NRC·CNRC

Flood Loads Data Generation Case Studies to Support Design of Flood-Resistant Buildings in Canada

Report No.: NRC-OCRE-2021-TR-021
Date: March 31, 2021
Authors: M.N. Khaliq, A. Attar

Ocean, Coastal and River Engineering Research Center

National Research Council Canada
Conseil national de recherches Canada

Canada

Cat. No. NR16-349/2021E-PDF

ISBN 978-0-660-38321-7

Acknowledgements

To support the design of flood-resistant buildings within the Climate Resilient Buildings and Core Pubic Infrastructure project, which is funded by the federal government of Canada through Infrastructure Canada, a number of flood modelling case studies were undertaken in different parts of Canada in collaboration with Canadian consulting firms. This report presents an overview of these case studies, which reflect the nature of flood loads that can be expected in riverine, coastal and urban environments in Canada. The much needed support of the following collaborators from the Canadian consulting firms for completing these case studies, in spite of the COVID-19 related unprecedented circumstances, is very much appreciated: Derek Williamson and Derek Eden from Baird and Associates; Alexander Wilson and Vincent Lays from CBCL; Stephen Bohrn and Raj Mannem from Hatch; Dan Hailey from Northwest Hydraulic Consultants; and Gilles Rivard from LaSalle | NHC.

The flood modelling and flood loads data generation case studies are expected to support the work related to the development of guidelines and prescriptive requirements for the design of flood-resistant buildings for the National Building Code. This work is being conducted through a joint collaboration between the NRC and the international codes experts from the US, with guidance and oversight from two technical committees (i.e. the Technical Committee for Flood-Resistant Buildings and the Steering Committee on Flood Resilience of Buildings) consisting of experts from private, government and academic sectors. All members of both committees are thanked for their oversight and useful suggestions. The two guidelines documents that will come out of this collaborative effort are expected to evolve overtime as new knowledge about flood characteristics, improved understanding of flood-resistant design methodologies and new flood-resistant materials will become available in the future, along with new information from additional flood modelling and flood loads data generation case studies, similar to the ones summarized in this report.

Dave Kriebel and Bill Coulbourne from Coulbourne consulting provided considerable technical guidance to Canadian consulting firms and reviewed generated data and approaches multiple times. This immense support is gratefully acknowledged.

Executive Summary

The National Research Council Canada (NRC) is leading the Climate Resilient Buildings and Core Public Infrastructure (CRB-CPI) project, with funding from the Federal Government of Canada through Infrastructure Canada. The focus of the project is to develop decision-support tools, including codes, guides and models, to enhance the resilience of Canada's buildings and core public infrastructure against climate change and extreme weather events, including floods.

The rising costs of floods over the last two decades in Canada have resulted in major economic losses and hardships for many communities across the country. There is also an increasing likelihood that the frequency and intensity of future flood events will be impacted by the anticipated climate change. Therefore, improving the performance of buildings exposed to flooding was recognized as an important research and development need early on within the CRB-CPI project. To advance research along these lines, the NRC launched a major effort, in collaboration with national and international partners, to develop prescriptive and performance-based requirements for the design of flood-resistant buildings, as well as guidelines for improving flood resistance of existing buildings. The outcomes of this effort will address a critical gap in the current National Building Code (NBC) of Canada, i.e. currently there are no provisions in the NBC for designing buildings against flood forces and flood loads, typically experienced in riverine, coastal and urban environments in Canada.

The work on the development of guidelines for the design of flood-resistant buildings and improving flood resilience of existing buildings is being conducted through a joint collaboration between the NRC and Coulbourne Consulting from the US, with guidance and oversight from two technical committees (i.e. the Technical Committee for Flood-Resistant Buildings and the Steering Committee on Flood Resilience of Buildings), consisting of experts from the private, government and academic sectors. The Coulbourne Consulting team was heavily involved in the development of ASCE7-17 in the US and developing design requirements for flood-resistant buildings. To underpin the development of these guidelines for Canada, a number of flood modelling case studies were undertaken in collaboration with Canadian consulting firms to generate flood loads data, from riverine, coastal and urban environments in Canada. This report presents an overview of these case studies and the information on the generated data.

In general, buildings and are subjected to two types of flood loads in floodplains, i.e. hydrostatic loads and hydrodynamic loads. Hydrostatic loads are associated with the standing water and originate from the hydrostatic pressure which is exerted on various components of buildings, e.g. wall assemblies, when they come in contact with flood waters. Hydrodynamic loads are associated with the forces of moving water when it impinges on or passes by building components.

This report is divided into ten chapters and a section on references. The background information on the design of flood-resistant buildings initiative is discussed in Chapter 1 in order to provide

the reader with sufficient contextual information on the topic. Objectives and limitations of the report are also discussed in this chapter. This introductory information was necessary to understand the technical information, flood modelling and mapping procedures, and flood loads data presented in other chapters of the report. An introductory primer on concepts associated with different types of flood loadings on buildings and building components and some general information on selected case studies for generating flood loads data is provided in Chapter 2. Chapter 3 of the report provides an overview of two riverine case studies from Alberta and discusses important highlights of the results obtained. These case studies were completed by Northwest Hydraulic Consultants from Edmonton. Chapter 4 presents a similar overview as given in Chapter 3, but for the four case studies completed in Atlantic Canada (Newfoundland and Labrador, New Brunswick and Nova Scotia). These case studies were conducted by CBCL Limited and cover both coastal and/or riverine flooding. Chapter 5 presents an overview of two coastal case studies from British Columbia. These were completed by Northwest Hydraulic Consultants from Vancouver. Chapter 6 presents an overview of two riverine case studies, one from Manitoba and another from Saskatchewan. These were completed by Hatch from Winnipeg. Two large lake coastal case studies for Lake Erie, completed by Baird from Ottawa, are presented in Chapter 7. After this, two case studies covering riverine and urban flooding from Quebec, completed by LaSalle | NHC from Montreal are presented in Chapter 8. One northern case study from Northwest Territories is covered in Chapter 9. This case study was completed by Baird from Ottawa. Chapter 10 presents an overall perspective on the case studies and discusses some important aspects related to flood loads data, generated in these case studies. This chapter also explores avenues of future research and discusses potential recommendations to strengthen the flood loads database derived from the selected case studies, presented in Chapters 3 to 9 of this report.

Table of Contents

List of Tables

List of Figures

List of Acronyms

Acronym	Description
ASCE	American Society of Civil Engineers
CHS	Canadian Hydrographic Society
CRB-CPI	Climate Resilient Buildings and Core Public Infrastructure
CSHORE	Cross-Shore Numerical Model for Waves, Currents, Sediment Transport and Beach Profile Evolution
AEP	Annual Exceedance Probability
CCFR	Climate Change Floodplain Review (CCFR)
CGVD28	Canadian Geodetic Vertical Datum of 1928
CHS	Canadian Hydrographic Society
DCE	Dike Crest Elevations
DFL	Designated Flood Level
DFO	Department of Fisheries and Oceans
DHI	Danish Hydraulic Institute
EVA	Extreme Value Analysis
FDRP	Flood Damage Reduction Program
FEMA	Federal Emergency Management Agency
GCM	General Circulation Model
GEV	Generalized Extreme Value
GIS	Geographical Information System
GP	Generalized Pareto
HEC-HMS	Hydrologic Engineering Centre Hydrologic Modelling System
HEC-RAS	Hydrologic Engineering Centre River Analysis System
HHWLT	Higher High Water Large Tide
IDF	Intensity Duration Frequency
IPCC	Intergovernmental Panel on Climate Change
IWD	Inland Waters Directorate
LiDAR	Light Detection and Ranging
LIO	Land Information Ontario
LLWLT	Lower Low Water Large Tide
LP3	Log Pearson Type 3
MIKE21	Hydrodynamic Model from DHI
M21FM	MIKE21 Flexible Mesh
M21SW	MIKE21 Spectral Wave
MRI	Mean Recurrence Interval
MS	Microsoft
MSC	Meteorological Service of Canada
NBC	National Building Code

NDMP	National Disaster Mitigation Program
NE	Northeast
NHC	Northwest Hydraulic Consultants
NOAA	National Oceanographic Atmospheric Administration
NRC	National Research Council
PCSWMM	Personal Computer Stormwater Management Model
POT	Peaks-Over-Threshold
RSLR	Relative Sea Level Rise
SCS	Soil Conservation Service
SLR	Sea Level Rise
SW	Southwest
SWMM	Stormwater Management Model
TPR	Town of Peace River
TWL	Total Water Level
USACE	US Army Corp of Engineers
USEPA	United States Environmental Protection Agency
USGS	United States Geological Survey
WIS	Water Information Studies
WL	Water Level
WSA	Water Security Agency

1 Introduction

1.1 Background

The National Research Council Canada (NRC) is leading the Climate Resilient Buildings and Core Public Infrastructure (CRB-CPI) project, with funding from the Federal Government of Canada through Infrastructure Canada. The focus of the project is to develop decision-support tools, including codes, guides and models, to enhance the resilience of Canada's buildings and core public infrastructure against climate change and extreme weather events, including floods (Infrastructure Canada, 2016; Global News, 2017). The rising costs of floods over the last two decades in Canada have resulted in major economic losses and hardships for many communities across the country. There is also an increasing likelihood that the frequency and intensity of flood events will be impacted by climate change in the future. Therefore, improving the performance of buildings exposed to flooding was recognized as an important research and development need early on within the CRB-CPI project. To advance research along these lines, the NRC launched a major effort in collaboration with national and international partners to develop prescriptive and performance-based requirements for the design of flood-resistant buildings, as well as guidelines for improving flood resistance and performance of existing buildings. The outcomes of this effort will address a critical gap in the current National Building Code (NBC) of Canada, i.e. currently there are no provisions in the NBC for designing buildings against flood forces and flood loads, typically experienced in riverine, coastal and urban environments in Canada.

The development of guidelines for the design of flood-resistant buildings and improving flood resistance of existing buildings is being carried out through a joint collaboration between the NRC and Coulbourne Consulting from the US, with guidance and oversight from two technical committees (i.e. the Technical Committee for Flood-Resistant Buildings and the Steering Committee on Flood Resilience of Buildings), consisting of experts from the private, government, and academic sectors, as well as not-for-profit organizations and municipalities. The Coulbourne Consulting team had previously participated in the development of ASCE7-16 in the US and was also involved in the development of design requirements for flood-resistant buildings. To underpin the development of design guidelines for Canada, a number of flood modelling case studies were designed and undertaken in collaboration with Canadian consulting firms to generate flood loads data from riverine, coastal and urban environments in Canada. This data acts as the backbone of numerous engineering calculations, which are required to be executed for the design of flood-resistant buildings and improving flood resistance of existing buildings.

In general, buildings are subjected to two types of flood loads in floodplains, i.e. hydrostatic loads and hydrodynamic loads. Hydrostatic loads are associated with the standing water and originate from the hydrostatic pressure which is exerted on various components of buildings, e.g.

wall assemblies, when they come in contact with flood waters. Hydrodynamic loads are associated with the forces of moving water when it impinges on or passes by building components. To develop a preliminary understanding of the type and magnitude of flood loads that can be expected on buildings and to generalize some guiding principles, the NRC supported two riverine case studies in Alberta, two costal case studies in British Columbia, two riverine case studies in Saskatchewan and Manitoba, two large lake case studies in Ontario, two riverine and urban case studies in Quebec, four riverine/coastal case studies in Atlantic Canada, and one coastal case study in northern Canada. This report presents an overview of these case studies and some general information on the generated data.

For generating information on flood loads, both hydrological and hydraulic investigations, involving multiple modelling tools, are generally required to be undertaken for the site of interest. For hydrologic investigations in rural and urban settings, long-term streamflow observations and extreme rainfall events play a critical role. However, most of the Canadian river network is ungauged and recorded observations are available frequently in southern parts of the country and much less so for northern areas, north of the 60 degrees parallel. In the absence of recorded observations, information on relevant high streamflow indices (e.g. 100-year or 200-year flood magnitudes and levels) at ungauged locations is obtained through indirect means, e.g. by transposing known or processed information from gauged to ungauged locations, following a set of established scientific and hydrologic principles, or through transforming extreme design rainfall amounts into design flow magnitudes and levels. Hydraulic modelling and investigations in riverine environments pertain to obtaining information on flow velocities and depths at various points within the floodplain and also to capture respective variabilities. These aspects are important since hydrostatic forces on building components are expressed in terms of depth of water and hydrodynamic forces in terms of velocity of water. For coastal settings, information on design water levels is obtained by analyzing various wave characteristics, wave run-up and storm surge elevations. All of the above efforts culminate in the creation of flood depth and flood velocity maps for the region of interest and these maps then act as the main source of information for deriving flood loads and load combinations, required for building design purposes.

Conventionally, all of the above analyses and investigations are performed using observed or transposed data assuming a stationary climate. Due to climate change as projected by Global Climate Models (GCMs) and documented in various reports of the Intergovernmental Panel on Climate Change (IPCC) (IPCC, 2007, 2013), the assumption of a stationary climate has become questionable and therefore the applicability of flood frequency magnitudes and water levels, derived from recorded historical observations and transposed data under the assumption of stationarity, has also become questionable. It is worth pointing out that many human related activities clearly affect the climate system. Most importantly, emissions of greenhouse gases, especially carbon dioxide and methane, are causing more heat to be trapped within earth's atmosphere. Therefore, the case for significant climate change is compelling in both the

empirical observations and theoretical predictions. A warmer air mass can hold more water (i.e. warmer air has a higher saturation vapor pressure) and therefore, it is reasonable to expect higher amounts of water vapor in the air, leading to intensification of the hydrologic cycle, with impacts ranging from one region to another and from one component of the water cycle to another (Khaliq, 2019). However, it is not so straightforward to consider the impacts of a changing climate when deriving flood frequency relationships, specifically when those relationships are transposed at various ungauged points of interest within a target region. Though openly recognized and acknowledged, the topic of non-stationary climate was not considered for the case studies and in the generation of flood loads, except in the case of two coastal studies in British Columbia, where the impact of sea level rise was considered. To address this topic, systematic guidelines have been incorporated on integrating climate change information with flood loading components in the guidelines related to the design of flood-resistant buildings (Coulbourne Consulting, 2021a). This report is specifically focused on flood loads data generation case studies. However, information on technical aspects and complex mathematical concepts involved in numerical hydrodynamic modelling is kept at the minimum. For the reader's convenience, a primer on flood loads on buildings is provided in Chapter 2, while Chapters 3 to 9 of the report pertain to the 13 flood loads data generation case studies from across the country. A high level summary and a set of potential avenues that can be explored in the future for improving quality of data on flood loads are provided in Chapter 10. Additional relevant detail, specific objectives and limitations of this report are provided below.

1.2 Objectives

The objectives of this report are to:

- Document an overview of the findings, modelling procedures, and generated data on flood loads that were realized through targeted flood modelling and mapping case studies, which were commissioned by the NRC, with funding from Infrastructure Canada, to support design of flood-resistant buildings in Canada;
- Identify and document the variety of techniques that were deployed in flood loads data generation case studies, reflecting the diversity and the range of engineering procedures used; and
- Carve a path forward for future research and development efforts in order to enrich and improve the quality of data on flood loads that are expected in urban, riverine and coastal environments across Canada.

1.3 Organization of the Report

This report is divided into ten chapters, including this introduction chapter, and a section on references. The background information on the design of flood-resistant buildings initiative is discussed in Chapter 1 in order to provide the reader with sufficient contextual information on

the topic. Objectives and limitations of the report are also discussed in this chapter. This introductory information is crucial to understand the technical information, flood modelling and mapping procedures, and flood loads data presented in the subsequent chapters of the report. An introductory primer on concepts associated with flood loads on buildings and building components, as well as some general information on selected case studies on flood loads data generation are provided in Chapter 2. Chapter 3 of the report provides an overview of two riverine case studies from Alberta and discusses important highlights of these case studies, which were completed by Northwest Hydraulic Consultants from Edmonton. Chapter 4 presents a similar overview as given in Chapter 3, but for the four case studies completed in Atlantic Canada (Newfoundland and Labrador, New Brunswick and Nova Scotia). These case studies were conducted by CBCL and cover both coastal and/or riverine flooding. Chapter 5 presents an overview of two coastal case studies from British Columbia; these were completed by Northwest Hydraulic Consultants from Vancouver. Chapter 6 presents an overview of two riverine case studies, one from Manitoba and another from Saskatchewan. These case studies were completed by Hatch from Winnipeg. Two large lake coastal case studies for Lake Erie, completed by Baird from Ottawa, are presented in Chapter 7. After this, two case studies covering riverine and urban flooding from Quebec, completed by LaSalle | NHC from Montreal are presented in Chapter 8. One northern case study from Northwest Territories is covered in Chapter 9. This case study was also completed by Baird from Ottawa. Chapter 10 presents an overall perspective on the case studies and discusses some of the main findings and limitations of the generated flood loads data. This chapter also explores avenues of future research and discusses potential recommendations to strengthen flood loads database derived from the selected case studies, presented in Chapters 3 to 9 of this report.

1.4 Convention on the Usage of Acronyms and Other Considerations

A number of acronyms are used in this report, which were used in the original reports compiled by five different consultants on 13 different case studies. Some of the acronyms are chapter-specific, while others are utilized throughout the report. Therefore, to facilitate easy comprehension and smooth readability, the acronyms are reintroduced in their expanded form in each chapter so that each chapter can be read independently.

Various aspects of open channel flow play a significant role in generating flood loads data. The terms like design river flow, design streamflow, or simply design flood, reflecting open channel flow and overland flow conditions, are considered equal in terms of meanings in this report. In a similar manner, design water levels or flood construction levels corresponding to stated return periods are also considered equal in terms of meanings, especially in the context of coastal flood modelling and mapping. It was necessary to clarify this point upfront since different terms are used in different case studies and merely using the word “flow” or “water level” does not convey true meanings of the contextual analyses, conducted for generating information on flood loads

from urban, riverine, or coastal floodplains. In addition, the terms “return period” and “mean recurrence interval” are used interchangeably and both have the same meanings.

1.5 Scope and Limitations

The overview of various analyses and technical procedures provided in this report are intended for individuals that have some basic understanding of runoff-generating mechanisms in riverine and urban environments, methods pertaining to streamflow analysis and the statistical theory involved in the estimation of design flows and water levels for flood mapping in urban, riverine and coastal conditions.

The technical/scientific information and published sources considered for this report are those which were originally considered in the technical reports prepared by all consultants, i.e. NHC (2021a, 2021b, 2021c, 2021d), CBCL (2021), Baird (2021a, 2021b), Hatch (2020) and LaSalle | NHC (2021), in addition to the findings documented in these reports.

The scope of this current report is limited to only hydrological and hydraulic investigations and coastal analyses pertaining to the development of flood maps for generating flood loads data. Since most of the case studies were conducted in areas where detailed studies already existed, detailed information on the data that underpin these studies is beyond the scope of this report. Some of these datasets were not available in the public domain and therefore those were of proprietary nature, either belonging to the consultant or to the funding authority that supported the original study. Detailed descriptions of theoretical aspects that underpin various statistical methods considered for deriving design flood magnitudes or water levels are outside the scope of this report. For such descriptions, scientific articles, technical reports or text books associated with these methods can be consulted.

2 Flood Loading on Buildings

2.1 General

For flood-resistant construction, it is important to ensure that new buildings in flood hazard areas are designed and constructed to resist the effects of flooding and resulting forces on building components. Thus, there are a number of important elements that need to be considered about flooding before determining the type of flood loads that are important for providing resistance within the structural elements of a building. Also, it is important to know, how does various flooding aspects affect buildings in floodplains? Certainly if flood water surrounds a building then the building could collapse and the interior contents could flood. This and other impacts can occur depending upon the depth of water. In addition, flood water comes with some velocity and hence the moving water could dislocate the building from its foundation. Flood water can rise very rapidly causing a flash flood, which can also dislodge buildings from their foundations and could also destroy inside contents and assets. Not only the flood depth and velocity, flood duration can also become an important parameter in certain situations. Flood waters can also carry debris, which can vary from large logs, cars, floats, to ice floes, etc., which can impact buildings in various ways. In coastal areas, flooding can cause damage to buildings as breaking waves extend to buildings and building components. To estimate expected flood loads for a given site of interest, it is important to determine flood conditions, i.e. information about flood depths, velocities, scour/erosion, wave forces, debris impacts, etc. (FEMA, 2011).

In order to find what flood risks exist or could exist at any building site within a floodplain, two pieces of information are generally required, i.e. information about flood depth, and information about flood velocity. From a building design perspective, it is important to know how to determine flood design depths and velocities at the building site from the information available from floodplain maps. The flood loads caused by water depths and velocities and other mechanisms are further discussed below, with respect to the Canadian floodplain maps.

2.2 Hydrostatic Loads

The depth of flooding causes hydrostatic loading on vertical surfaces or buoyancy or uplift on horizontal surfaces (see Figure 2.1 and Figure 2.2). In fact, this is the most obvious flood load and the easiest to compute from a practical standpoint. However, the information available on most Canadian flood maps is quite insufficient to estimate these loads in a reliable manner. Many existing flood maps show greater than or less than a meter of depth, which in some provinces delineate the distinguishing features of floodway and flood fringe (see Figure 2.3). Therefore, determination of actual flood loads due to hydrostatic forces requires more precision in flood depth than is currently available on flood maps. Flood depth from existing flood maps can be determined by subtracting the ground elevation from the mapped flood levels corresponding to

the design flood or the regulatory flood or from the flood construction levels, a term often used in coastal settings.

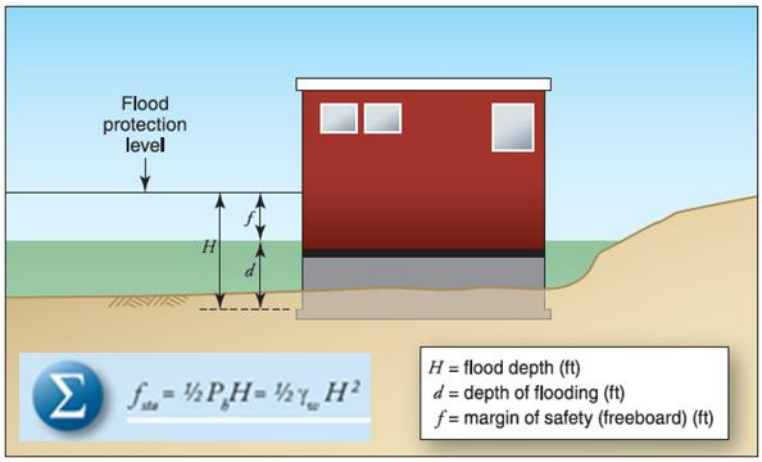

Figure 2.1: Schematic of hydrostatic loading on buildings and building components. Source: FEMA (2012, 2013).

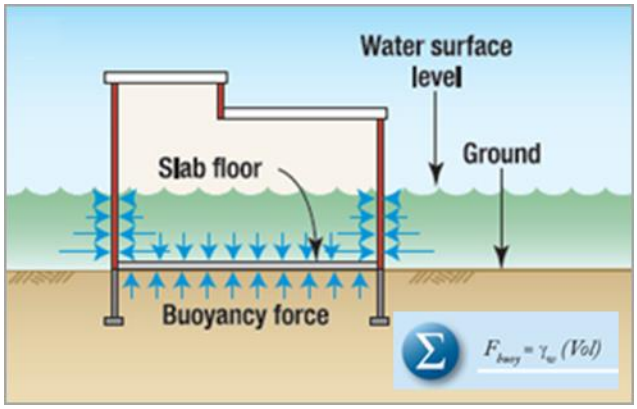

Figure 2.2: Schematic of buoyancy or uplift forces on horizontal surfaces. Source: FEMA (2012, 2013).

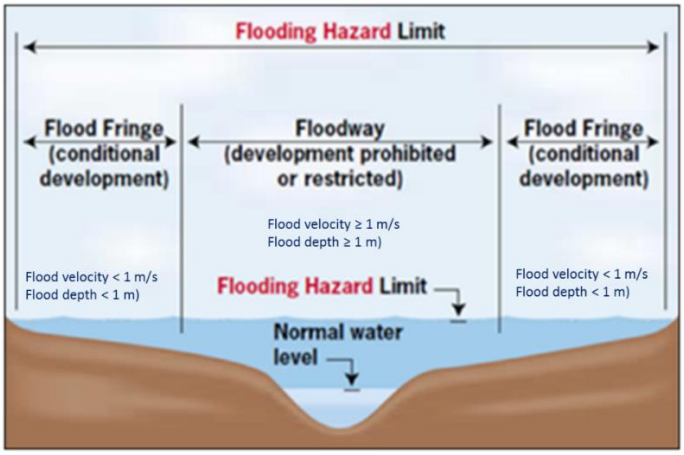

Figure 2.3: Schematic diagram showing floodway and flood fringe, identified based on flood velocity and depth criteria. Source: Ontario Ministry of Natural Resources and Forests.

2.3 Hydrodynamic Loads

Apart from flood depth, discussed above, flood velocity is also an important variable for load calculations (see Figure 2.4). Flood velocity is an important variable because faster moving flood waters can cause significant damage to buildings that are located in floodplains. This variable is used in flood load equations for calculating hydrodynamic loads, and debris loads as well. Flood velocity is not generally mapped as part of most Canadian provincial mapping programs. In many cases, there are indications on the map that the velocity is less than or greater than one meter per second because that helps define location of floodway and flood fringe (see Figure 2.3). However, that level of information is not fine enough for determining realistic flood loads from moving waters. Compared to hydrostatic loads, hydrodynamic loads are more difficult to determine and may require engineering consultations and detailed investigations. If detailed modelling results are available, then standard methods for estimating open channel flow velocities can be employed. In coastal areas, there is more uncertainty in estimating flood velocity, which is not associated with breaking waves. A number of FEMA references demonstrate how to calculate velocity as a function of still water depth (e.g. FEMA, 2011). In many cases with coastal flooding, water slowly rises and floods lands and then withdraws. In these situations, there are not large net velocities and these can safely be neglected. On the other hand, there are also coastal regions where strong currents are encountered and those must be considered for load calculations.

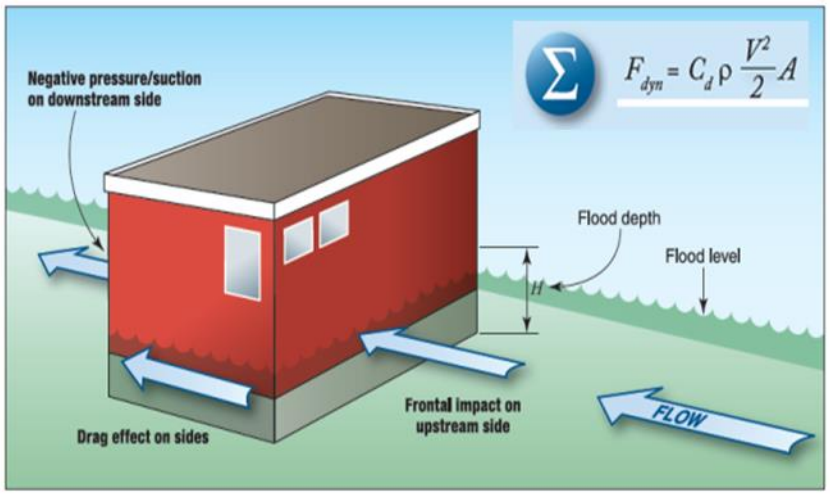

Figure 2.4: Schematic of hydrodynamic loading on buildings and building components, shown as a function of flood velocity (V), contact area (A), density of water (ρ) and drag coefficient (C_d). Source: FEMA (2012, 2013).

2.4 Debris Impacts

Debris is basically an impact load as debris in moving waters can impart a considerable impact load when it comes in contact with buildings and building components. Typical examples of debris are logs and woody debris, floating ice floes, man-made debris, small boats, cars, trucks,

field equipment, and shipping containers. The presence and the types and sizes of debris cannot be determined from flood maps and flood risk assessment studies. The debris and ice loads can arise due to two mechanisms. One is due to accumulation of debris or ice jamming against buildings; they are driven by the velocity of the flow and are usually treated as static loads. The other is due to the impacts of individual pieces of debris or individual ice floes and other objects. There is no clear perception and guidance in the literature regarding how to handle these loads properly, given that these are of very short duration, and could be treated dynamically by structural engineers. ASCE/SEI 7-16 (ASCE/SEI 7-16, 2017) commentary on flood loads, provides some guidance for the consideration of debris impact loads. During flood load calculations, ice is treated as a type of debris. Of all debris types, ice is most thoroughly investigated, for bridge piers and much less is known about the interaction of ice with residential and commercial buildings (ASCE/SEI 7-16, 2017).

2.5 Wave Loads

Wave loads are important in large lake (e.g. Great Lakes) and coastal environments. These loads depend largely on wave height, which is a function of still water depth, which can be estimated from water level records maintained by Canadian Hydrographic Society (CHS) or through numerical modelling approaches. According to ASCE/SEI 7-16 (ASCE/SEI 7-16, 2017), the magnitude of wave loads can be 10 times or more, stronger than wind forces. In coastal areas, wave loads are due to breaking waves and loads due to wave runup. Both are treated as dynamic loads for building design purposes. Wave heights over 0.9 m can cause extreme structural damage (FEMA, 2013). For breaking wave loads on vertical walls, more commonly engineers use Goda equations (Goda, 2010) for wave interactions with large vertical structures. None of the wave impacts is really mapped on flood maps, individually. Somehow, the information would have to be inferred from water depths shown on flood maps or through perusing the detailed numerical modelling outputs for load calculations. In general, the coastal flood depth mapping requires storm surge plus tide levels and some additional elevation considerations for waves and wave runoffs and freeboard (if considered). Future conditions are suggested to be shown for new maps.

2.6 Erosion and Scour

Erosion and scour may affect the stability of foundations as both lower the ground surface next to the building. Consequently, the loss of supporting soils should be considered because it affects flood loads on walls, columns, and piles that support various structural components of buildings. FEMA (2011) provides some guidance on the effects of erosion and scour.

2.7 Duration of Flooding

Flood duration parameter is not included in standard floodplain maps in any part of the world. Though flood duration does not directly contribute to flood loads, it is a flood condition that warrants consideration because long duration flooding is more likely to delay re-occupancy in residential buildings and is also an important factor in dry flood proofing for non-residential buildings. Flood duration definitely affect damage levels, creates lots of potential mould and if flood water is enclosed in the building for a longer time, it can affect the resistance of materials below the flood level. Additionally, long duration flooding is likely to cause non-structural damages even if the buildings are strengthened with flood-resistant materials.

2.8 Initiation of Flood Loads Data Generation Case Studies

Across the country, particularly in populated riverine and coastal communities, many buildings already exist in floodplains, so retrofitting options may require estimates of flood loads. Similarly, certain critical buildings may be required to be located in floodplains and for that matter, estimates of flood loads are generally required. Currently, the mapping standards in Canada range from 100-year return period flood levels (in most provinces and territories) to 200-year levels in British Columbia and 500-year levels in Saskatchewan (Khaliq and Attar, 2017; Khaliq et al., 2018). In the case of a higher return period regulatory level (e.g. the 500-year level for the whole country), many buildings will probably be allowed to be built in the expanded flood zone. Therefore, there are several reasons for considering flood forces on buildings and building components.

In Canadian floodplains, flood loads for building design purposes must be determined at a minimum for (i) flood depth, (ii) flood velocity, (iii) waves generated by moving water in coastal locations, and (iv) debris impact including that from ice, similarly to the approach suggested in the American Society of Civil Engineers Standards ASCE/SEI 7-16 (ASCE/SEI 7-16 2017). Flood provisions in ASCE/SEI 7-16 include those related to: hydrostatic loads; hydrodynamic loads; erosion and scour; wave conditions and wave loads; and flood-borne debris and debris impact loads. Therefore, at the minimum, floodplain maps showing spatial patterns of both velocity and depth of flood water for flood-prone areas both for coastal and riverine environments will be useful for estimating flood loads on buildings and developing related code provisions, guidelines and standards.

In Canada, most of the floodplains were mapped through the federal government funded Flood Damage Reduction Program (FDRP), which started in 1976 and was led by Inland Waters Directorate (IWD) (IWD, 1976; Environment and Climate Change Canada, 2016). In 1995/96 when the FDRP ended, most of the flood-prone areas and vulnerable major population centers across the country were flood risk mapped. The majority of the flood maps produced within the FDRP were targeted to show flood extents following the two zone concept, i.e. floodway and

flood fringe. The floodway is the portion of the floodplain where flood velocities are expected to equal or exceed 1 m/s and/or water depths equal or exceed 1 m. The flood fringe is the remainder of the flood zone where the flood velocities are under 1 m/s and the water depth is below 1 m. New flood-prone areas were mapped and existing maps were undated in certain jurisdictions under the National Disaster Mitigation Program (NDMP) of Public Safety Canada (https://www.publicsafety.gc.ca/cnt/mrgnc-mngmnt/dsstr-prvntn-mtgtn/ndmp/index-en.aspx). Most of the new and existing flood maps show inundation extent and spatial distribution of flood water depth in terms of floodway and flood fringe (Khaliq and Attar, 2017; Khaliq et al., 2018). Detailed spatial information about flood depths and velocities is available only for a few west and east coast communities, where new mapping initiatives were recently undertaken. This information is absolutely required if flood-resilience is required at the building footprint level in flood-prone areas across Canada.

To fill the gap between the detailed information required for flood-resistant design of buildings and what is currently available from flood maps, and to support the development of guidelines for flood-resistant design of buildings initiative of the CRB-CPI project, a number of flood loads data generation case studies were designed and undertaken in collaboration with Canadian consulting firms. The distribution of these case studies, reflecting riverine, coastal and urban conditions, is shown in Figure 2.5. The outputs of these studies will support development of generalized prescriptive guidelines for flood design and retrofitting of existing buildings included in the two guidelines documents, i.e. Flood-Resistance Design of Buildings (Coulbourne Consulting, 2021a) and Improving Flood-Resistance for Existing Buildings (Coulbourne Consulting, 2021b).

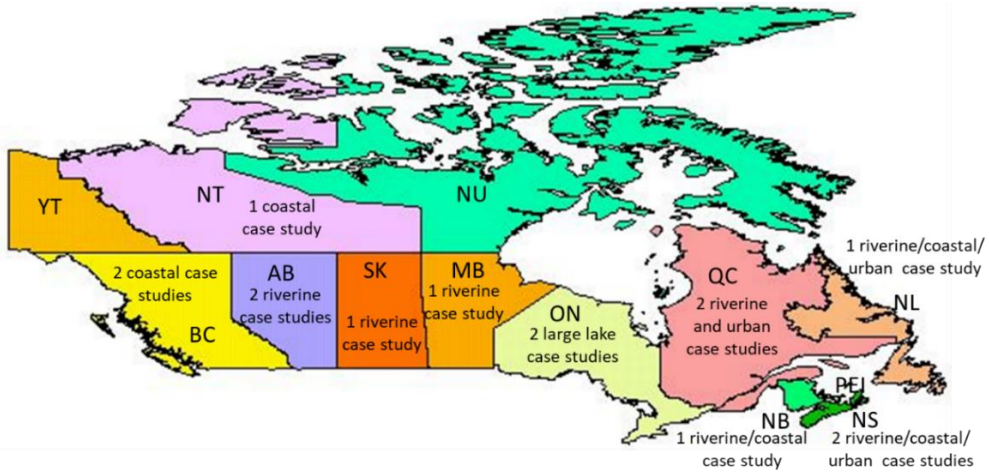

Figure 2.5: Flood loads data generation case studies undertaken in riverine, urban and costal environments across Canada to support design of flood-resistant buildings initiative of the NRC. Two/three letter abbreviations used for provinces and territories are: AB-Alberta; BC-British Columbia; MB-Manitoba; NB-New Brunswick; NL-Newfoundland and Labrador; NS-Nova Scotia; NT-Northwest Territory; NU-Nunavut; ON-Ontario; PEI-Prince Edward Island; QC-Quebec; SK-Saskatchewan; and YT-Yukon Territory.

3 Alberta – Riverine Flooding Case Studies

3.1 General

Northwest Hydraulic Consultants Ltd. (NHC) Edmonton were contracted to undertake riverine flood modelling and flood loads data generation case studies in Alberta. Two representative riverine floodplain mapping studies were selected where most of the required supporting datasets were readily available. These datasets included: bathymetry data, LiDAR data, orthorectified aerial imagery, and flood hydrology. The first case study is of the North Saskatchewan River at Edmonton and the second is of the Peace River at Peace River. For these case studies, NHC already completed detailed floodplain mapping studies for Alberta Environment and Parks (AEP). By selecting these case studies where previous detailed studies existed, considerable efficiencies were realized as much of the background data sources were already compiled and the models were already set up. There were also considerable gains in terms of data pre-processing and modelling experience. NHC extended these existing studies to satisfy the requirements of flood loads data generation initiative of the NRC. In doing so, NHC also obtained appropriate permissions from AEP for sharing of data and models.

The material included in this chapter is extracted directly from the reports prepared by NHC (Northwest Hydraulic Consultants, 2021a, 2021b). Detailed information on the modelling procedures, assumptions made, compromises on data availability, data sources, and data preparation and modelling procedures is available in this reference. Here, in this chapter, the North Saskatchewan River case study is presented first, followed by the Peace River study.

3.2 North Saskatchewan River Case Study

3.2.1 Project Area and Representative River Cross-Sections

First limits of the project area for floodplain mapping from the previously completed study were determined and then representative cross-section locations were identified within the project area. The project area covers a range of conditions for river and floodplain morphology and land use. Figure 3.1 depicts the project area and representative cross-sections. In this figure, the 100-year flood extents are also shown for contextual purposes.

Each representative cross-section was divided into segments (denoted as “panels”) covering the left overbank, main channel and right overbank portions of the river cross-section. The convention used to denote left and right overbanks corresponds to a viewer looking in the downstream direction. A uniform panel width of 20 m was adopted for the overbanks and main channel. This was considered to be a representative order of magnitude dimension for a typical development footprint. The edges of the panel segments were set to align with the left and right bank stations (the boundary between the main channel and overbank portions of the channel).

Since the width of the main channel and overbank portions were not evenly divisible by the 20 m panel width, a shorter panel width remained in each of the far left and right overbanks, and middle of the main channel. Figure 3.2 provides plots of 6 (out of 11) representative cross-sections depicting: the bank stations, the channel, the left and right overbanks, the panel segments, and water levels for the 20-, 100-, 500-, and 2500-year flood scenarios (chosen for demonstration purposes). The midpoint of each panel is denoted herein as a “save point”. Characteristic parameters were extracted from the modelling results for each panel / save point location. Panel widths and corresponding save points were set to a fixed location for all scenarios. This strategy facilitated comparisons between scenarios at a given location.

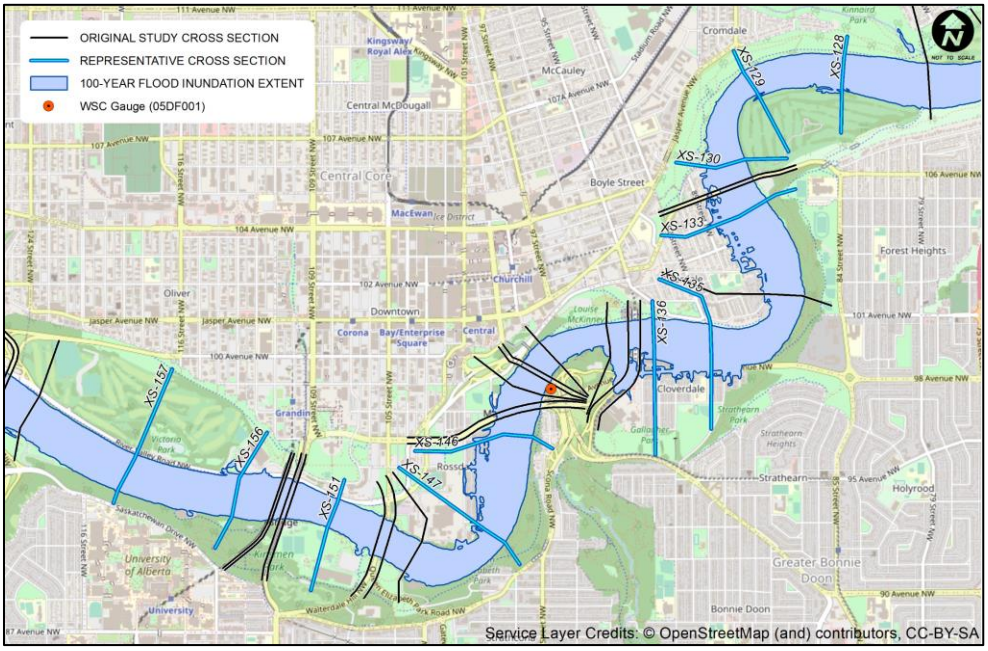

Figure 3.1: North Saskatchewan River project area. Existing and representative cross-sections and the 100-year floodplain are also shown. WSC: Water Survey of Canada.

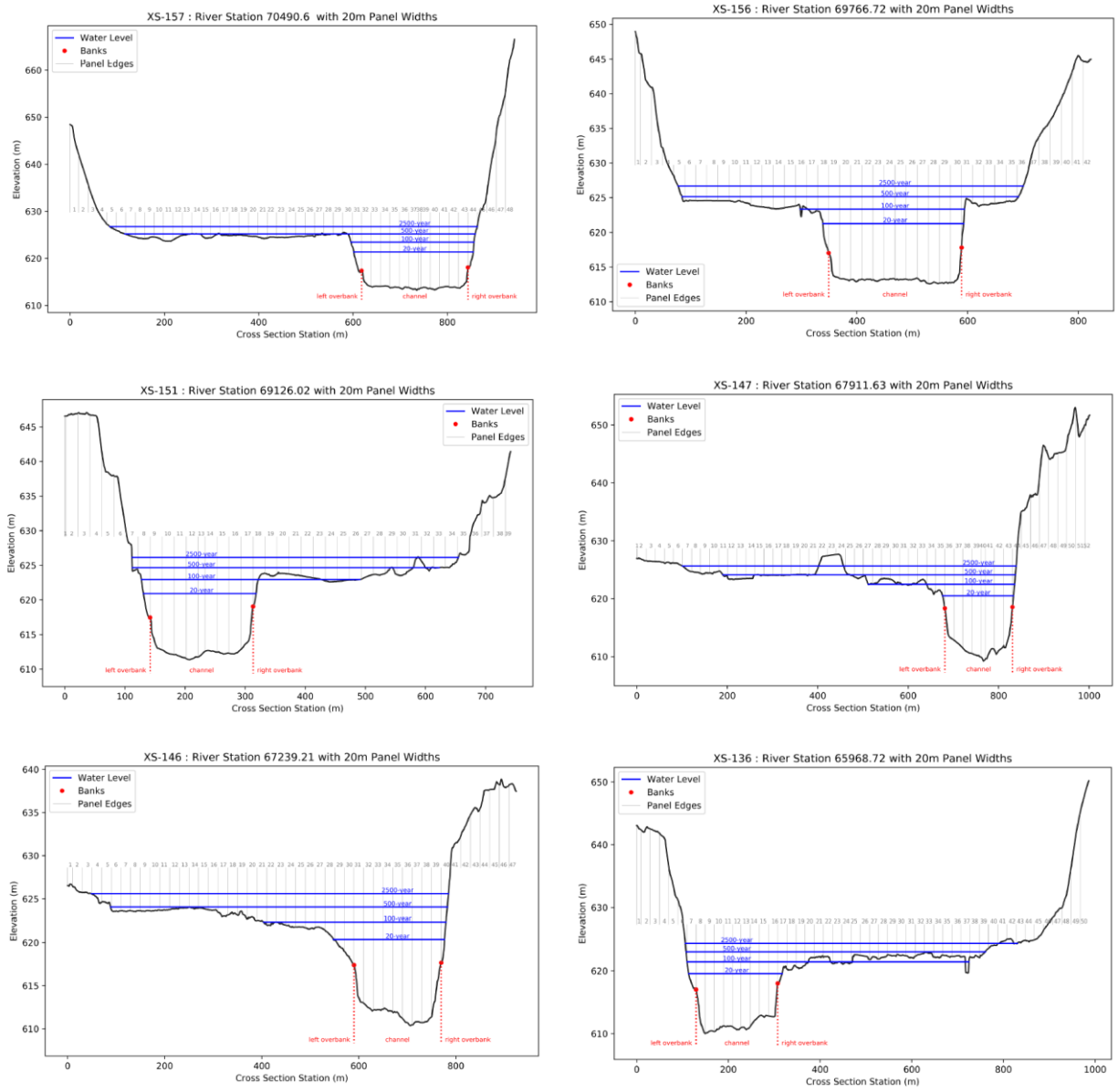

Figure 3.2: Six selected cross-sections (i.e. XS-157, XS-156, XS-151, XS-147, XS-146, and XS-136; shown at the top of each graphic) with 20 m panel width.

3.2.2 Flood Scenarios

Flood frequency values were estimated from historic annual extremes, extracted from the data collected at the Water Survey of Canada (WSC) gauge in Edmonton. The discharges were naturalized as part of the original study (NHC, 2020) to account for the effects of regulation. In the original study, flood magnitudes were derived for return periods ranging from 2 to 1000 years. For this study, flood scenarios were required for 10-, 20-, 50-, 100-, 200-, 500-, 1000-, and 2500-year return periods. The 2500-year flood scenario was estimated by extending the flood

frequency relationship used in the original study. Figure 3.3 depicts the flood frequency curve with the 95% confidence limits. Additional information on the flow naturalization techniques and flood frequency analysis is available in NHC (2020). Table 3.1 lists the flood frequency values used to determine flood levels, inundation extents, and the characteristic parameters of flood loads, summarized later in this report.

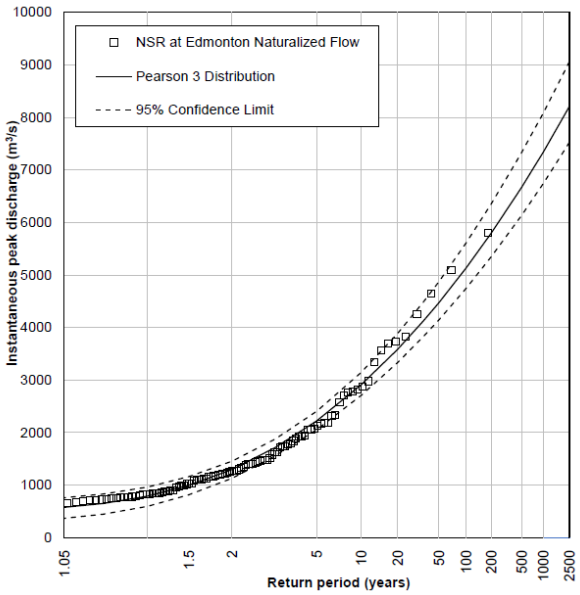

Figure 3.3: Annual maximum naturalized flows, the fitted Pearson Type 3 distribution and the 95% confidence band.

Table 3.1: Flood frequency estimates for the North Saskatchewan River at Edmonton.

Return period (years)	Annual probability of exceedance (%)	Discharge (m^3/s)	
		Magnitude	95% confidence limits
2500	0.04	8,210	7,530 – 9,060
1000	0.10	7,330	6,730 – 8,070
500	0.20	6,670	6,140 – 7,330
200	0.50	5,800	5,350 – 6,350
100	1.00	5,130	4,750 – 5,610
50	2.00	4,470	4,140 – 4,870
20	5.00	3,580	3,330 – 3,880
10	10.00	2,910	2,710 – 3,140

Floodplain maps for all flood scenarios were developed and delivered to the NRC (i.e. NHC, 2021a). However, the flood extents for this study were generated in a slightly different manner than the original study (NHC, 2020). The original study involved a complex series of operations using ArcGIS tool sets and detailed manual inspection for smoothing flood limit lines and removal of small isolated wet and dry areas in the floodplain and main channel. Whereas, the flood extents presented in this study were derived directly from the HEC-RAS RASMapper

toolset. Thus, flood limits depicted for this study vary slightly from the ones provided in the original study. Three sample flood maps are shown in Figure 3.4, Figure 3.5 and Figure 3.6.

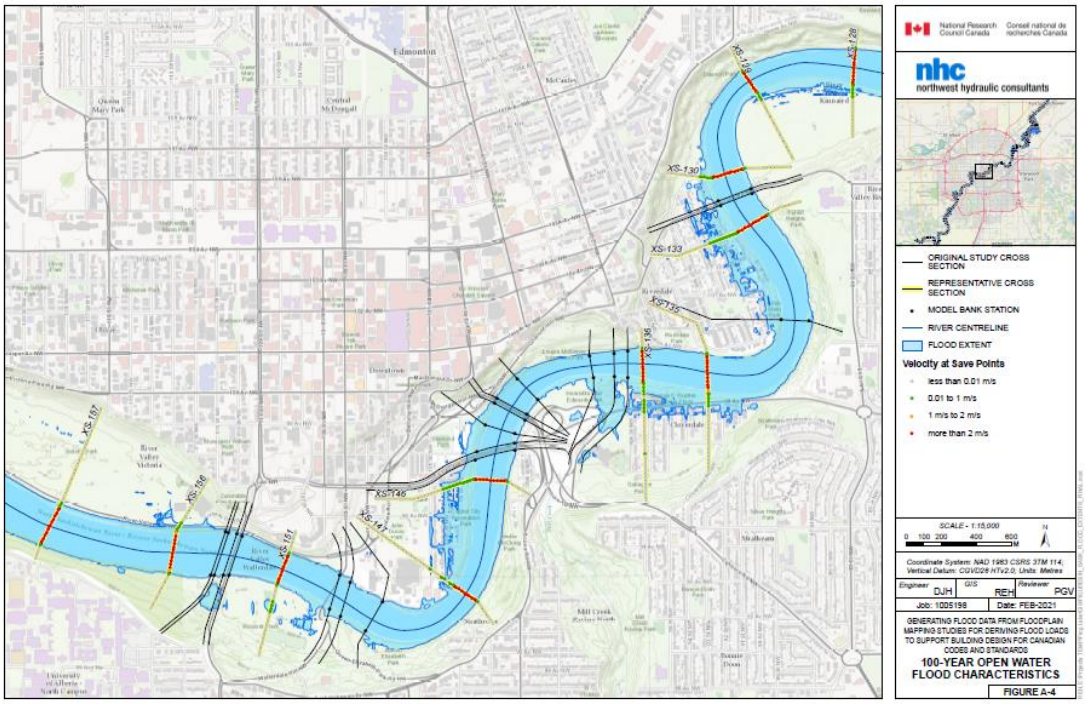

Figure 3.4: Flood inundation extents for the 100-year event.

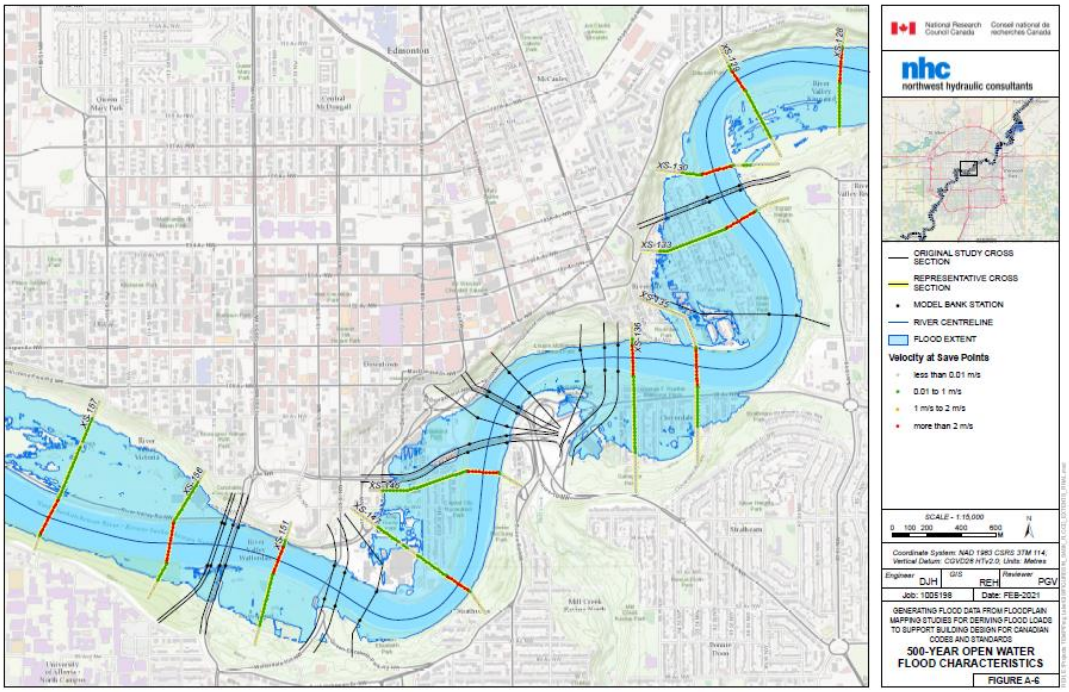

Figure 3.5: Flood inundation extents for the 500-year event.

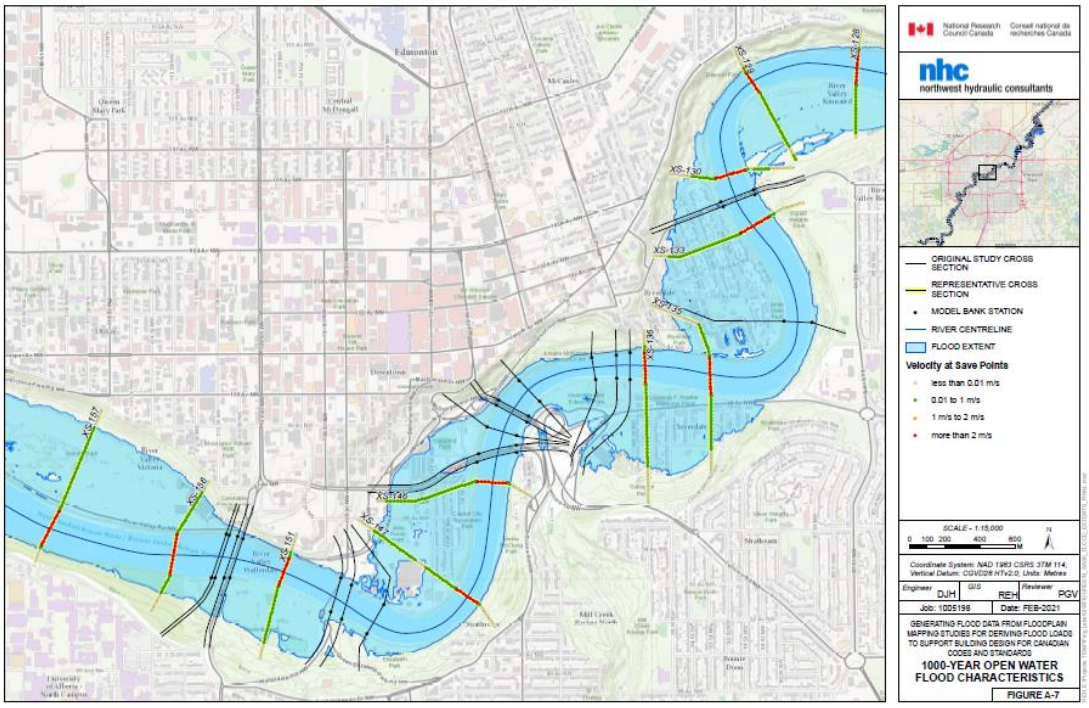

Figure 3.6: Flood inundation extents for the 1000-year event.

3.2.3 Flood Characteristics

Flood characteristics were extracted from the flood modelling and mapping results for each of the eight flood scenarios. Data was extracted for each cross-section and for each individual panel (save point) along the cross-section.

Cross-Section Characteristics

For each representative cross-section, the geographic location (Northing and Easting of the cross-section at mid-channel) and stream-wise distance from downstream limit of the original study reach were determined. The following additional cross-section characteristics were obtained for the various flood scenarios considered.

- River discharge;
- Water level;
- Cross-sectional area of the wetted portion of the channel and floodplain (total area, left overbank area, main channel area, and right overbank area);
- Mean flow velocity of the channel and floodplain (average velocity over the entire cross-section, average velocity for the left overbank area, average velocity for the main channel area, and average velocity for the right overbank area); and
- Kinetic energy coefficient “alpha”.

Panel (Save Point) Characteristics

The following characteristics were extracted from the modelling results for each flood scenario at the evenly spaced save point locations along the individual cross-sections. Characteristics for each save point were derived from the geometry and hydraulic properties of the associated panel.

- Northing and Easting of the mid-point of each panel, denoted as the save point;
- Location with respect to the floodway or flood fringe;
- Average bed/ground elevation;
- Water surface elevation;
- Flood depth (average and maximum) for the panel;
- Panel area;
- Panel velocity; and
- Panel roughness (Manning's n value).

Save point characteristics were tabulated separately and delivered to the NRC in MS Excel format. Cross-section width varies from one section to the other and therefore the number of panels also varies from one section to the other. Furthermore, the wetted portions of a particular section vary from one flood scenario to another scenario, and the same is the case with the number of wetted panels. To facilitate comparisons between flood scenarios at a particular save point location, the panels were set based on the entire cross-section width and kept constant for all flood scenarios. All panels, including the dry panels, were tabulated for each cross-section. For the user's convenience and quick lookup purposes, dry panels were denoted with zero values for flood depth, panel area and panel velocity, where applicable.

3.2.4 Flood Statistics

Summary statistics (in the form of mean and standard deviation) were determined for the specific flood parameters (i.e. flood depth and velocity) as noted below. Dry panels were excluded from these calculations. Statistics were derived:

- According to the flood scenario (corresponding to 10- to 2500-year return periods) separately for the left overbank; main channel; right overbank; left and right overbanks combined; and full flood extent (i.e. main channel, left, and right overbanks).
- For all combined flood scenarios (i.e. one grand sample of all points combined).

A summary of the flood loading variables was also prepared in the form of a table.

3.2.5 Concluding Discussion

The information on flood loading variables was extracted from the modelling outputs that were available from the original study for 10-, 20-, 50-, 100-, 200-, 500-, and 1000-year floods. The same model that was used in the original study (NHC, 2020) was then rerun to generate outputs

for the 2500-year flood, which was estimated by extrapolating the flood frequency curve used in the original study. Given the typical record lengths of 30-50 years of hydrological variables, the flood frequency estimates are considered to be reasonable and adequate for return periods up to about 200 years. The estimates for more extreme events (e.g. 500-year, 1000-year or 2500-year floods), obtained by extrapolating the frequency curve, are expected to be associated with considerable uncertainties and therefore the corresponding results should be used with caution.

As pointed out above, the statistics assembled for the NRC's study were derived from the information developed under a much larger and complex flood hazard mapping study completed by NHC (NHC, 2020) for AEP. Therefore, additional information and details pertaining to hydrologic aspects, hydraulic modelling, flood mapping procedures, risk assessment, and supporting data (e.g. geo-spatial and hydrographic surveys) can be found in that study.

3.3 Peace River Case Study

3.3.1 Project Area and Representative River Cross-Sections

For this site, the limits of the project area for floodplain mapping were determined first and then representative cross-section locations were identified within the project area. This study area also covers a range of conditions for river and floodplain morphology and land use. The project area and representative cross-sections are shown in Figure 3.7. The 100-year flood extents are also shown in this figure for contextual purposes.

Figure 3.7: Peace River project area. Existing and representative cross-sections and the 100-year floodplain are also shown.

For the selection of representative cross-sections, number of panels and panel widths, exactly the same procedure was used as described above for the North Saskatchewan River case study. The naming convention for the left and right overbanks and save point locations was also kept the same. Figure 3.8 provides plots of six representative cross-sections showing: the bank stations, the channel, the left and right overbanks, the panel segments, and water level elevations for the 20-, 100-, 500-, and 2500-year flood scenarios.

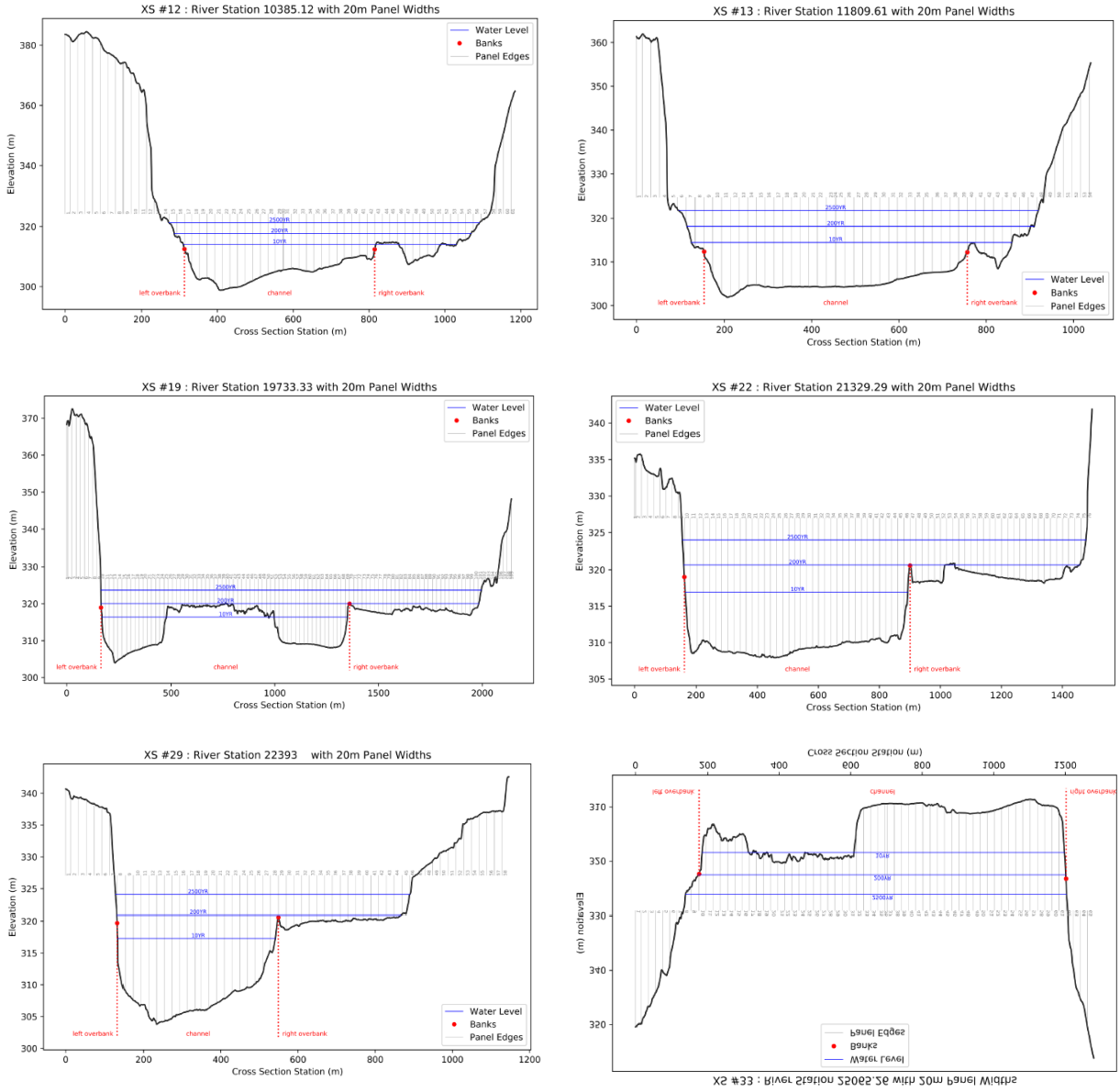

Figure 3.8: Six selected cross-sections (i.e. XS #12, XS #13, XS #19, XS #22, XS #29, and XS #33; show at the top of each graphic) with 20 m panel width.

3.3.2 Flood Scenarios

Flood frequency values were estimated from historic annual extremes, extracted from the data collected at WSC gauge in Peace River. The discharges were naturalized as part of the original study by NHC (NHC, 2017) to account for the effects of regulation. In the original study, flood magnitudes were derived for return periods ranging from 2 to 1000 years. For this study, flood scenarios were required for 10-, 20-, 50-, 100-, 200-, 500-, 1000-, and 2500-year return period floods. The 2500-year flood scenario was estimated by extending the flood frequency relationship used in the original study. Figure 3.9 depicts the flood frequency curve with the 95% confidence limits at the Town of Peace River (TPR). Additional information on the flow naturalization techniques and flood frequency analysis procedures can be found in NHC (2017). Table 3.2 lists the flood frequency values used to determine flood levels, inundation extents, and characteristics of flood loading variables considered for this study.

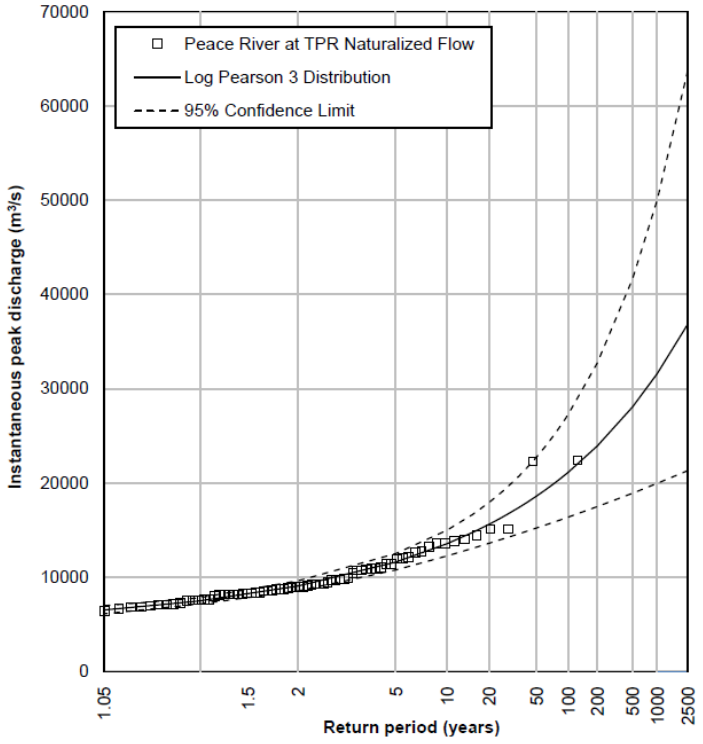

Figure 3.9: Annual maximum naturalized flows, the fitted Log Pearson Type 3 distribution and the 95% confidence band for the Town of Peace River (TPR).

Table 3.2: Flood frequency estimates for the Peace River above and below the Smoky River.

Return period (years)	Annual probability of exceedance (%)	Peace River above Smoky River		Peace River below Smoky River	
		Discharge (m^3/s)	95% confidence limits	Discharge (m^3/s)	95% confidence limits
2500	0.04	21,500	15,500 – 30,000	36,800	21,300 – 63,700
1000	0.10	19,600	14, 800 – 26,000	31,600	20,000 – 50,000
500	0.20	18,200	14,200 – 23,400	28,100	18,900 – 41,600
200	0.50	16,500	13,500 – 20,200	23,900	17,500 – 32,700
100	1.00	15,200	12,800 – 18,000	21,100	16,400 – 27,300
50	2.00	13,900	12,100 – 16,000	18,600	15,200 – 22,800
20	5.00	12,300	11,100 – 13,600	15,600	13,600 – 17,900
10	10.00	11,100	10,200 – 12,000	13,500	12,200 – 15,000

Floodplain maps for all flood scenarios were developed and delivered to the NRC. However, the flood extents for this study were generated in a slightly different manner than the original study (NHC, 2017). The original study involved a complex series of operations using ArcGIS tool sets and detailed manual inspection for smoothing flood limit lines and removal of small isolated wet and dry areas in the floodplain and main channel. Whereas, the flood extents presented in this study were derived directly from the HEC-RAS RASMapper toolset. Thus, the flood limits depicted for this study are slightly different from the ones provided in the original study. Three sample flood maps are shown in Figure 3.10, Figure 3.11 and Figure 3.12.

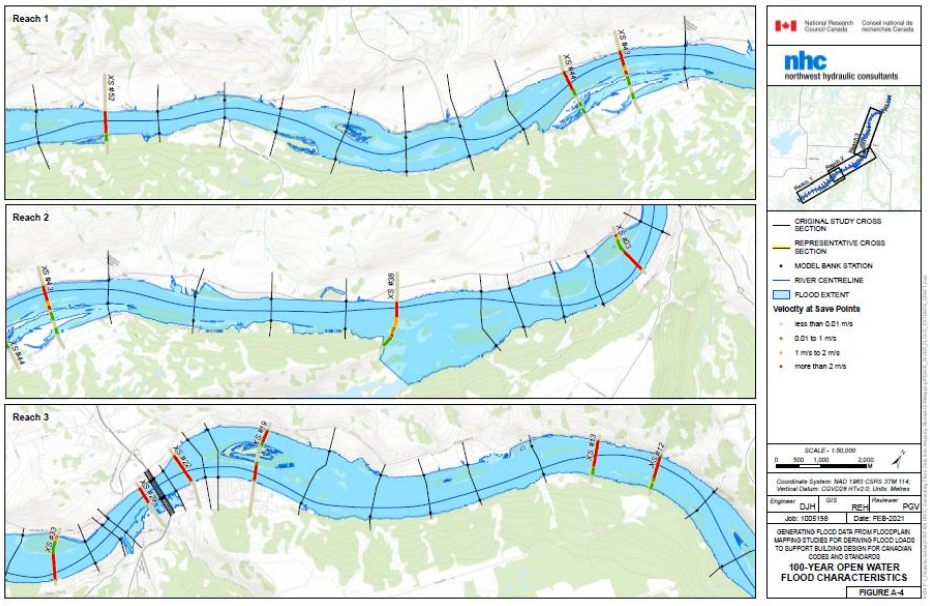

Figure 3.10: Flood inundation extents for the 100-year event.

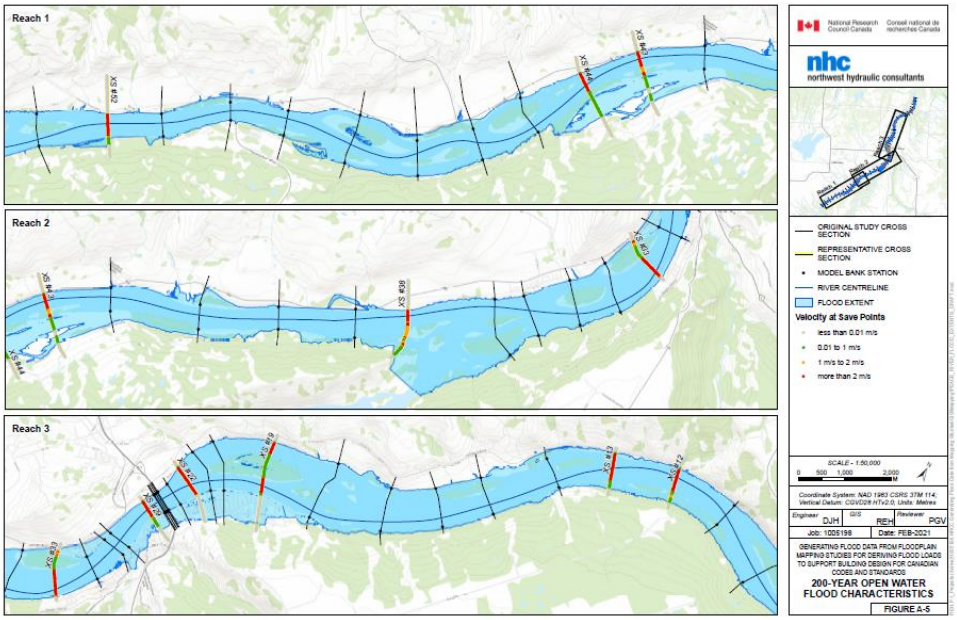

Figure 3.11: Flood inundation extents for the 200-year event.

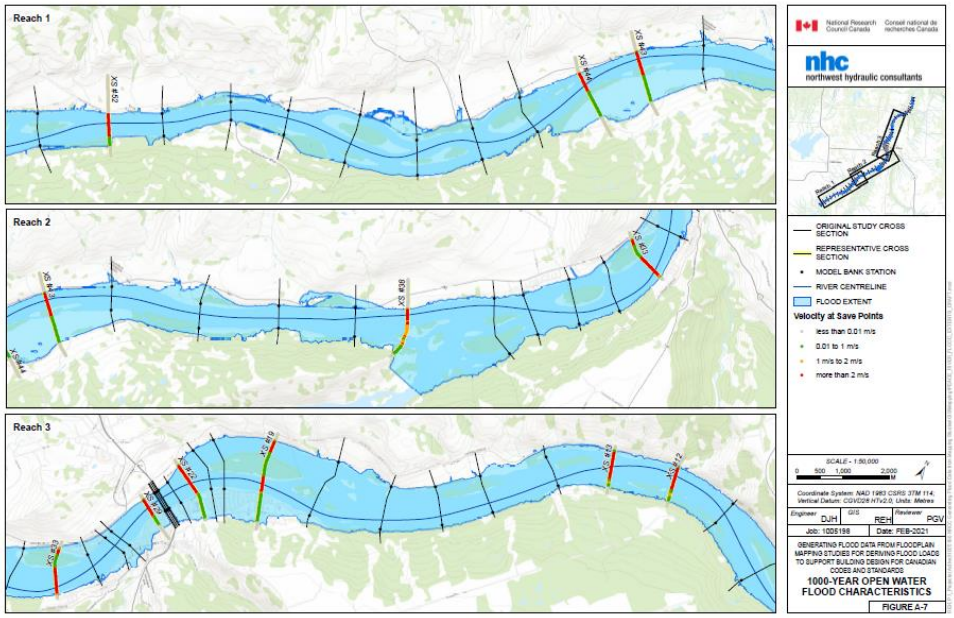

Figure 3.12: Flood inundation extents for the 1000-year event.

3.3.3 Flood Characteristics

Flood characteristics were extracted from the flood modelling and mapping results for each of the eight flood scenarios. Data was extracted for each cross-section and for each individual panel (i.e. save point) along the cross-section. The same characteristics as listed in Section 3.2.3 were extracted from all cross-sections and panels. Save point characteristics were tabulated separately

and delivered to the NRC in MS Excel format. Cross-section width varies from one cross-section to the other and therefore the number of panels also varies from one cross-section to the other. Furthermore, the wetted portions of a particular section vary from one flood scenario to another, and the same is the case with the number of wetted panels. To facilitate comparisons between flood scenarios at a particular save point location, the panels were set based on the entire cross-section width and kept constant for all flood scenarios. All panels, including the dry panels, were tabulated for each cross-section. For quick lookup purposes, dry panels were denoted with zero values for flood depth, panel area and panel velocity, where applicable.

3.3.4 Flood Statistics

Exactly the same statistics were derived as described above for the case of North Saskatchewan River. That is, summary statistics (in the form of mean and standard deviation) were determined for the specific flood parameters (i.e. flood depth and velocity): (1) according to flood scenario (corresponding to the selected 10- to 2500-year return periods) for the left overbank; main channel; right overbank; left and right overbanks combined; and full flood extent (i.e. main channel, left and right overbanks); and (2) for all combined flood scenarios (i.e. considering one grand sample of all points combined). A summary of the flood loading variables was also prepared in the form of a table.

3.3.5 Concluding Discussion

The work completed during the original study, which was completed in 2017 and updated in 2019 (NHC, 2017), laid the foundation for generating flood loads data in an efficient manner. Previous modelling results were used to generate information corresponding to the 10-, 20-, 50-, 100-, 200-, 500-, and 1000-year flooding scenarios. The same model (i.e. HEC-RAS) as used in the original study was extended to generate results for the 2500-year flood, which was estimated by extrapolating the flood frequency curves used in the original study. As discussed above, the flood frequency estimates are generally considered to be reasonable for return periods up to about 200 years, given the 30-50 years long historical observations. Consequently, NHC noted that the estimates for more extremal events (e.g. 500-year, 1000-year or 2500-year floods) obtained by extrapolating the flood frequency curve could be associated with large uncertainties and therefore the corresponding results should be used with caution. Details pertaining to hydrologic aspects, hydraulic modelling, flood mapping, risk assessment, and supporting datasets is available in the much larger and complex flood hazard mapping study, which was completed by NHC (NHC, 2017) for AEP.

4 Atlantic Provinces – Riverine and Coastal Flooding Case Studies

4.1 General

CBCL Halifax (CBCL hereafter) were contracted to undertake riverine and coastal flood modelling and flood loads data generation case studies in Atlantic Provinces. After careful review of a range of existing studies and associated models, supporting data and availability of rainfall and coastal water level records, four sites were selected for the project: Truro in Nova Scotia, the Waterford River in Newfoundland, Mahone Bay in Nova Scotia, and Saint John in New Brunswick. Based on historical perspectives, these locations were found to be highly vulnerable to both riverine and coastal flooding. According to the review conducted by CBCL, all models for these study sites were adequately set up and calibrated based on historical events. However, where necessary, CBCL made some adjustments to satisfy requirements for the NRC's flood loads data generation case studies project. By selecting these sites where previous detailed studies existed, considerable efficiencies were realized as much of the background data sources were already compiled and the models were already tested on historical events. There were also considerable gains in terms of data pre-processing and modelling experience. Where applicable, CBCL also obtained appropriate permissions for sharing of data and modelling results as the original projects were completed for different municipal entities and under different initiatives.

The information included in this chapter is extracted directly from the report prepared by CBCL (CBCL, 2021). Detailed information on the modelling procedures, assumptions made, compromises on data availability and transferability, data sources, and data preparation and modelling procedures is available in this reference. In this chapter, the four case studies are presented in the following order, i.e. Site 1: Truro (Section 4.2); Site 2: Waterford River (Section 4.3); Site 3: Mahone Bay (Section 4.4); and Site 4: Saint John (Section 4.5). Before discussing hydrologic and hydraulic considerations for these sites, it is important to know how various flood scenarios were developed and some background information on statistical methods and data that were used to derive extreme rainfall amounts and river and coastal water levels corresponding to targeted return periods, ranging from 10 to 2500 years.

4.1.1 Flood Scenarios and Model Simulations

For the selected case studies, development of flood scenarios involved either extreme rainfall amounts, river discharges or extreme storm surge elevations corresponding to 10-, 20-, 50-, 100-, 200-, 500-, 1000-, and 2500-year return periods. All model simulations were considered to have flood mechanisms dominated by either rainfall events or storm surge events. Joint probability approach for estimating the likelihood of a rainfall event of a given magnitude, occurring at the same time as the storm surge, was not considered for these studies. However, an average event of the non-dominant process was combined with the target return period event of the dominant

process. Based on this strategy, following 16 flood scenarios were formulated and analysed (Table 4.1).

Table 4.1: Flood scenarios considered for the NRC's project.

Scenario ID	Flood scenario	Rainfall event return period (years)	Storm surge event return period (years)
1	10-year rainfall	10	2
2	20-year rainfall	20	2
3	50-year rainfall	50	2
4	100-year rainfall	100	2
5	200-year rainfall	200	2
6	500-year rainfall	500	2
7	1000-year rainfall	1000	2
8	2500-year rainfall	2500	2
9	10-year storm surge	2	10
10	20-year storm surge	2	20
11	50-year storm surge	2	50
12	100-year storm surge	2	100
13	200-year storm surge	2	200
14	500-year storm surge	2	500
15	1000-year storm surge	2	1000
16	2500-year storm surge	2	2500

4.1.2 Statistical Analyses

Statistical analyses were conducted to estimate rainfall amounts and coastal and river water levels for 2-, 10-, 20-, 50-, 100-, 200-, 500-, 1000-, and 2500-year return periods. The output of the statistical analyses were used for hydrologic and hydraulic analyses. Additional information is provided below.

Rainfall Magnitudes and Hyetographs

For developing intensity duration frequency (IDF) relationships for the four selected sites, rainfall observations from Truro (for the Truro study site), St. John's Airport (for the Waterford River case study), Western Head (for the Mahone Bay case study), and Saint John (for the Saint John case study) were used. Rainfall magnitudes corresponding to various return periods, noted above, for 5, 10, 15, 30 and 60 minutes, and 2, 6, 12, and 24 hours were estimated using the Gumbel distribution, fitted by the method of maximum likelihood. For these estimates, confidence intervals were developed using the profile likelihood method.

After estimating the rainfall magnitudes, the alternating block method was used to estimate synthetic hyetographs that were then used as input to the hydrological component of the modelling framework. The alternating block method converts rainfall magnitudes for various durations (i.e. 15- and 30-minute, and 1-, 2-, 6-, 12- and 24-hour) for a particular return period

into rainfall hyetographs. The maximum incremental rainfall is placed at the centre of the storm and the remaining incremental values are arranged in descending order, alternating right and left of the centre. This way, synthetic hyetographs were created for 2-, 10-, 20-, 50-, 100-, 200-, 500-, 1000-, and 2500-year return periods.

Coastal Water Levels

For the Bay of Fundy, extreme value analysis (EVA) was conducted based on 106 years of hourly total water levels in Saint John and employing the peaks-over-threshold (POT) approach for extracting extreme values. Generalized Pareto Distribution (GP) was fitted to declustered water levels and the fitted GP distribution was used to derive water levels corresponding to selected return periods. It is important to note that, for the EVA of total water levels, the extreme values should be larger than the Higher High Water Large Tide (HHWLT) in order to have a physical justification and that ensured during the analysis.

River Water Levels

For water levels of Oakpoint River and Saint John River, block maxima approach was used with the Generalized Extreme Value (GEV) distribution, fitted using the maximum likelihood method. The fitted GEV distribution was used to derive return values corresponding to various return periods, selected for the study.

Extreme Wind and Waves

To describe offshore wave climate, CBCL utilized the Environment Canada MSC50 offshore wind and wave model hindcast from January 1954 to December 2015 which contains hourly time series of wind and wave parameters. This dataset is a state-of-the art hindcast, wherein data from all existing wind and wave measurements were re-analysed and input to a 0.1-degree resolution ocean wave model that included the effect of ice cover (Swail et al., 2006). The MSC50 hindcast was developed by Oceanweather Inc. and is distributed by Environment Canada.

For the Truro study site, the MSC50 hourly time series of wind and wave parameters at the Upper Bay of Fundy (45.3°N, 64.6°W) was used. This dataset also includes hurricane wind fields. Extreme value analysis based on the POT approach was conducted on the MSC50 wind data to derive extreme wind conditions. For this project, various exposure directions were also considered. After analyzing different wind fields and a number of wind directions, it was found that the most critical wind direction for Truro is southwest, which also aligns with the Bay of Fundy and produces large surges that propagate into the Minas Basin and reaches the town of Truro.

For the Saint John site, extreme value analyses were conducted on the offshore wave data to derive offshore wave conditions for numerical modelling purposes. For the analysis, storm peaks were derived using the POT method and three directions of exposure for waves and winds were

considered, i.e. wave and wind conditions coming from southeast, north and west. The waves and winds coming from the southeast direction were found to be the dominant ones for the Saint John harbour and along the southern facing coastline area. The northern winds were used as input to calculate wave conditions for the northern shoreline of Saint John facing the Kennebecasis River. The west winds were used to derive wave conditions for the shoreline facing west for areas upstream of the reversing falls.

4.2 Site 1: Truro

The residents of Truro have endured repeated flooding from rivers at an increasing frequency, and similar flooding is likely to continue in the future. As part of an effort to reduce local flood risks, a flood risk management study commissioned by the Joint Flood Advisory Committee was undertaken. This was a very comprehensive study and it involved extensive stakeholder consultations, as well as 1D, 2D and 3D modelling of runoffs, tides, sediments and ice jams. In this study, floodlines were delineated, climate change aspects were considered and more than 40 flood mitigation options were modelled and ranked to provide solutions and produce a capital works plan.

An integrated 1D-2D PCSWMM model was calibrated and used for this site to simulate one-dimensional channel flows and two-dimensional floodplain flows. PCSWMM modelling tool integrates Version 5 of the Storm Water Management Model (SWMM) with a GIS engine and is capable of performing both hydrologic and hydraulic modelling. Developed by the US Environmental Protection Agency (USEPA), SWMM conducts unsteady flow calculations to simulate water backup, pooling and culvert hydraulics by dynamically solving the continuity and momentum equations with a finite difference scheme.

For flood load data generation purposes, no modification was made to the already calibrated model, except changing boundary conditions and using smaller routing time steps. Inputs to the model included synthetic rainfall hyetographs and coastal water levels corresponding to different return periods, required for the study. In the absence of tide gauge data for Truro, CBCL used a 2D hydrodynamic model to obtain extreme coastal water levels.

4.2.1 Placement of Transects

Ten representative transects were selected along the river channels, including the Salmon River, North River, Farnham Brook and McClures Brook. These transects were selected to cover most of the floodplain with likelihood of severe flooding, especially in urban areas (Figure 4.1). In particular, the transect numbers 2, 3, 9, and 10 represent interactions between the Salmon River flows and extreme coastal water levels, while transect numbers 1,4, 5, 6, 7, and 8 represent flooding conditions in major tributaries of the Salmon River.

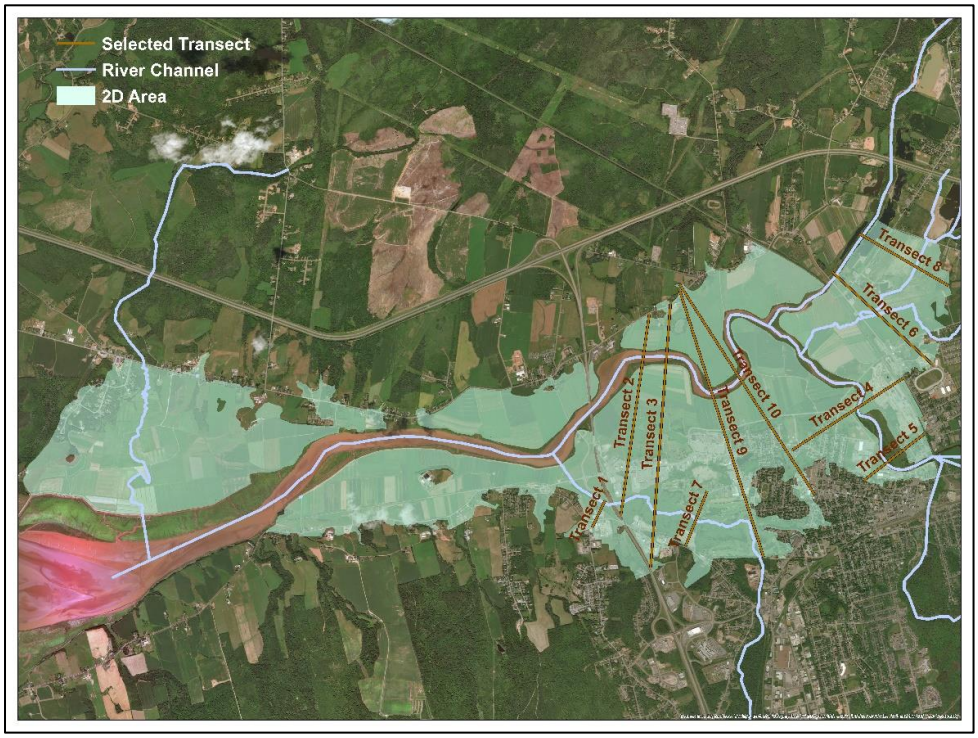

Figure 4.1: Truro study area, showing river channels and selected transects.

4.2.2 Hydrologic and Hydrodynamic Modelling

Extreme Coastal Water Levels

In a previous study, CBCL developed a 2D hydrodynamic model of the Bay of Fundy to obtain extreme coastal water levels. For this study, the same model was refined within the Minas Basin and extended to include Truro. The hydrodynamic model was calibrated by comparing predicted tidal levels within the Minas Basin from Webtide and with water level measurements at the Avon River Estuary. The Environment Canada MSC50 offshore wind model hindcast was used to define extreme wind conditions, already discussed in Section 4.1.2. This dataset comprises hourly time series of wind speed and direction for the period of January 1954 to December 2018 and is recognized as being high quality dataset.

Storm surge modelling was completed by running the full tidal model for two-weeks to determine the peak tidal levels near Truro. The outputs from the tidal model was then used as initial conditions for the surge model which was run over a period of 48 hours. Estimated extreme wind values were combined with a normalized storm shape to force the surge model. The peak of the developed storm, which coincided with the peak tidal elevations, was considered to estimate extreme total water levels. The developed model was used to provide extreme (still) water levels along the existing shoreline in Truro. The 24-hour time series of TWL for different return periods were used as the coastal boundary conditions for the PCSWMM modelling.

Estimates of Channel and Floodplain Flows

For the original study, a hydrologic analysis was carried out for the modelling domain (Figure 4.2) to delineate watersheds and determine watershed characteristics, including surface slope, overland flow length, surface roughness, imperviousness, and soil characteristics, to be used as input parameters. Historical flow and water level data for five hydrometric stations along the Salmon and North Rivers and their tributaries were used for model calibration purposes. Based on radar and gauged rainfall data, a representative rainfall event was associated with each watershed. Field measured information on bridges, culverts and aboiteaux was incorporated in the modelling. The main branches of the Salmon River, North River, Farnham Brook and McClures Brook were modelled using cross-sections that were 20 m and 50 m apart. Twenty meter apart cross-sections were used to model the urban floodplain, where more detail was necessary, while 50 m apart cross-sections were used to model upstream areas of the watershed. The urban floodplain downstream of the Bible Hill CNR Bridge (Salmon River) and the Onslow CNR Bridge (North River) were modelled with a 2D mesh, which included portions of the Town of Truro, the Village of Bible Hill and Onslow. The 2D mesh was developed using the LiDAR data and was comprised of a 40 m resolution hexagonal grid. Break lines were included in the mesh at locations where sharp changes in elevation, such as raised roadways and railways, to ensure that these locations are modelled with sufficient detail. Coastal boundary conditions were used as inputs at the mouth of the Salmon River.

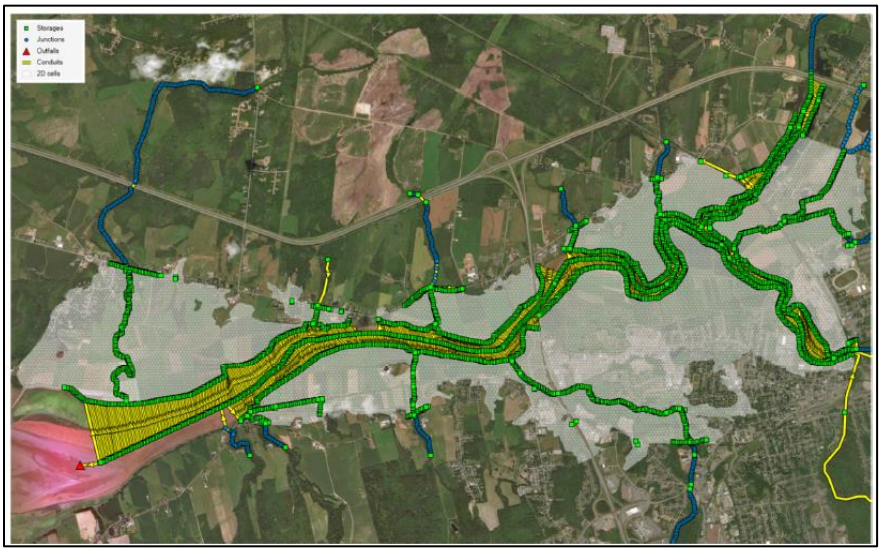

Figure 4.2: PCSWMM modelling domain for the Truro case study.

For the NRC's flood loads data generation project, synthetic hyetographs generated from the rainfall analysis, discussed above in Section 4.1.2, and the extreme coastal water levels obtained from the 2D hydrodynamic model, discussed above, were used as inputs for the already calibrated PCSWMM to simulate flows and water levels under different flooding scenarios, required for the study.

4.2.3 Flood Maps

Flood maps for 16 different scenarios were developed. These maps show flood lines corresponding to both rainfall and storm surge events of different return periods. In comparison terms, the most severe flooding for this site was noted for the rainfall related events, especially the 2500-year event. One flood map for the 500-year coastal conditions is shown in Figure 4.3, and that for the 500-year rainfall event is shown in Figure 4.4.

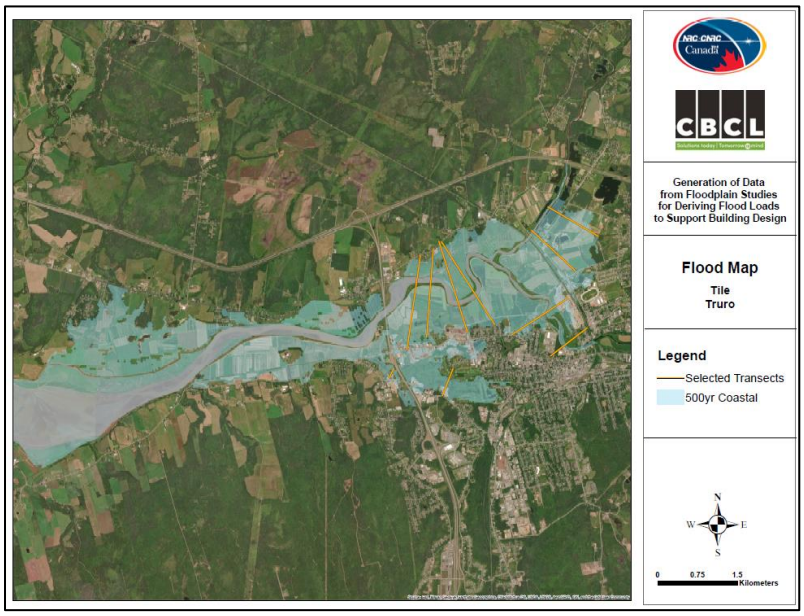

Figure 4.3: Floodplain map corresponding to 500-year coastal conditions for the Truro study area.

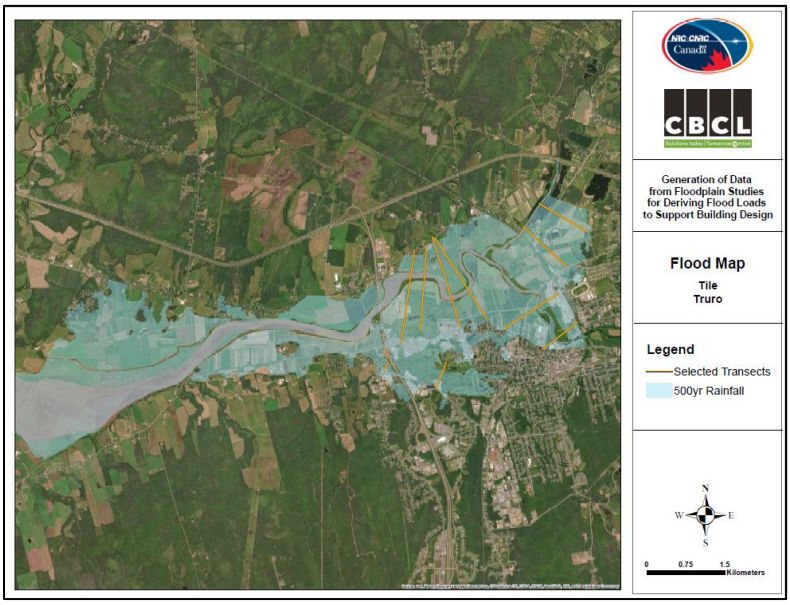

Figure 4.4: Floodplain map corresponding to the 500-year rainfall event for the Truro study area.

4.2.4 Data Extraction

Information on flood loading variables was extracted for each transect and save point, and summary statistics were prepared and delivered to the NRC in MS Excel format. In the tables, the transect geometry and water surface elevation from left to right, looking in the downstream direction, for different flood scenarios, was described. Extracted data from the PCSWMM included topographic elevations, river discharges for the entire transects, the maximum water surface elevation, the maximum water depth and the maximum velocity at the 1D channel and 2D cells along the transects. Ground elevations and the maximum water surface elevations were used for calculating flow areas at each transect and save point.

4.3 Site 2: Waterford River

In the past, significant rainfall events in the Waterford River Basin led to repeated flooding in the City of St. John's, including damages to hydraulic structures, washouts, and bank erosion. For long-term planning purposes, the Government of Newfoundland and Labrador funded a floodplain mapping update study through the Department of Municipal Affairs and Environment, Water Resources Management Division. The Waterford River drainage area totals 66.3 km^2 and extends over three municipalities: the City of St. John's, the City of Mount Pearl, and the Town of Paradise. A combination of the HEC-HMS and HEC-RAS models were developed for this site and used for simulating one-dimensional flows in both the channel and the floodplain. For the NRC's project, no modification was made to the available calibrated models, except extending the width of various transects. Required inputs included synthetic hyetographs of rainfall events and coastal water levels corresponding to the selected return periods. At this site, tide gauging data was available to support estimation of extreme coastal water levels.

4.3.1 Placement of Transects

As shown in Figure 4.5, ten representative transects were selected along the Waterford River and its major tributaries. All transects were placed in urban areas and were located in areas with relatively uniform flow. All transects are wide enough to include both the river channel and the floodplain and represented typical flooding conditions in the Waterford River.

Figure 4.5: Waterford River study area, with river channels and selected transects.

4.3.2 Hydrologic and Hydrodynamic Modelling

For the Waterford River, hydrologic modelling was carried out using the HEC-HMS model to obtain river flows for different rainfall events and those were used as input to the 1D HEC-RAS model to estimate water levels corresponding to different flood scenarios. Following stream network and sub-basin delineations, physical characteristics, such as stream length and slope, longest flow paths, centroidal flow lengths, and basin slopes were extracted from the terrain data using the HEC-GeoHMS extension. Calibration of the HEC-HMS model was achieved by simulating a recorded precipitation event and comparing the simulated flows with the recorded flows.

A 1D steady flow analysis was conducted using the HEC-RAS model for the Waterford River and its major tributaries, including South Brook, Tributary from Nevilles Pond, Donovans Tributary, Tributary from Branscombe's Pond to Waterford River, and Kilbride Brook (Figure 4.6). A 2D analysis was not considered because the flow and velocity in the floodplain were expected to follow the path of the main river and was not expected to spread out in multiple directions. Surveyed cross-sections and LiDAR data were used to set up the model. In total, there were 433 surveyed cross-sections and 664 interpolated cross-sections in the model geometry. At the mouth of the Waterford River, water levels are influenced by tides. Therefore, to model the boundary conditions at the mouth of the river, an estimate of the HHWLT was obtained for St. John's from the Canadian Hydrographic Service (CHS) nautical chart 4846: Motion Bay to Cape St. Francis. Calibration of the HEC-RAS model was achieved by simulating a historical event and comparing the output water levels to recorded water levels.

These calibrated models were used to generate information on flood loading variables for the NRC project. However, prior to the numerical modelling for different flood scenarios, some cross-sections were extended and resampled at 1 m spacing using the LiDAR data. Synthetic hyetographs of rainfall events for 2-, 10-, 20-, 50-, 100-, 200-, 500-, 1000-, and 2500-year return periods were used as input to the HEC-HMS model. The resulting flow rates and coastal water levels corresponding to the same return periods were used as inputs to the HEC-RAS model. The steady state analysis was conducted with the hydraulic model, with the coastal TWLs for various return periods applied directly at the downstream boundary of the modelling domain.

Figure 4.6: Modelling domain for the HEC-RAS 1D model for the Waterford River.

4.3.3 Flood Maps

Flood maps for 16 flooding scenarios were developed, with maps showing floodlines for both rainfall and storm surge events. The most severe flooding, however, was noted for rainfall events, specifically for the 2500-year return period event. Extreme coastal water levels at the downstream boundary were found to have limited effects on flooding conditions in the Waterford River. Two sample flood maps are presented in Figure 4.7 and Figure 4.8.

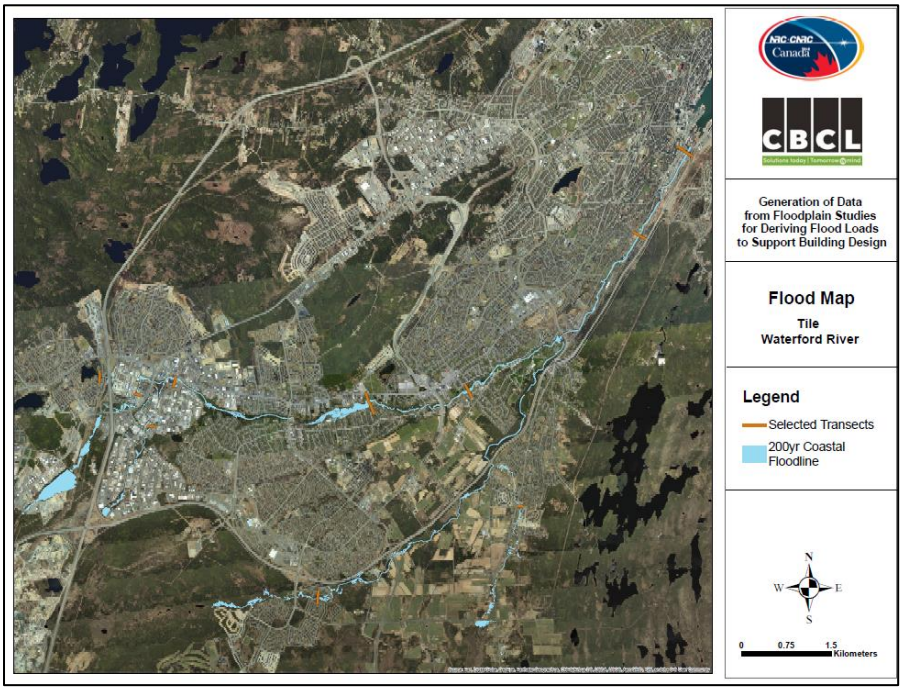

Figure 4.7: Floodplain map corresponding to 200-year coastal conditions for the Waterford River study area.

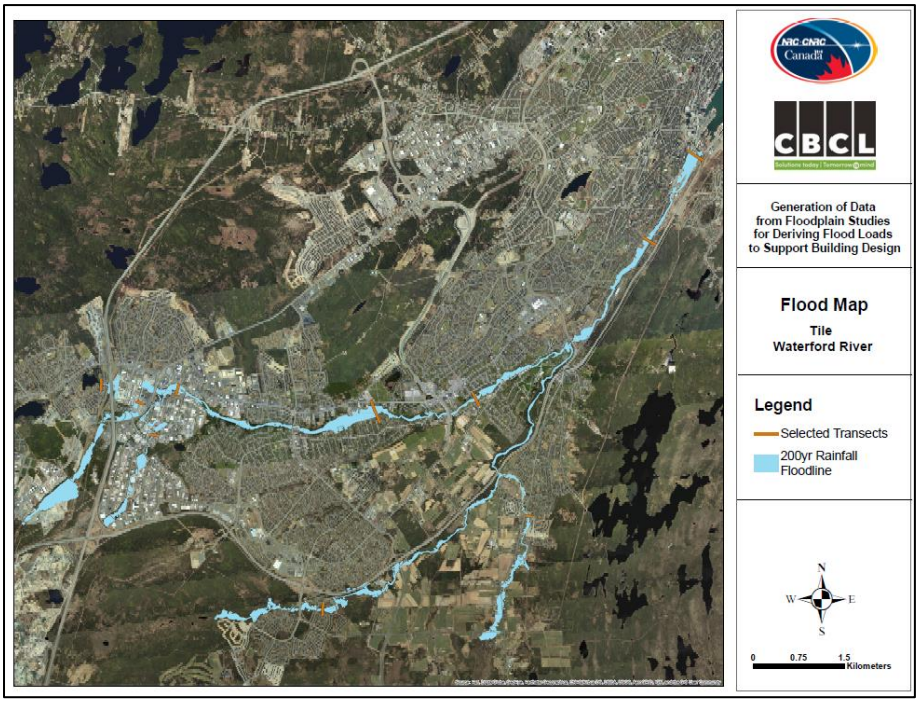

Figure 4.8: Floodplain map corresponding to the 200-year rainfall event for the Waterford River study area.

4.3.4 Data Extraction

Data on flood loading variables was extracted for each transect and save point, and the summary statistics were developed in MS Excel format. In the tables, the transect geometry and water

surface elevation from left to right, looking in the downstream direction, for different flood scenarios, was included. Extracted data from the HEC-RAS model included the cross-sectional elevation, flow areas at all transects, flow magnitude and the average velocity for the entire transect and for each save point, alpha coefficient, the water surface elevations, and the water depths. The topography and water surface elevation for each save point were used for the calculation of flow area.

4.4 Site 3: Mahone Bay

The Town of Mahone Bay, with its scenic coastal zone, is a popular location for residential housing, as well as for commercial and recreational activities. However, this town like many waterfront towns is highly vulnerable to flooding due to storm surges, wave conditions and sea level rise. The original project, which was funded by the Town of Mahone Bay, involved increasing the resilience of the town and its waterfront to the impacts of coastal flooding and climate change. In addition to the detailed modelling of sea levels, waves and river flows, the project also aimed to enhance the waterfront's attraction for residents and tourists. This included creation and restoration of pathways, vistas, and coastal habitat.

An integrated 1D-2D model based on the PCSWMM was developed for this site and used for simulating one-dimensional channel and two-dimensional floodplain flows. For the NRC's study, no modification was made to the already calibrated model, except changing the boundary conditions and using smaller routing time steps. Inputs to the model included synthetic hyetographs of selected rainfall events and coastal water levels for different return periods. The closest available tide gauge was located in Halifax, approximately 50 km away from the site, but was on the same coast. Data from this gauge was considered representative of water levels at Mahone Bay.

4.4.1 Placement of Transects

As shown in Figure 4.9, six transects along the river channel and four perpendicular to the coastline were selected as representative of flooding conditions in this area. These transects were wide enough to include both the river channel and floodplain.

Figure 4.9: Selected transects and river channels for the Mahone Bay study site.

4.4.2 Hydrologic and Hydrodynamic Modelling

For the original study, hydrologic and hydraulic modelling was carried out using the integrated 1D-2D PCSWMM to simulate one-dimensional channel and two-dimensional floodplain flows corresponding to different design flood scenarios. The modelling domain is shown in Figure 4.10. For modelling the hydrologic component of the study, watershed characteristics, including surface slope, overland flow length, surface roughness, imperviousness, and soil characteristics, were determined separately and used as inputs to the hydrologic model. Model calibration was conducted by simulating a recent flood event and comparing the results from the model to the flooding information gathered through meetings with the Town Staff and residents (i.e. by exploiting anecdotal flooding information). In the development of the integrated 1D-2D hydrodynamic model of the river channels that pass through the Town of Mahone Bay, LiDAR data and field measurements of water levels along the river and coastline were used. The 2D river floodplain was connected to the 1D model components (bridges, culverts, river channels, etc.) through orifices. The resolution of the 2D mesh varied from 2.5 m to 10 m based on the land use. Break lines were included in the mesh at roadways to ensure that locations with sharp changes in elevation were modelled with sufficient detail. Outfalls were uniformly distributed along the coastline to simulate the effects of coastal water levels.

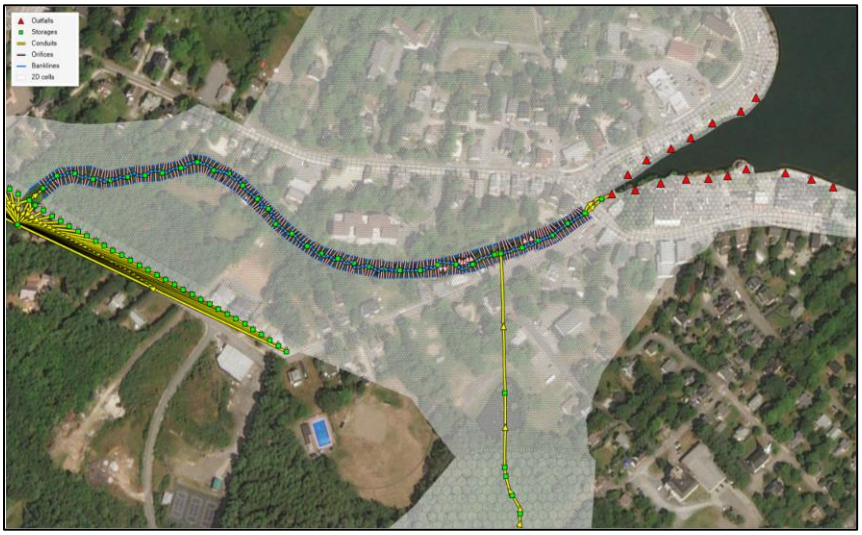

Figure 4.10: PCSWMM modelling domain for the Mahone Bay study site.

For the NRC's project, existing 2D areas were reduced within the river banks of the Ernst Brook, which was then represented as a 1D channel with cross-sections resampled every 10 m along the river channel based on LiDAR data. Existing 2D areas were also extended in the coastal part of the domain to capture areas likely to be flooded during extreme storm surge events. An unsteady analysis was conducted, with 24-hour time series of rainfall amounts and coastal water levels as inputs to the model. Time series of coastal water levels used in the model were in the form of sine waves constructed from the HHWLT, Lower Low Water Large Tide (LLWLT), and TWL for different return periods calculated using the statistical analysis.

4.4.3 Flood Maps

Flood maps for 16 flooding scenarios were developed. These maps show floodlines for rainfall and storm surge events of different return periods. As mentioned earlier, the study area is exposed to both riverine and coastal flooding. However, the most severe flooding along the coastline was observed for the 2500-year storm surge event, while the most severe flooding along the river channel was observed for the rainfall event of 2500-year. Thus, coastal areas were dominated by storm surge related flooding and riverine parts with rainfall related flooding. Two sample flood maps for the study area are shown in Figure 4.11 and Figure 4.12.

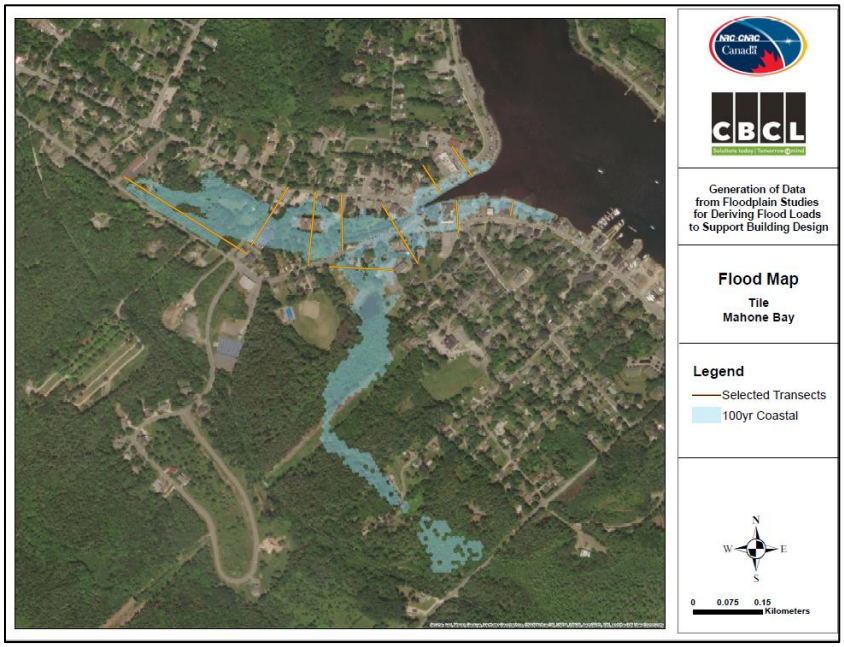

Figure 4.11: Floodplain map corresponding to 100-year coastal conditions for the Mahone Bay study area.

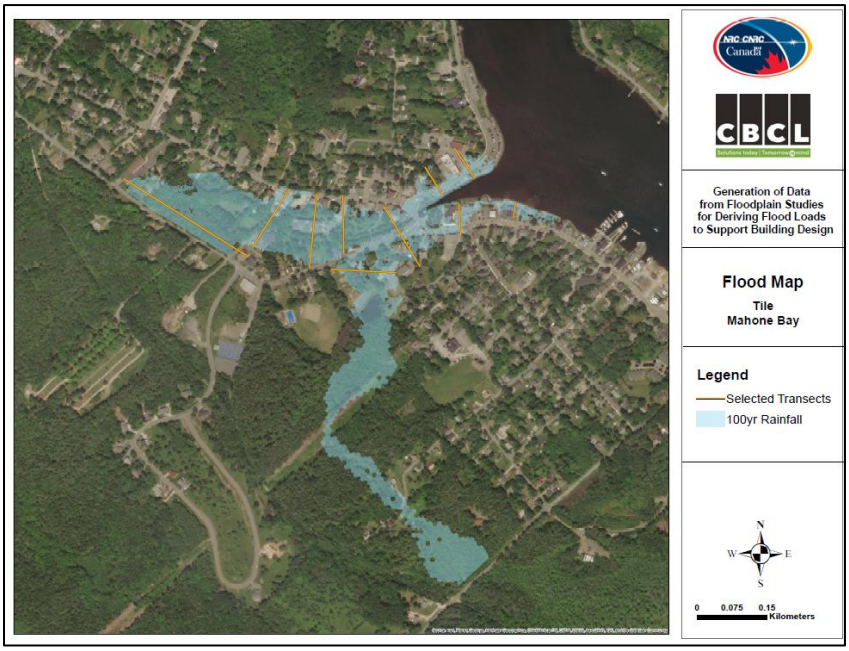

Figure 4.12: Floodplain map corresponding to the 100-year rainfall event for the Mahone Bay study area.

4.4.4 Data Extraction

Data for flood loading variables was extracted for each transect and save point, and the summary statistics were developed in MS Excel format. In the tables, the transect geometry and water surface elevation from left to right, looking in the downstream direction, for different flood scenarios, was described. Extracted data from the PCSWMM modelling results included

topographic elevations, flows at the entire transects, the maximum water surface elevation, the maximum water depth and the maximum velocity for each 1D channel and for each 2D cell. The ground elevations and maximum water surface elevations were used for the calculation of flow areas for each save point and transect.

4.5 Site 4: Saint John

Saint John is located in a very dynamic area, where large tides meet strong river flows. For this location, the study area can be divided into three main sections, i.e. the coastal area near the harbour, the channel area west of Saint John city, and the shoreline located north of the city. In the past, many models have been developed for the Saint John Harbour Authority to investigate currents, water levels and sedimentation around the Port of Saint John. The harbour area is partially sheltered from prevailing waves from the south and southeast. The marine physical environment of the Saint John harbour is very complex and dynamic, and therefore presents challenges and requires advanced modelling methodologies and numerical models. Key parameters such as water level, water density and flow velocities are highly variable in time and space due to the interaction of very large tides with strong freshwater inflow from the Saint John River. According to the provincial flood database, historic records indicate that the Saint John River has been subject to flooding on ten different occasions since 1962. In Saint John, flood stage is generally reached when water levels exceed 4.2 m. Before the flood of 2018, the two largest water levels were noted for the floods of 1973 (5.31 m) and 2008 (5.20 m).

As mentioned above, a unique characteristic of the Saint John harbour is that the large tides are being countered by strong river flows. The river discharges in the harbour across an upstream sill and then through a narrow rock gorge which is approximately 100 m wide at its narrowest point. The sill and passage through the constriction, known as the Reversing Falls, only allows a relatively small volume of water to discharge in and out over a tidal cycle. This hydraulic control allows a significant difference in the water levels to build up on either side of the constriction, creating locally strong currents alternating in direction. Currents flow in the seaward direction when the river level is higher than the tide level, and in the reverse direction when the tide level is higher than the river level.

4.5.1 Placement of Transects

Eleven different transects were selected to represent hydrodynamic conditions of the study area (see Figure 4.11). Transects 1 through 6 were in the north of Saint John, transect 7 was placed on the west side of Saint John, transects 9 and 10 were on the harbour side of Saint John, and the final transect 11 was placed upstream of the Reversing Falls. Each transect was divided into save points to represent the water surface elevation and depth averaged currents along a transect. Due to the perpendicular nature of transects to the coastline and also due to the nature of coastal flooding, some save points will remain dry for many flooding scenarios. Therefore, in order to ensure a minimum of 11 save points for data extraction, a total of 21 save points were considered

to maximize the potential of generating sufficient usable data to drive flood loads calculations. All transects were defined sufficiently wide to include both river channel/harbour channel and floodplain/shoreline.

4.5.2 Hydrodynamic Modelling

The Danish Hydraulic Institute's (DHI) three-dimensional MIKE3 model was used to evaluate flow patterns and water levels at the site. The modelling domain for the area of interest is shown in Figure 4.13. As shown in the figure, finer meshing covers areas that are prone to flooding or areas with steep bathymetric gradients where mesh resolution is important to adequately reproduce physical processes.

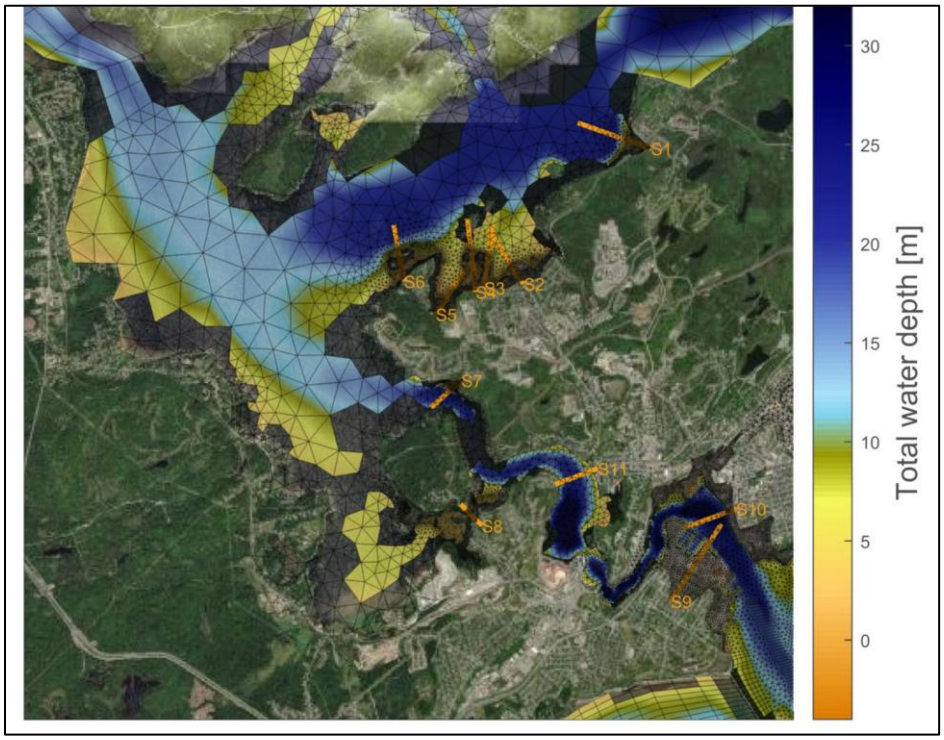

Figure 4.13: Computational mesh (shown in black), defined transects (S1 to S11; shown in orange) and total water depth as schematized in the hydrodynamic and wave model (color scale).

Water level observations at Oakpoint (Environment Canada river gauge) and Saint John harbour (DFO tide gauge) were used as upstream and downstream boundary conditions, respectively. In addition, discharge values at the Kennebecasis River were studied to better understand freshwater forcings and dynamic behaviour of water levels in the study area. The water level variation is well represented for different areas, showing amplification upstream near Oakpoint and some reduction closer to the mouth of the Saint John River. The hydrodynamic regime was well reproduced, with a strong surface ebb current peaking at low tide and a well-defined flood induced current. Strong currents occurred in the main channel immediately outside the entrance of the harbour.

4.5.3 Wave Modelling

For coastal areas, including the Saint John harbour, the MIKE21 Spectral Wave (MIKE21SW) model from DHI was used in fully spectral mode with a quasi-stationary time-domain approach (i.e. steady state). The model was run to evaluate extreme conditions under selected return period scenarios.

Within river areas, the Bretschneider wind-wave growth formulation was used. This formulation took into account the wind speed, the fetch length and the average water depth over the corresponding fetch. Regional model boundary conditions were derived from the MSC50 offshore wind and wave hindcast data. The results of wave modelling in terms of wave characteristics were summarized for north, west and southeast directions for 10-, 20-, 50-, 100-, 200-, 500-, 1000-, and 2500-year return periods.

The interdependency of wave extremes and water level extremes was not considered in this study. Instead, CBCL considered the extremes as independent events. The wave model was used to extract wave parameters at each of the defined transects, from which runup heights were determined using schematized profiles.

4.5.4 Wave Runup Modelling

Based on the nearshore wave conditions, obtained from wave modelling, the estimated runup height was calculated using the XBeach numerical model (Smit et al., 2010; Roelvink et al., 2015). XBeach is a powerful open-source numerical wave model that includes the following hydrodynamic processes: (1) short wave transformation (refraction, shoaling and breaking); long wave (infragravity wave) transformation (generation, propagation and dissipation); wave-induced setup and unsteady currents; and short and long wave runup.

The original XBeach model, with funding from the US Army Corps of Engineers, was developed to assess hurricane impacts on sandy beaches. Since then, the model has been extended, applied and validated for storm impacts on urbanized coastal regions for flood risk assessments, and the non-hydrostatic version of the model has been validated with laboratory experiments and field measurements to estimate overtopping. For this study, the 1D non-hydrostatic version was forced with the nearshore output from MIKE21SW model to calculate wave propagation and wave runup. The XBeach model was developed for three representative shore perpendicular transects with a cross-shore spatial resolution of about 1 m.

4.5.5 Flood Maps

Flood maps for16 different flooding scenarios were developed and Figure 4.14, Figure 4.15 and Figure 4.16 show sample outputs from models. Figure 4.14 shows bed level (black solid line), the maximum surface elevation (blue dashed line) and the maximum depth averaged current speed for each save point (colour bar). The plot shows the results for a combination of a 2-year event on the Saint John River side and a 2-year water level on the Saint John harbour side. When

the profiles were dry, no data was included in the plots. Figure 4.15 shows the maximum water surface elevation, when the peak water from Oakpoint coincides with the peak water level at the Saint John harbour. All elevations are in metres and referenced to CGVD28. Figure 4.16 shows the current speed for the time step when peak water levels coincide.

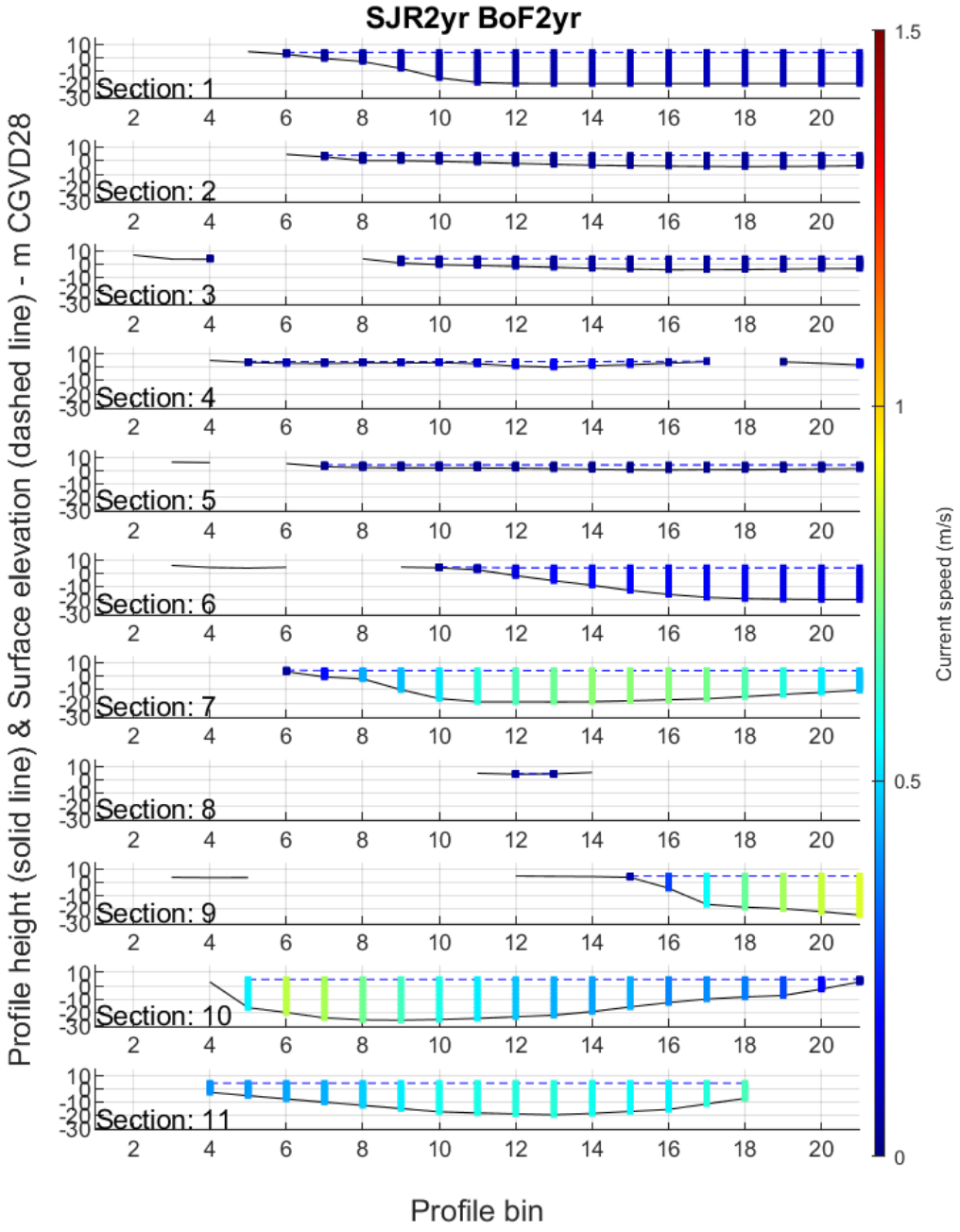

Figure 4.14: Bed level (black solid line), maximum water surface elevation (blue dashed line) and maximum current speed (color bar) for each save point (x-axis) and all the 11 transects (graphic panels 1 through 11) for the Saint John study site. SJR2yrBoF2yr reflects 2-year event on the Saint John River side and a 2-year water level on the Saint John harbour side.

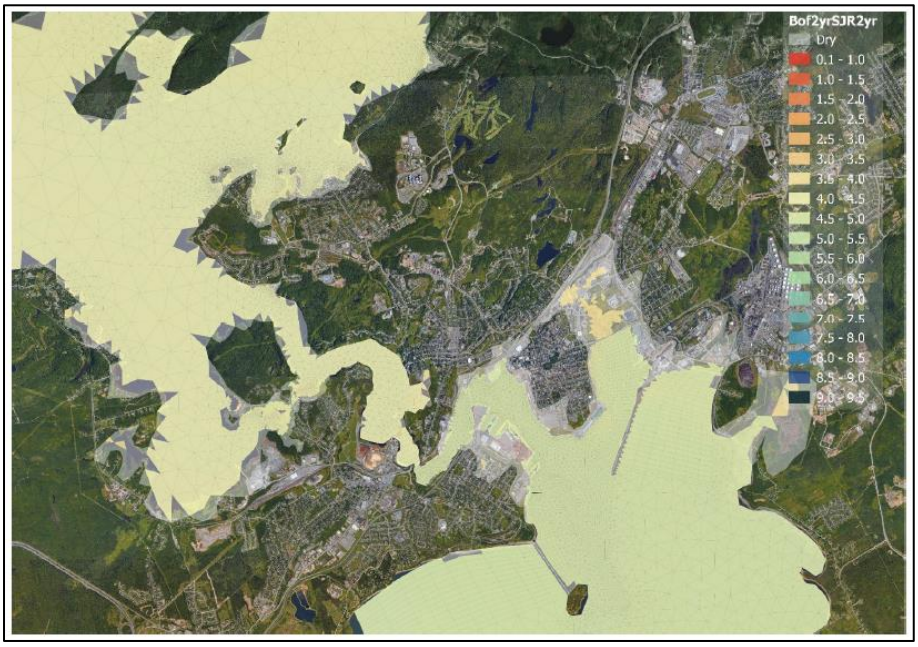

Figure 4.15: Surface elevation map corresponding to the 2-year storms for the Saint John River and the Bay of Fundy.

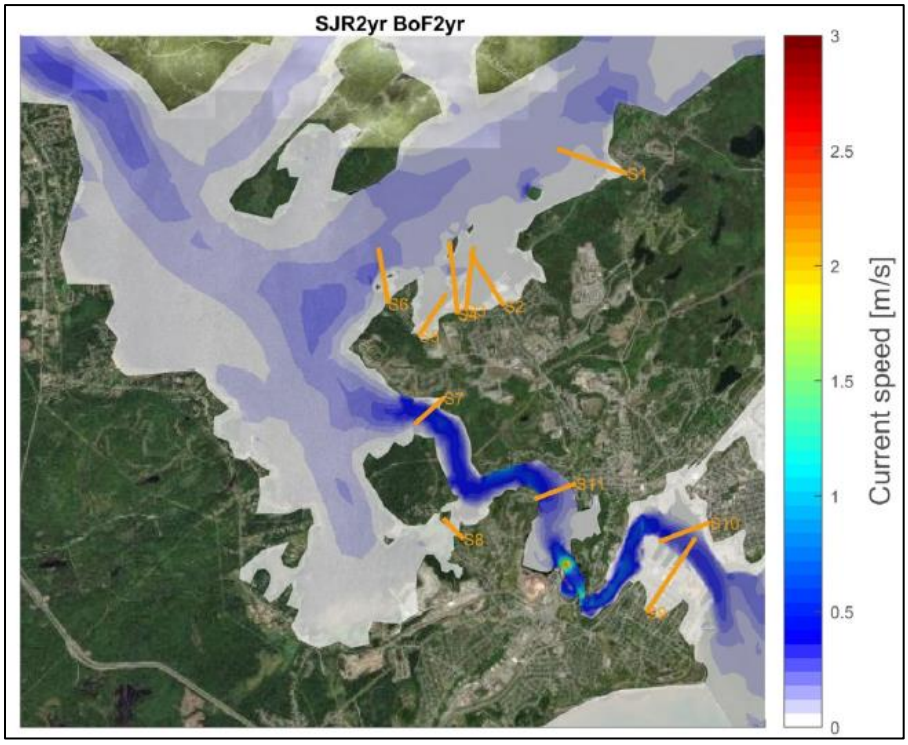

Figure 4.16: Current speed map corresponding to the 2-year storm for the Saint John River and the Bay of Fundy.

4.5.6 Data Extraction

Data extracted for each transect and save point, and summary statistics were prepared in MS Excel format and delivered to the NRC. Some information about the data extracted and variable names are presented below:

- Bank Elevation for save points was manually defined based on the transect shape.
- Water Level reflects the modelled water level for each save point at the peak of the simulated events.
- Flood Velocity represents the depth averaged flow velocity at the time of the peak water level of the simulated events.
- Flood Wave (from channel banks) represents the difference between the mean of the maximum water level per transect minus the defined bank elevation.
- Wave run-up (pertains to wind generated waves).
- Flow velocities can vary depending on the tidal cycle and river discharge, and are stronger at other moments that do not coincide with the maximum water level (e.g. max ebb/flood).

4.5.7 Concluding Discussion

The four case studies discussed above were conducted by CBCL for locations where adequate hydrologic, hydraulic and coastal analyses and associated models already existed. In certain cases, adjustments were also made to accommodate requirements of flood loads data generation case studies to support NRC's flood-resistant design of buildings initiative. These adjustments included changing mesh resolutions, bathymetry, as well as extending the cross-sections and extents of 2D meshes, to capture the range of extreme events considered. The events modelled considered flooding under rainfall and storm surge conditions, for return periods of 10, 20, 50, 100, 200, 500, 1000, and 2500 years. Statistical analyses were conducted to obtain return values for each of the return periods, noted above, for rainfall, coastal water levels, winds, and wave heights. Joint probability analyses of rainfall and coastal water levels were not considered.

The flooding processes for the selected four sites can be summarized as follows:

- Truro, Nova Scotia: Flooding in this area is influenced by extreme tides from the Bay of Fundy, sediment accumulation and ice jams, and is also somewhat dominated by extreme rainfall events. The urban areas, concentrated within the floodplains, are very vulnerable to flooding.
- Waterford River, Newfoundland: The Waterford River is an urban river in the centre of St. John's. Flooding in the Waterford River occurs as a result of extreme rainfall events, and encroachments due to developments within the floodplain.
- Mahone Bay, Nova Scotia: Mahone Bay is a touristic destination in Nova Scotia that faces the Atlantic Ocean. Its picturesque setting is threatened by increasing risks of flooding from tides, waves, storm surges, and also due to extreme rainfall events.

- Saint John, New Brunswick: In this area flooding is mainly driven by: (1) coastal storm surge for the inner harbour downstream of the Reversing Falls, and (2) extreme river levels associated with precipitation, snow melt and runoff for the estuary upstream of the Reversing Falls. The Reversing Falls act as a hydraulic control point which separates the region into two areas, with distinct flooding regimes.

Although the format of data generated from these case studies varies with respect to the models used, i.e. PCSWMM, HEC-RAS 1D, and MIKE3, efforts were made to convert the generated data into a consistent format to be used for flood load calculations.

5 British Columbia – Coastal Flooding Case Studies

5.1 General

Northwest Hydraulic Consultants Ltd. (NHC), Vancouver were contracted to undertake coastal flood modelling and flood loads data generation case studies in British Columbia. Two representative coastal flood modelling studies were selected where most of the required supporting datasets and calibrated modelling tools were already available. These datasets included: bathymetry data, LiDAR data that extends into the intertidal zone, tidal elevations, storm data, and offshore (or deep-water) sea state conditions of wave heights, direction, and period. The first study was completed for the City of Vancouver and the second for the City of Surrey.

By selecting these case studies, where previous detailed studies already existed, considerable efficiencies were realized as much of the background data sources were already compiled and the models were already set up. There were also considerable gains in terms of data pre-processing and modelling experiences. However, NHC extended the original studies to satisfy the requirements of flood loads data generation initiative of the NRC. In doing so, NHC also obtained appropriate permissions from the municipal governments for sharing of data and modelling results. Highlights from both case studies are presented below one after the other. The information provided here is derived from the case studies reports, completed by NHC (i.e. NHC, 2021c, 2021d).

5.2 Case Study 1

5.2.1 Project Area and Representative Transects

The City of Vancouver (the City) is a coastal, seaport city on the mainland of British Columbia. Located on the western half of the Burrard Peninsula, Vancouver is bounded to the north by English Bay and the Burrard Inlet and to the south by the Fraser River. The City's coastal shoreline can be divided into four coastal zones (see Figure 5.1) based on the prevailing coastal and shoreline conditions.

Since Zone 4 is relatively sheltered from offshore waves, Zones 1, 2 and 3 were selected for this case study. Figure 5.2 shows representative transects identified for the study. Each transect was further divided into 11 save points where characteristic parameters for flood load calculations were assembled.

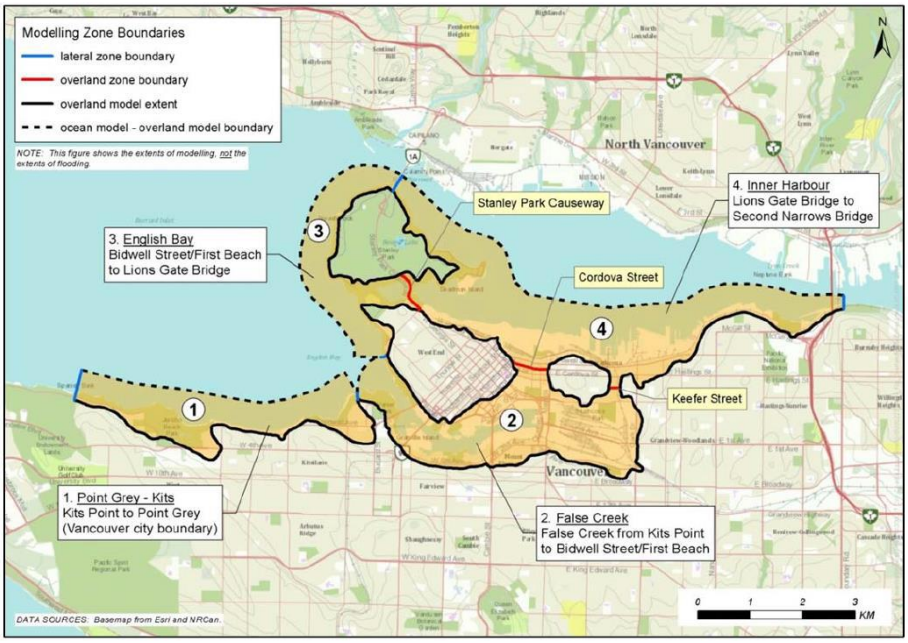

Figure 5.1: City of Vancouver flood modelling zones in Burrard inlet.

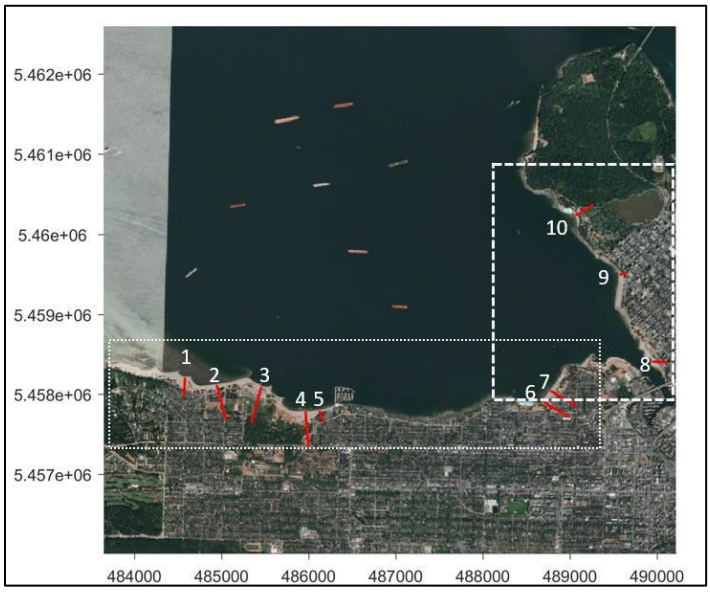

Figure 5.2: Modelling domain with sub-grid extents (white dashed lines) and selected transect locations (red lines).

5.2.2 Overview of Design Event Estimation

In the original study, completed by NHC for the City of Vancouver, the joint probability of individual designated flood level (DFL) components (i.e. storm surge, tide, waves, and wind setup) was assessed using a long term continuous coastal simulation for the 1963–2012 period, and carrying out an extreme value analysis to determine the DFL for several specified events corresponding to 1-in-200 through 1-in-10,000 year return periods. Sea level rise was also

considered prior to conducting model simulations. For this study, the DFL was defined as the sum of tide, surge, wind setup, wave setup, sea level rise, and local uplift/subsidence.

With the future sea level rise (SLR) scenarios considered, part of the City was expected to be inundated, making a wave effect metric based on the wave amplitude more appropriate for the site. However, given the significant variations in wave amplitude that can occur in shallow water, it was important to model wave propagation on land. Water levels for the wave model were set to the maximum elevation calculated by the overland flood model for each return period. Design wind conditions, determined from the wind analysis, were applied over the modelling domain to simulate the wind-generated component of the waves in the model.

5.2.3 Design Flood Scenarios

This case study specifically focuses on areas where overland flooding is expected and where waves could reach structures and other elements. The Higher High Water Large Tide (HHWLT) at Point Atkinson, which is located at the entrance to Burrard Inlet, was found to be 1.9 m CGVD28; the CGVD28 was used in this study unless otherwise stated; the HHWLT was defined as the average of the highest high water levels, one from each of the 19 years of predictions. Most of the land along the City's shoreline is situated above 3 m and, based on the original analyses, only a small area along the City's shoreline was expected to be inundated under present day conditions. Therefore, the corresponding results were of limited use for calculating flood loads. Due to this reason, flood scenarios from the original study with consideration of future SLR to the year 2100 were considered for this study.

An important element in any coastal flood analysis is establishing appropriate wind and wave effects for DFLs associated with the selected return periods. For the purposes of the original study, the wind-generated wave conditions were selected by conducting an extreme value analysis of wind data at Point Atkinson and constructing variable wind fields based on representative magnitudes. Wind magnitudes were determined for a variety of events corresponding to various return periods ranging from 1 to 2,500 years and modelled along with the designated flood elevation, which provided some level of sensitivity in flood load statistics due to considering different wind events. Flood scenarios were developed considering 1.0 m SLR, 500-year return period DFL and 10 different wind conditions corresponding to 1-, 5-, 10-, 20-, 50-, 100-, 200-, 500-, 1000-, and 2500-year return periods (Table 5.1).

Table 5.1: Flood scenarios for the City of Vancouver case study.

Scenario	SLR (m)	DFL return period (years)	Wind condition return period (years)	
1	1.0	500	1	
2	1.0	500	5	
3	1.0	500	10	
4	1.0	500	20	
5	1.0	500	50	
6	1.0	500	100	
7	1.0	500	200	
8	1.0	500	500	
9	1.0	500	1000	
10	1.0	500	2500	

5.2.4 Project Area and Representative Transects

The modelling results for a selected scenario for Zone 1 are shown in Figure 5.3 and those for Zones 2-3 are shown in Figure 5.4. In these figures, wave height is shown by colour shading and wave direction and relative heights are shown by vectors.

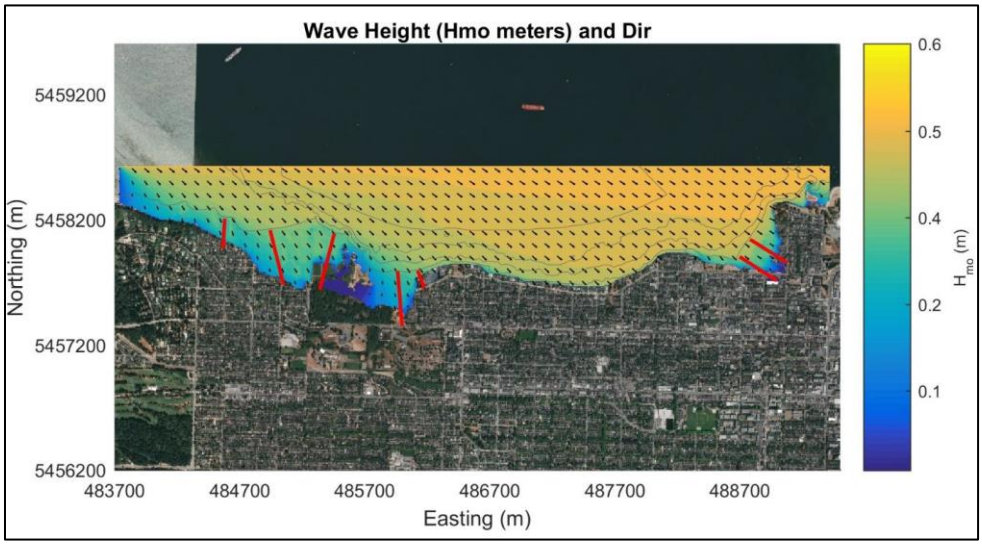

Figure 5.3: Wave modelling results for Zone 1, considering Scenario 3 (1.0 m SLR; 500-year DFL; and 10-year wind conditions) for transects 1 through 7.

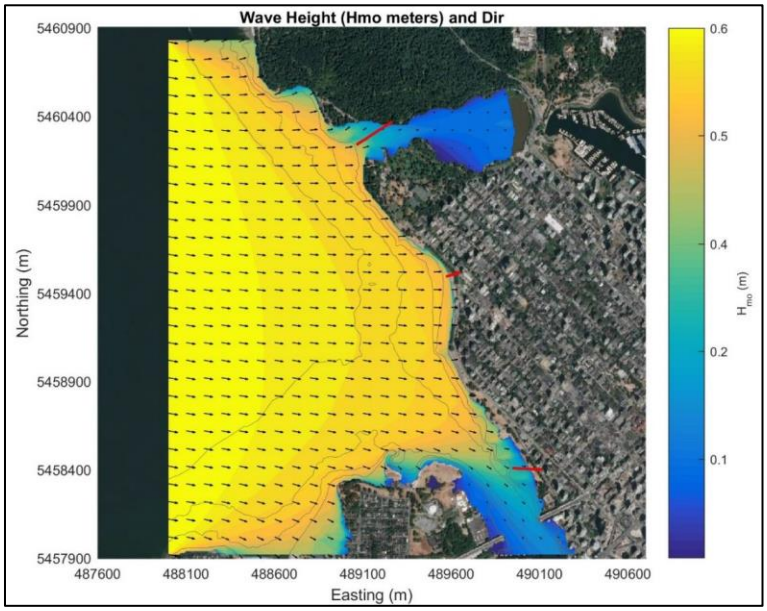

Figure 5.4: Wave modelling results for Zones 2-3, considering Scenario 3 (i.e. 1.0 m SLR; 500-year DFL; and 10-year wind conditions) for transects 8 through 10.

5.2.5 Flood Characteristics and Flood Loading Variables

Flood loading variables were extracted from the modelling results for all flood scenarios, considered in the study. Relevant information was extracted for each transect and for each individual panel (save point) along a given transect.

Transect Characteristics

- Transect location (latitude and longitude);
- Mean sea level used;
- Tidal conditions/elevation considered;
- Still water level for transect (with storm surge effect but without wave setup effects);
- Wave runup limit for the transect;
- Ground elevation for the transect (lowest, highest and the elevation at set distances landwards from the present day natural boundary from a common datum);
- Maximum water level and depth along each transect; and
- Maximum landward depth of water and averaged velocity at the natural boundary and landward locations.

Panel (Save Point) Characteristics

The following characteristics were extracted from the modelling outputs for each flood scenario at the evenly spaced save point locations along the transect. Save point zero was taken at the origin of the transect, with save point numbers increasing in a landward direction. Characteristics

for each save point were derived from the geometry and hydraulic properties of the associated panel.

- Northing and Easting of the mid-point of each panel, denoted as the save point;
- Ground elevation;
- Local water level;
- Local flood/water depth;
- Local wave height and period; and
- Current velocity.

For each save point, several parameters were recorded and those included easting, northing, distance along the transect, bottom elevation, water depth, wave height, mean wave period, peak wave direction, orbital wave velocity, and wave-induced force per surface area (see Figure 5.5). The data was assembled in MS Excel spreadsheet format and delivered to the NRC.

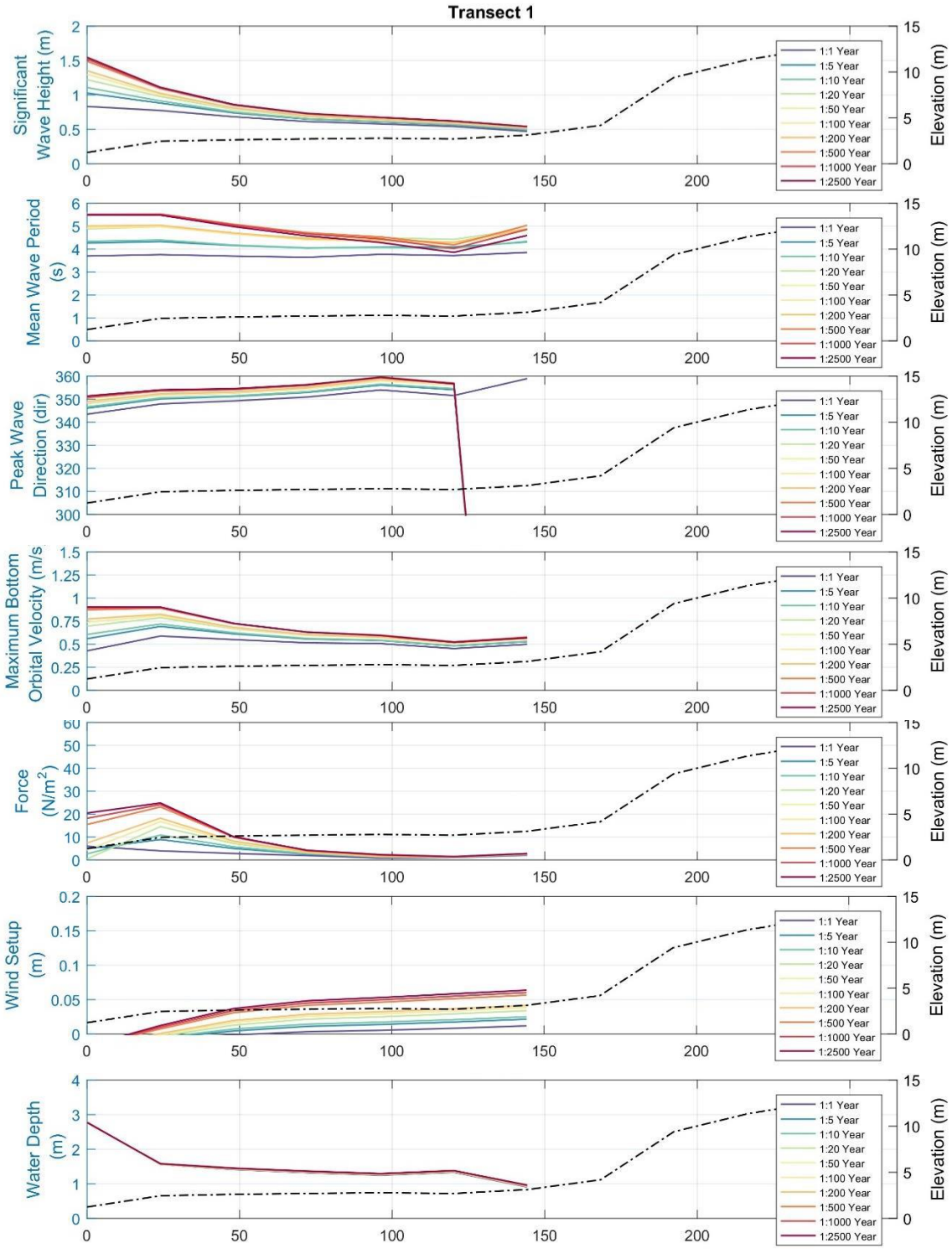

Figure 5.5: Wave and other relevant parameters at save points along transect 1 for Zone 1.

5.2.6 Flood Load Statistics

Summary statistics (i.e. mean and standard deviation) of flood loading variables (e.g. local flood depth, maximum velocity and wave height) at each save point was calculated for scenarios with 1.0 m SLR and a 1-in-500 year design still water level. A large sample of estimated values of each parameter were assembled for Zone 1 and Zones 2-3 for calculating overall statistics.

5.2.7 Concluding Discussion

The nature of coastal flooding is notably different from river flooding in several ways. Coastal flood risk involves both direct flooding of upland areas for short periods of time as well as exposure to waves. Some insights on coastal flooding mechanisms are discussed below.

Shoreline Flooding:

The tidal influence on the coasts causes a large change in the shoreline water levels of several metres twice each day and as a result any coastal flooding due to combinations of high tides and storm surge (atmospheric forcing) is relatively short lived with peak water levels only lasting for one to two hours before the falling tide occurs and the coastal flooding recedes. Storm surge refers to an increase in the ocean levels due to low atmospheric pressure. Perhaps the most famous examples of storms generating high surge levels are Hurricanes and Typhoons, but any large area of low pressure over an ocean will generate some degree of storm surge. High pressure systems can also lead to the opposite effect which is sometimes referred to as negative storm surge.

Along the Pacific Coast of Canada and within the Strait of Georgia, storm surge levels of between 0.1 and 0.5 m occur frequently each year. Statistical analysis of historical storm surge suggests an annual expected maximum storm surge of 0.7 m for the Strait of Georgia, while the 100-year return period storm surge level is about 1.2 m (NHC, 2021c). Storm surges typically last for several days in association with large weather fronts, but peak only for a period of 3 to 6 hours. For this reason, the peak storm surges do not always coincide with the timing of high tides and a large storm surge that occurs during a low tide period will go largely unnoticed by property owners on shorelines. Conversely, a large storm surge that is coincident with a large tide can result in shoreline flooding of low lying areas.

SLR is a long-term process and is believed to be a consequence of climate change. There is no doubt that SLR is occurring as it is being directly measured, with a global rate varying between 3 and 4 mm per year. There is also a general scientific consensus that the annual rate of SLR will increase in the future. However, there is deep uncertainty around the timing of SLR and when certain levels of SLR (such as 1 m or 2 m) will occur. This is partly due to the fact that future policy decisions and behaviours by humans will affect the severity of future climate change and hence the future rates of SLR.

The above mentioned phenomena have direct implications for the future flood levels in coastal regions. What is an extreme total water level at the shoreline today will eventually, with sufficient SLR, become a daily high tide level. With additional SLR, this level may eventually become a frequently occurring mechanism during the daily tide cycle. One can also argue that, given high levels of uncertainties in the timing of future SLR, it is difficult to place high confidence in predictions of future flood levels in coastal regions.

Wave Exposure:

Coastal shorelines may be exposed to large waves that are generated in deep water during wind storms. During a coastal flood event, the nature of wave forces striking shoreline structures is fundamentally different than hydraulic forces from moving water due to river currents. Wave forces are cyclical and non-uniform. Waves break in different ways depending upon the nature of the shoreline; steep shorelines can produce plunging waves while more gently sloping shorelines create spilling waves. As larger waves approach a shoreline they become depth limited and break, with different sized waves breaking at different distances from the shore depending on depth (the surf zone). For a coastal flood situation in which an upland area is temporarily flooded under shallow water the larger waves break on submerged beaches and smaller waves or bores propagate landward across the flooded areas. Vegetation and coastal structures serve to dissipate the wave energy.

The data generated in this study are representative of a variety of coastal areas in the City of Vancouver. The numerical model that was setup for the analysis provided outputs on the significant wave height and spectral mean wave period along each transect, as well as the maximum wave orbital velocity and net horizontal force induced from the waves at each location. Coastal flood studies do not typically consider flow velocity from flooding alone as the overland currents tend to be weak compared to tidal currents in deeper waters offshore and the velocity of wave bores.

5.3 Case Study 2

5.3.1 Project Area and Representative Transects

The City of Surrey (the City) is a coastal city on the mainland of British Columbia, located to the south of the City of Vancouver. The City is bounded to the south and west by the Strait of Georgia, and to the north by the Fraser River. Two major rivers create a floodplain (denoted here Zone 1 and Zone 2) located within the low lying areas within the bounds of the City that slowly meander towards the Strait of Georgia. The City’s coastal shoreline can be divided into five general coastal zones based on the prevailing coastal, riverine and shoreline conditions (Figure 5.6).

Figure 5.6. City of Surrey coastal zones (Zone 1 to Zone 5). Zone 1 and Zone 2 are impacted by river flows.

Representative transects were selected from Zones 1, 2 and 3 for this study. Figure 5.7 shows the project area and the representative transects. Each transect was then further divided into 11 save points where characteristic parameters were reported.

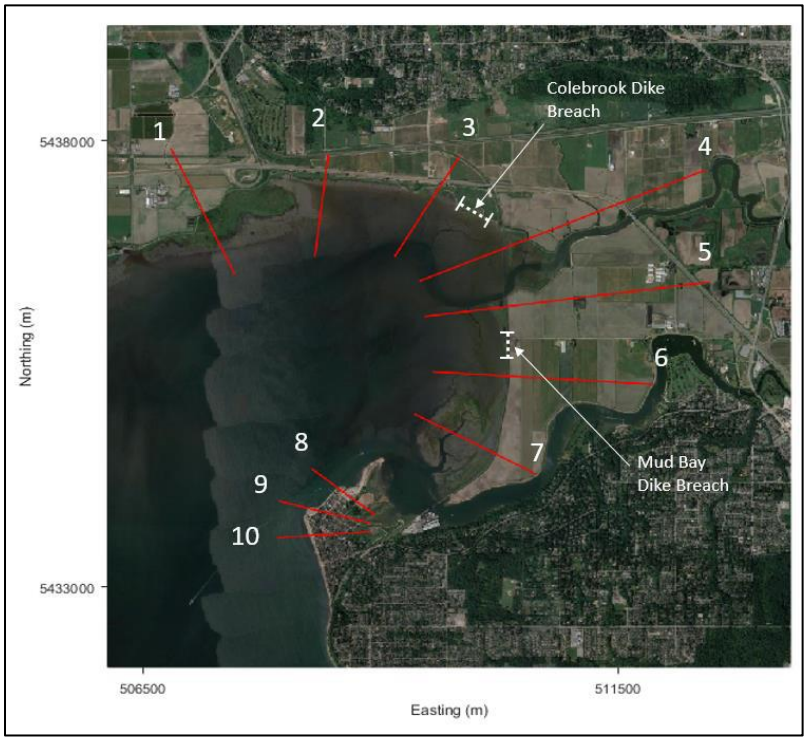

Figure 5.7: Representative transect locations (red lines) for the City of Surrey case study.

5.3.2 Overview of Previously Completed Studies

Inundation of the Serpentine/Nicomekl River floodplain is a complex function of rainfall, sea level and hydraulic response of the watersheds to the hydrologic inputs and sea level. In the previously completed study (NHC, 2015), a long term continuous simulation of sea levels and rainfall for the 1963–2012 period was used and the simulated annual peak water levels were subjected to conventional frequency analysis to determine the designated food level (DFL).

The Phase 1 of the climate change floodplain review (CCFR) study that was completed by NHC in 2012 (NHC, 2012) developed a scientifically defensible modelling approach to characterize flood hazards under sea level rise and undertook a preliminary assessment of infrastructure vulnerability and flood risk from ocean and riverine sources. Following this, Phase 2 of the CCFR study (NHC, 2015) refined and expanded on Phase 1 and incorporated climate change impacts on precipitation and updated subsidence estimates. In addition to the base year 2010 and year 2100, the modelling was also extended to include year 2020, 2040, 2070 and 2200. Floodplain extents corresponding to estimated 200-year flood levels were evaluated for all modelling scenarios and preliminary vulnerability assessments were completed. Based on 2-dimensional modelling, water depths and flow velocities caused by select dike breaches were simulated.

The return period of total water levels corresponding to the dike crest elevations (DCE), as currently constructed, were calculated for nine coastal locations in the project area for current 2010 conditions and for the relative sea level rise conditions associated with the year 2020, 2040, 2070 and 2100. Provincial guidelines recommended a 1 m rise in sea level between 2010 and 2100 and assumed a linear rate of rise during this period (Ausenco Sandwell, 2011) and the same projections were used in this study. The total water level was calculated as the sum of relative sea level rise (RSLR), DFL and wave effect and the result was considered equivalent to a predicted future DCE without adding any freeboard allowance (NHC, 2015).

For each location and the target year, the RSLR and wave effects were used to adjust the distribution describing the relationship between water levels and return periods. The adjusted distribution was then used to estimate the return period associated with the current elevation of the dike. The estimated return periods of total water levels associated with the current DCEs are given in Table 5.2.

Table 5.2 shows that most of the City’s coastal dikes currently provide inadequate protection against flooding due to overtopping and breaching (NHC, 2015). As water levels will increase due to sea level rise, conditions are expected to continuously worsen overtime. For 2010 conditions, the return period ranges from 2 to 350 years, with only two of the dikes meeting 200-year ocean level standards. At present conditions, breaches could potentially result in some loss of life and extensive damage, whereas future breaches would be catastrophic with flood depths reaching over 3 m in some locations. Additional analysis was also performed and it was found

that the results are sensitive to the selected breach locations or their combinations, adopted parameters and water levels.

Table 5.2: Total water level return periods (in years) associated with the current DCE for selected years from 2010 to 2100.

Site	Location	DCE (m)	2010	2020	2040	2070	2100
1	Colebrook – Serpentine	2.84	22	8	2	<1	<1
2	Crescent Beach East	2.88	220	70	7	<1	<1
3	Mud Bay – Serpentine	3.00	28	11	2	<1	<1
4	Mud Bay – Nicomekl	2.98	350	110	10	<1	<1
5	Colebrook (Highway 99)	3.15	22	10	2	<1	<1
6	Crescent Beach North	2.90	2	1	<1	<1	<1
7	Crescent Beach South	3.30	70	22	3	<1	<1
8	BNSF Railway	3.20	7	3	<1	<1	<1
9	8th Avenue at Campbell	2.30	4	1	<1	<1	<1

5.3.3 Model Design Scenarios

NHC conducted a re-analysis of modelling results from the CCFR Phase 2 study (NHC, 2015), and extended where necessary, to generate information on flood loading variables along select transects arising from various combinations of water levels and wave forces.

Breach Events

For coastal dike failures, two breaches were modelled at the sea dike, one on the Colebrook Dike north of the mouth of the Serpentine River and another on the Mud Bay Dike between the mouths of the Serpentine River and Nicomekl River. The modelling was performed with tidal boundary conditions for a storm with a peak water level corresponding to the 10-year and 100-year joint probabilities. The 2D hydrodynamic model simulated the spill of water through the breaches and subsequently inundation across the floodplain over several tidal cycles.

For this study, hydraulic information (water depth and currents) from two model “snapshots” or model time steps were extracted from the breach modelling results and used as input for the wave model development. The first snapshot was obtained at the time step shortly after the breach occurred with high velocity flow going through the breach. The second snapshot was obtained couple of hours after the breach when the area behind the dike experienced the largest inundation.

Wind

An important element in coastal flood analysis is to establish appropriate wind and wave effects for each DFL. For the original study, the wind-generated wave conditions were selected by examining the significant wave height concurrent to large tidal residual events in the hindcast

simulation. This approach was selected in order to ensure that the assigned probability from each DFL return period remained the same. Additional scenarios, which considered less frequently occurring wind events coinciding with the DFL, were created to show the sensitivity of flood loads statistics due to altering wind events. The wind scenarios considered are summarized in Table 5.3. A total of 40 model simulations were completed, considering 2010 and 2100 breach scenarios, maximum velocity and maximum inundation, and all 10 wind scenarios.

Table 5.3: Wind scenarios corresponding to 10 selected return periods.

Model scenario	Return period (years)	Wind speed (km/h)	Wind direction (degrees)
1	1	65	202.5
2	5	71	202.5
3	10	76	202.5
4	20	80	202.5
5	50	83	202.5
6	100	88	202.5
7	200	91	202.5
8	500	95	202.5
9	1000	99	202.5
10	2500	103	202.5

Significant wave heights for the two breach events occurred when the maximum velocity and maximum inundation were observed. This can be seen in Figure 5.8, Figure 5.9, Figure 5.10, and Figure 5.11.

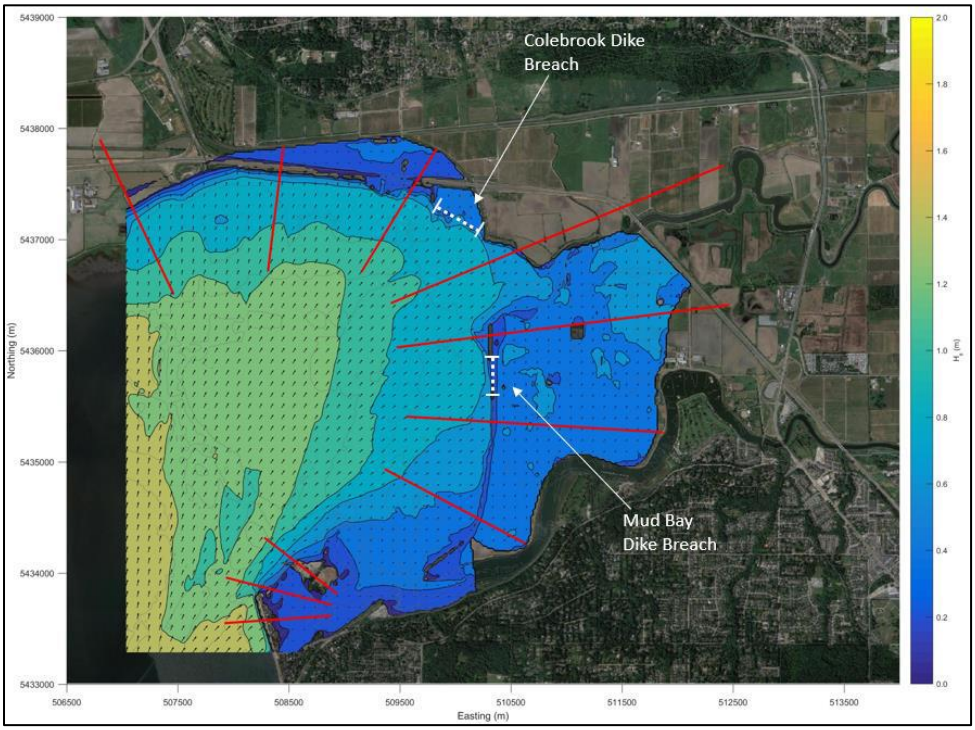

Figure 5.8: Wave modelling results of significant wave height for the 2010 breach event during maximum velocity for the 100-year wind speed. Black vectors represent wave direction, red lines represent transects, and white dashed lines represent breach event locations.

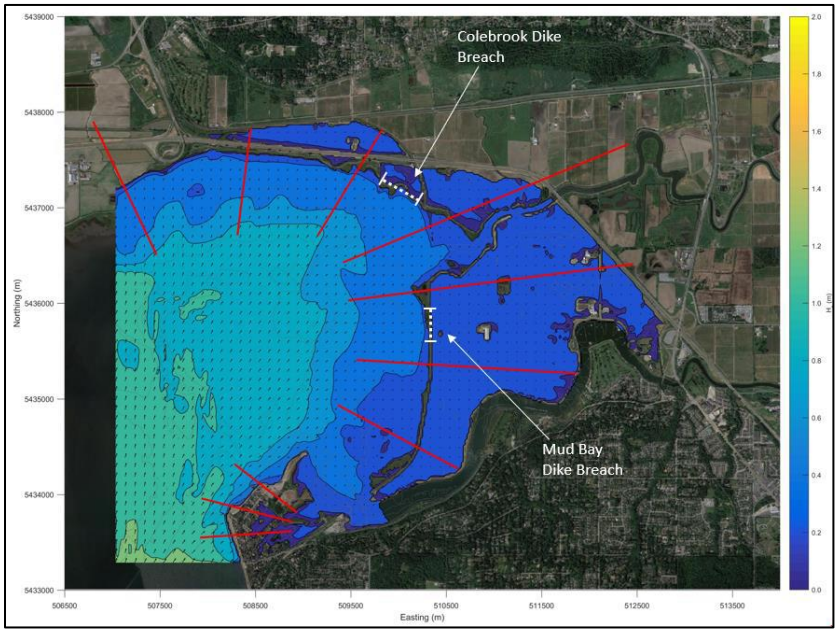

Figure 5.9: Wave modelling results of significant wave height for the 2010 breach event during maximum inundation for the 100-year wind speed. Black vectors represent wave direction, red lines represent transects, and white dashed lines represent breach event locations.

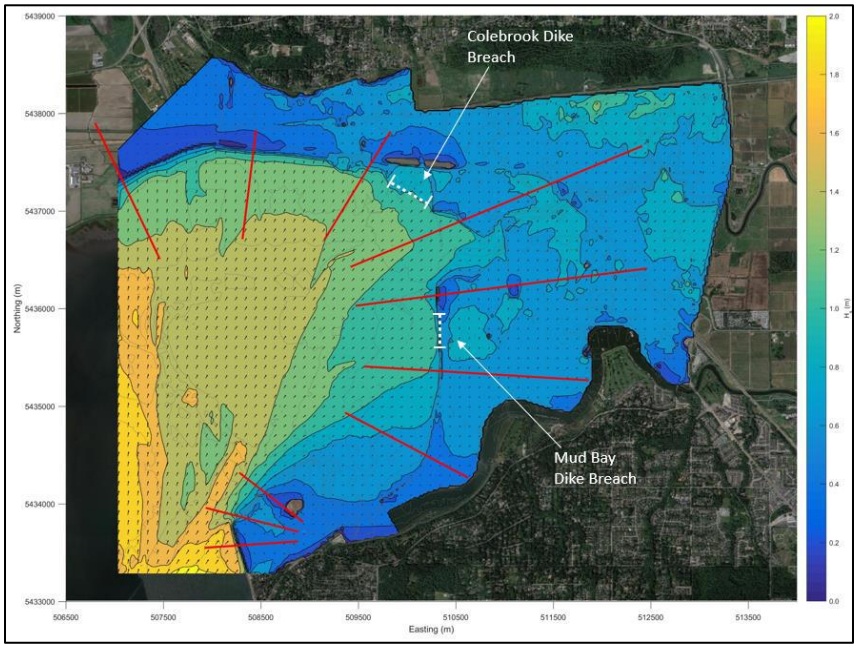

Figure 5.10: Wave modelling results of significant wave height for the 2100 breach event during maximum velocity for the 100-year wind speed. Black vectors represent wave direction, red lines represent transects, and white dashed lines represent breach event locations.

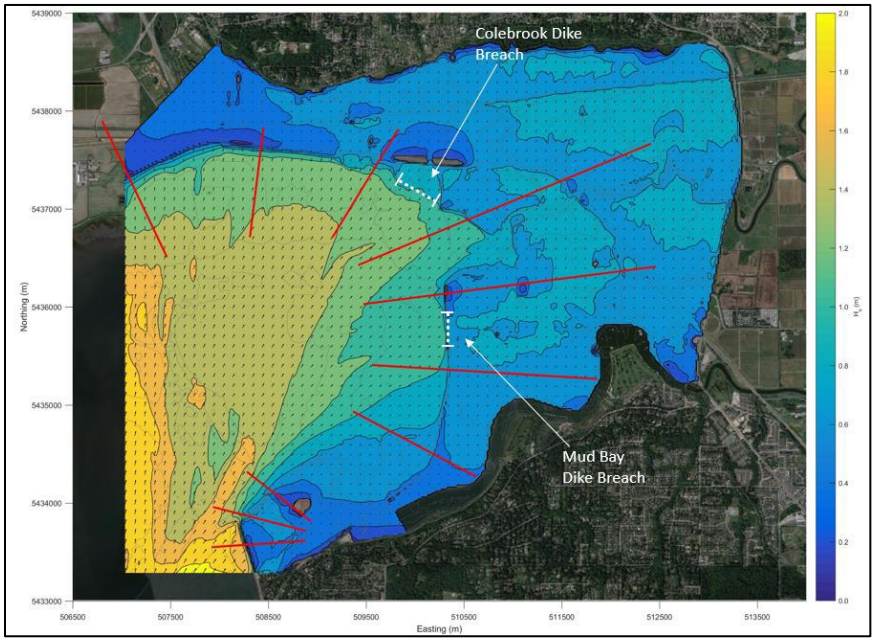

Figure 5.11: Wave modelling results of significant wave height for the 2100 breach event during maximum inundation for the 100-year wind speed. Black vectors represent wave direction, red lines represent transects, and white dashed lines represent breach event locations.

5.3.4 Flood Characteristics

Information on flood loading variables and other elements were extracted from the modelling results for each flood scenario and for each transect and for each individual panel (save point) along all transects. Generated flood characteristics are listed below.

Transect Characteristics:

The following characteristics were obtained for the various flood scenarios considered.

- Transect location (latitude and longitude);
- Mean sea level used;
- Tidal conditions/elevation considered;
- Still water level for transect (with storm surge effect but without wave setup effects);
- Wave runup limit for the transect;
- Ground elevation for the transect (lowest, highest and the elevation at set distances landwards from the present day natural boundary from a common datum);
- Maximum water level and depth along each transect; and
- Maximum landward depth, averaged velocity at the natural boundary and landward locations.

Panel (Save Point) Characteristics:

The following characteristics were extracted from the modelling results for each flood scenario at the evenly spaced save point locations along all transects. Save point zero was taken at the origin of all transects, with save point numbers increasing in a landward direction. Characteristics for each save point were derived from the geometry and hydraulic properties of the associated panel.

- Northing and Easting of the mid-point of each panel, denoted as the save point;
- Ground elevation;
- Local water level;
- Local flood/water depth;
- Local wave height and period; and
- Current velocity.

For each save point, multiple parameters were recorded. These included easting, northing, distance along transect, bottom elevation, depth, wave height, mean wave period, peak wave direction, orbital wave velocity, and wave-induced force per surface area (see Figure 5.12). All information was assembled in MS Excel worksheets, delivered to the NRC.

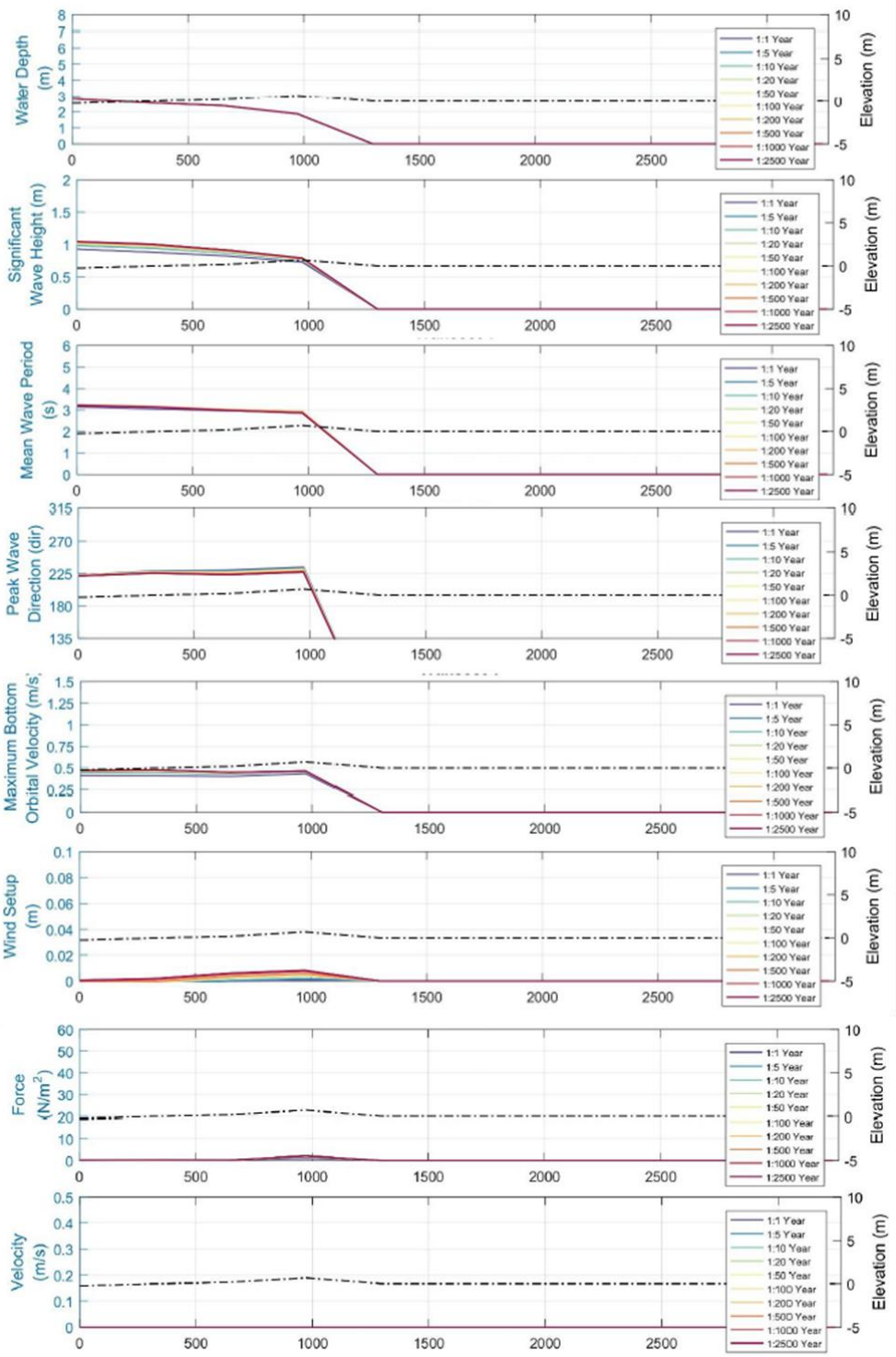

Figure 5.12: Wave and other parameters at save points for the 2010 breach event during maximum velocity at transect 4. Black dashed line represents elevation over the length of the transect (GD, m).

5.3.5 Flood Load Statistics

Summary statistics (mean and standard deviation) for each parameter (i.e. local flood depth, maximum velocity and wave height) at each save point were calculated for scenarios with 0.0 m and 1.0 m of SLR. A large sample of estimated values of each parameter were assembled and corresponding summary statistics were derived.

5.3.6 Concluding Discussion

The nature of coastal flooding is notably different from river flooding in several ways. Coastal flood risk involves both direct flooding of upland areas for short periods of time as well as exposure to waves. The data on flood loading variables generated in this study is representative of a variety of coastal areas in the City of Surrey. The numerical model provided outputs on the significant wave height and spectral mean wave period along each transect, as well as the maximum wave orbital velocity and net horizontal force induced from the waves at each location. The wave model was coupled with the hydrodynamic outputs from the previous study, completed in 2015 (NHC, 2015), to generate data for this study.

6 Manitoba and Saskatchewan – Riverine Flooding Case Studies

6.1 Overview

Hatch was contracted by the NRC to complete hydraulic modelling studies for riverine environments in Manitoba and Saskatchewan in support of flood loads data generation initiative of the NRC. Hatch carried out these studies by extending two previously completed hydraulic modelling studies for the Souris River in Manitoba and Saskatchewan. The Saskatchewan study was related to Rafferty-Alameda dams. By selecting these case studies where previous detailed analyses existed, considerable efficiencies were realized as much of the background data sources were already compiled and the models were already set up. The case study for the Souris River reach in Manitoba is referred to as Souris River (Manitoba) and the other pertaining to the river reach in Saskatchewan is referred to as Rafferty-Alameda (Saskatchewan) in the rest of this chapter. The first study was completed for Manitoba Infrastructure and the second for the Saskatchewan Water Security Agency (WSA). To reutilize data and models, Hatch obtained appropriate permissions from both provincial government departments. Information on flood depth and flood velocity for a variety of return periods was derived for both case studies. This information was delivered to the NRC in MS Excel worksheets and that can be used to determine the potential magnitude and nature of flood loads on buildings in riverine floodplains.

The information and perspectives on data and modelling approaches included in this chapter are extracted directly from the report prepared by Hatch (Hatch, 2020). Detailed information on the modelling procedures, assumptions made, data sources, data preparation and modelling procedures, and background perspectives on original studies is available in this report. The following sections briefly describe the methods adopted and the results that were reported by Hatch.

6.2 Hydraulic Modelling Domains

6.2.1 Souris River (Manitoba) Case Study

The modelling domain used in this study for generating flood loads was part of a previous study, which was completed by Hatch for Manitoba Infrastructure. In that study 1D HEC-RAS hydraulic model was used for the full extent of the Souris River in Manitoba, as well as a portion of the Plum Creek near Souris, to determine flood levels for various flood events, but up to the 300-year return period flood. The Souris River originates in southeast Saskatchewan. It flows south through North Dakota and then back north into Manitoba. Within Manitoba, the river passes through the communities of Melita, Hartney, Souris and Wawanesa, before reaching its confluence with the Assiniboine River at Treesbank (about 40 km south-east of Brandon). The main tributaries which flow into the Souris River in Manitoba are the Antler River,

Gainsborough Creek and Plum Creek. The Souris River has a total length of approximately 700 km (starting from Saskatchewan), with an approximate length of 273 km in Manitoba.

In the past, several large floods had occurred in the Souris River basin in Manitoba, e.g. the floods of 2011 and 1976. These floods had caused considerable damage to farmland and other properties along the river, in addition to evacuations of thousands of residents. For accurate prediction and mapping of water levels during extreme flow events and to effectively manage flooding and assess damages, Manitoba Infrastructure commissioned the original study, which was extended to satisfy requirements of the flood loads data generation initiative of the NRC. Six overflow weir structures were present along the Souris River in Manitoba and those were included in the HEC-RAS model, as well as 26 bridge crossings. Most of the bridge crossings were road and rail crossings with a complete deck and piers. Each of these structures were included in the model.

6.2.2 Rafferty and Alameda (Saskatchewan) Case Study

The Alameda and Rafferty dams are located in south eastern Saskatchewan, and were constructed in the early 1990's. The Saskatchewan WSA owns and manages these dams. During an evaluation, the WSA classified both Rafferty and Alameda dams as extreme consequences structures, following the guidelines from the Canadian Dam Association. This classification was the highest possible for these dams and reflects the potential damages and loss of life that could be caused if the dams were to fail. This led to the need for a detailed review and update of the previous inflow design flood selection and estimation procedures. To satisfy this need, the WSA commissioned Hatch to update design flood selection and estimation procedures for both dams, using the most up to date information and regulatory guidelines. This study involved the development of an updated HEC-RAS dam breach model for both the Souris River and Moose Mountain Creek, calibration of the model against the 2011 flood event, and evaluation of various dam break scenarios based on the calibrated model. Four flooding scenarios were evaluated, including the probable maximum flood, 1000-year event and two other flood events which were smaller than the probable maximum flood but larger than the 1000-year event. The Logarithmic Pearson Type 3 distribution, based on its good fitting to historical data, was used to estimate flood flows for various return periods. For the NRC's flood loads data generation initiative, the same modelling domain and the same hydraulic model were used to map flood levels and generate quantitative information on flood loading variables.

6.3 Model Hydrology

The hydraulic models for both reaches of the Souris River were driven using the peak flood flows corresponding to the 10-, 20-, 50-, 100-, 200-, 500-, 1000-, and 2500-year return periods. Initially the model was run in quasi steady-state at the peak flow for each of the selected events to avoid any stability issues and also to be consistent with the methodology that was used in the

original study. The model was slowly ramped up to the peak flow and held there long enough for the model to reach steady state in terms of water levels and velocities. The magnitudes of peak flows derived at selected locations of interest for each study case are summarized in Table 6.1 and Table 6.2. For the Manitoba case study, peak flows were provided by Manitoba Infrastructure's Hydrologic Operations Centre as part of the original Souris River modelling study and were updated by Hatch where necessary. The peak flows for the Rafferty and Alameda case were estimated by Hatch as part of a reconstituted hydrology report for the Souris River for the Saskatchewan WSA. The flood frequency analysis at all hydrometric stations was accomplished following the approach outlined in the USGS Bulletin 17B (http://water.usgs.gov/osw/bulletin17b/bulletin_17B.html).

Table 6.1: Estimated flood magnitudes at seven different locations within the Souris River (Manitoba) case study modelling domain. Water Survey of Canada station names/numbers and corresponding record lengths are also shown.

Flood event return period (years)	Estimated flood magnitudes (m^3/s)						
	Souris River at Westhope (05NF012) [88 years]	Souris River at Coulter (02NF016) [15 years]	Souris River near Melita (05NF009) [16 years]	Souris River at Melita (05NF001) [107 years]	Souris River at Napinka (05NG807) [20 years]	Souris River at Souris (05NG021) [53 years]	Souris River at Wawanesa (05NG001) [106 years]
10	150	153	177	190	194	220	256
20	240	244	274	294	301	341	389
50	405	411	445	480	493	560	617
100	576	584	613	661	683	800	837
200	794	805	820	885	920	1,057	1,104
500	1,171	1,171	1,232	1,254	1,319	1,528	1,541
1000	1,539	1,539	1,571	1,599	1,695	1,942	1,942
2500	2,200	2,200	2,225	2,225	2,300	2,650	2,650

Table 6.2: Estimated flood magnitudes at Rafferty and Alameda dam locations.

Flood event return period (years)	Estimated flood magnitudes (m^3/s)		
	Rafferty contribution	Alameda contribution	Total flow at Saskatchewan/US border
10	122.8	57.2	180
20	177.3	82.7	260
50	255.8	119.2	375
100	318.5	148.5	467
200	383.3	178.7	562
500	477.5	222.5	700
1000	560.0	261.0	821
2500	671.9	313.1	985

The river reach for the 'Souris River (Manitoba)' case study was broken into a series of segments with junctions for use in the hydraulic model. The local flow contribution within the incremental area was determined as the difference between two adjacent stations and then scaling it down

according to the incremental drainage area. The resulting incremental flow values for each segment of the domain were used as lateral inflows into the hydraulic models.

The hydrologic analysis that was completed for the Rafferty and Alameda consisted of a series of backrouting calculations for the available streamflow data on the Souris River in addition to the analysis that was completed in the study for the WSA. This backrouting was completed to remove the effect of regulation from the flow series to obtain naturalized flows. Observed flows from hydrometric gauges were examined and separated into periods where the flows were affected by regulation and where the flows represented natural conditions. For the periods since the Rafferty and Alameda dams were constructed, reservoir routing and hydrologic routing were used to derive naturalized time series. For frequency analysis of peak flows, the Log Pearson Type 3 distribution was used, following the USGS Bulletin 17B (http://water.usgs.gov/osw/bulletin17b/bulletin_17B.html).

6.4 Data Extraction Methodology

For both modelling domains, Hatch selected 10 transects and each was divided into 11 save points. Flood loading variables were recorded at each of these save points for the 10-, 20-, 50-, 100-, 200-, 500-, 1000-, and 2500-year return period floods. The transect sites were chosen to be spaced relatively evenly throughout the modelling domain, but also in areas where there was potential for some overland flooding to occur.

6.4.1 Souris River (Manitoba) Model

The selected transects for the Souris River (Manitoba) case are shown in Figure 6.1. These transects were numbered sequentially, starting at the upstream (south western) end of the domain. The transect numbers are also shown in this figure and the same numbering convention was used to tabulate and contextualize flood loading variables. The key information for these transects included latitude, longitude, flood event return period, river discharge, transect cross-sectional area, mean water level, mean flow velocity, and kinetic energy coefficient alpha.

Figure 6.1: Selected transects (shown in red) for the Souris River (Manitoba) modelling domain.

The plots of four selected (out of 10) transects along with the 2500-year water level and the panels used for local flood velocity calculation and depth estimation are shown in Figure 6.2. Flood maps were developed separately for 22 reaches of the river and one such map is shown in Figure 6.3.

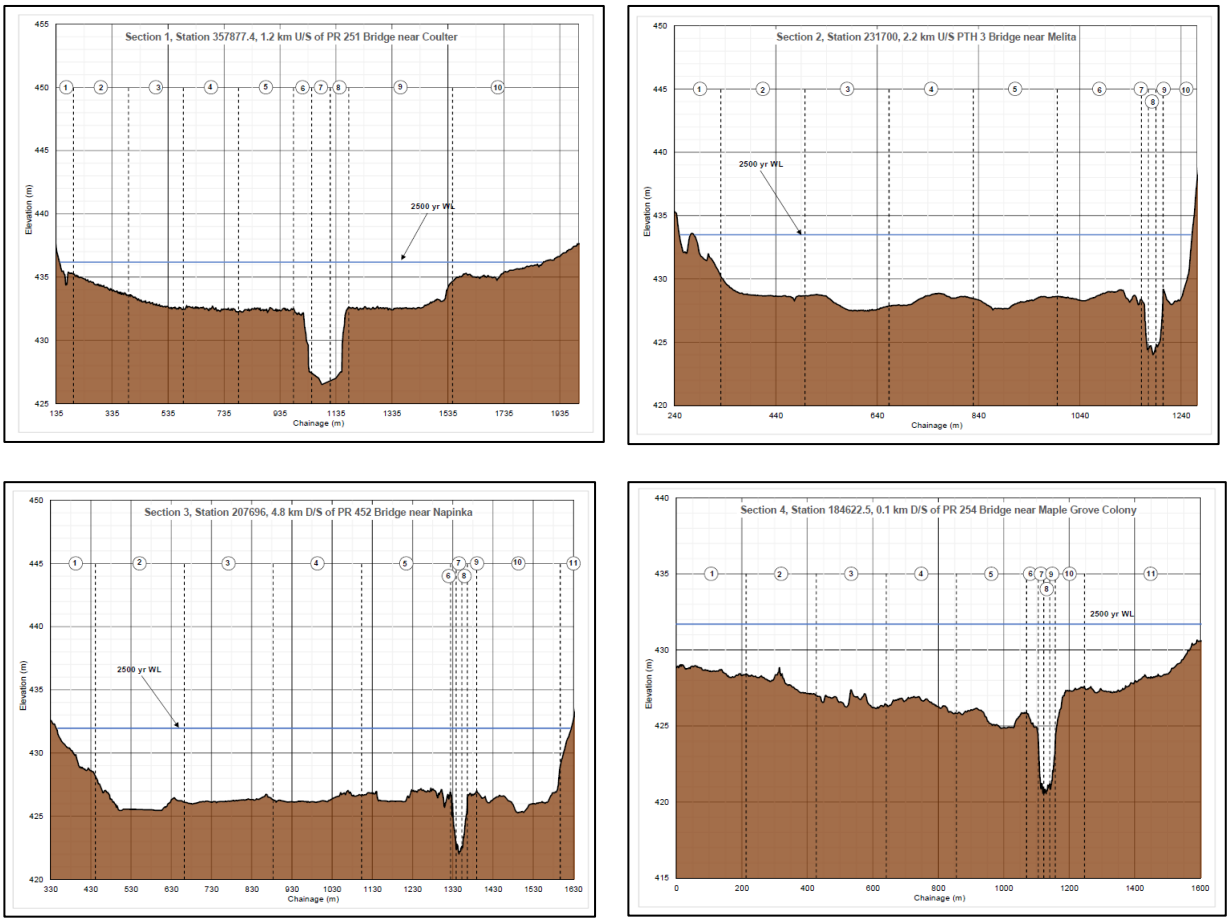

Figure 6.2: Four selected transects (i.e. river cross-sections), showing the 2500-year water level and the panels (i.e. save points) used for local flow velocity calculation and depth estimation for the Souris River (Manitoba) case study.

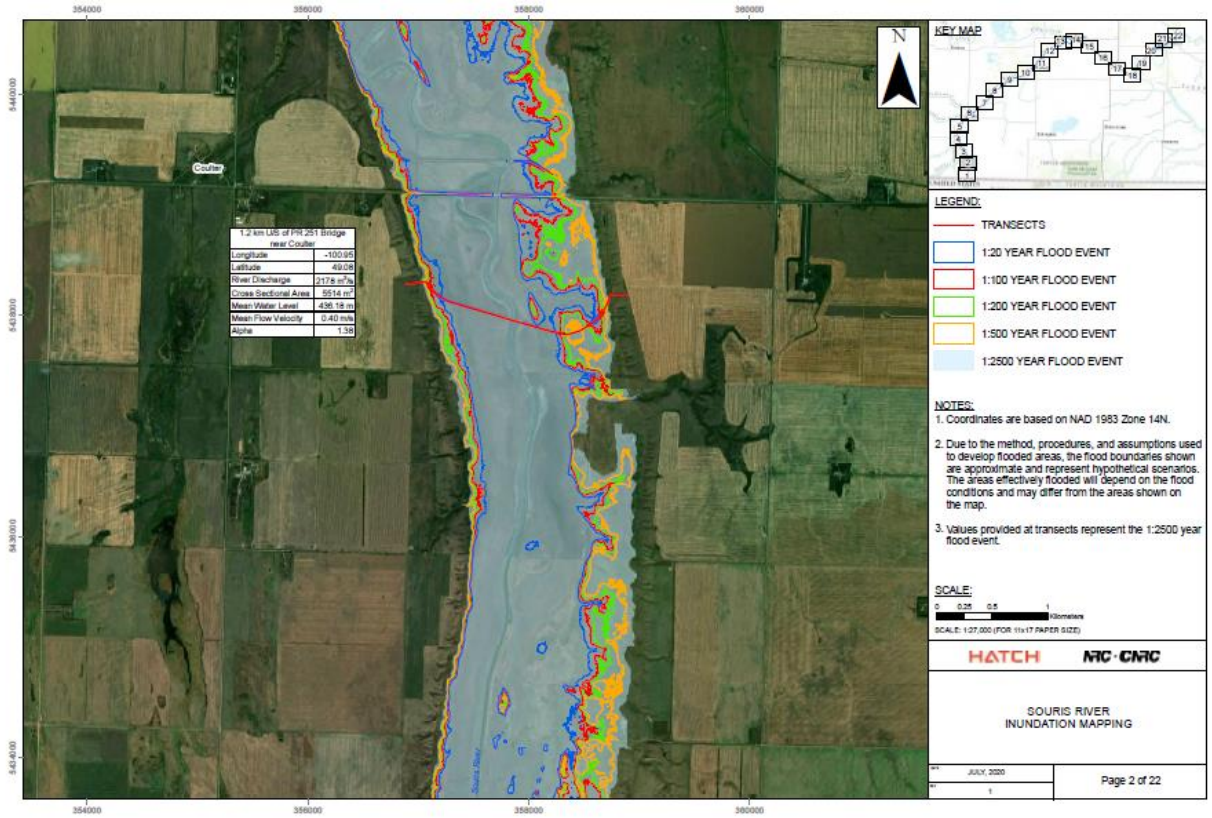

Figure 6.3: Flood map for one of the 22 reaches of the Souris River (Manitoba) model, showing inundation extents corresponding to selected flood events.

6.4.2 Rafferty and Alameda (Saskatchewan) Model

The selected transects for the Rafferty and Alameda (Saskatchewan) case are shown in Figure 6.4. These transects were numbered sequentially, starting at the upstream (western) end of the domain. The transect numbers are also shown in this figure and the same numbering convention was used to tabulate and contextualize flood loading variables. The key information for these transects included the same parameters as listed above for the Souris River (Manitoba) case, i.e. latitude, longitude, flood event return period, river discharge, transect cross-sectional area, mean water level, mean flow velocity, and kinetic energy coefficient alpha.

Figure 6.4: Selected transects (shown in red) for the Rafferty and Alameda (Saskatchewan) modelling domain.

The plots of four selected (out of 10) transects along with the 2500-year water level and the panels used for local velocity calculation and depth estimation are shown in Figure 6.5. Flood maps were developed separately for 22 reaches of the river and one such map is shown in Figure 6.6.

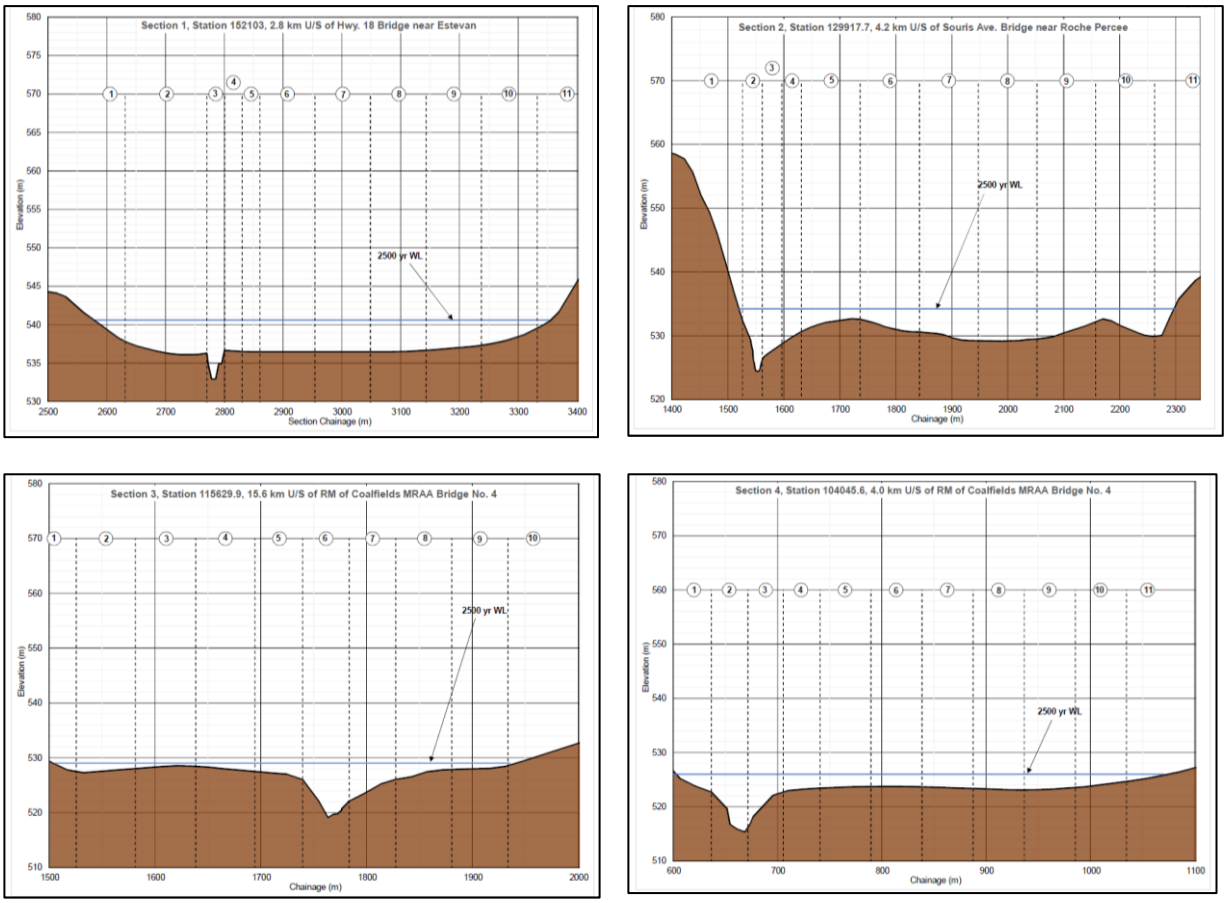

Figure 6.5: Four selected transects (i.e. river cross-sections), showing the 2500-year water level and the panels (i.e. save points) used for local flow velocity calculation and depth estimation for the Rafferty and Alameda (Saskatchewan) case study.

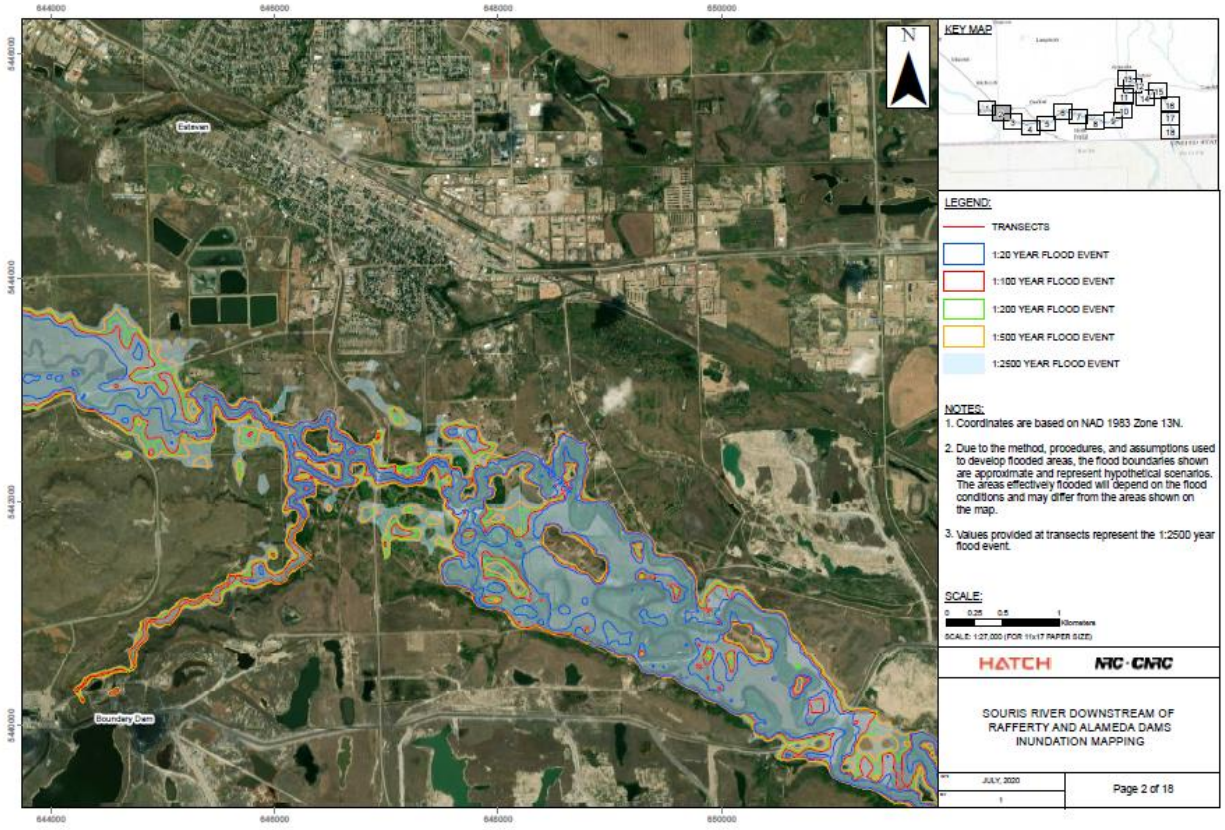

Figure 6.6: Flood map for one of the 18 reaches of the river for the Rafferty and Alameda (Saskatchewan) model, showing inundation extents corresponding to selected flood events.

6.5 Save Point Information

For the Souris River (Manitoba) model, a total of two transects had seven save points, two transects had eight save points, three transects had 10 save points, and another three transects had 11 save points. For the Rafferty and Alameda (Saskatchewan) model, a total of one transect had 10 save points, and nine transects had 11 save points. A further breakdown of these sections with respect to floodway and flood fringe was also carried out. For this purpose, the floodway was defined as anything that was wet for the 50-year flood. The flood fringe was the incremental area between the 50-year flood and the 2500-year flood extents.

Following the data generation guide, which was provided at the onset of the project, Hatch recorded a set of information for each save point corresponding to eight flood return periods. The information was gathered in tabular format in spreadsheets and were delivered with the report (Hatch, 2020). The information collected included location of the save point (within the channel or in the overbank area, and chainage along the cross-section for the save point), ground elevation, water level, flood depth (both section averaged and maximum), flow velocity, cross-sectional area, and Manning's n (roughness) value.

6.6 Flood Load Summary Statistics

Local flood depths and local flow velocities from all save points and from all transects were compiled to prepare summary statistics (i.e. mean and standard deviation) for individual cross-sections, as well as for the entire study reaches. These measures provided an indication of the degree of variability in the depth of flow and velocity across the selected river cross-sections. Maximum flow velocity was also extracted for each return period for each of the selected transects. Flood wave height for each transect was calculated as the height of the flood above the bank-full condition at the peak of the flood. This was defined using the elevations of the bank stations that were set in the model setup, which roughly represent the elevations where water leaves the channel banks and begins to flood the adjoining overland region. The results for the Souris River (Manitoba) case and the Rafferty and Alameda case are discussed below in two separate sections.

6.6.1 Souris River (Manitoba) Model

Mean and standard deviation of local flood depth, local flow velocity, maximum flow velocity, and flood wave height were estimated and reported corresponding to each of the eight selected return periods. Flood wave depth was measured from the channel bank elevation. A profile of the water level along the river for the 2500-year flood condition is shown in Figure 6.7. This profile shows how the elevation and slope of the Souris River changes along the length of the selected river reach, as well as the relative location of the water surface to the channel banks along the reach. This portion of the river is relatively flat for the majority of its length, with a significant increase in slope when approaching downstream end where it meets the Assiniboine River.

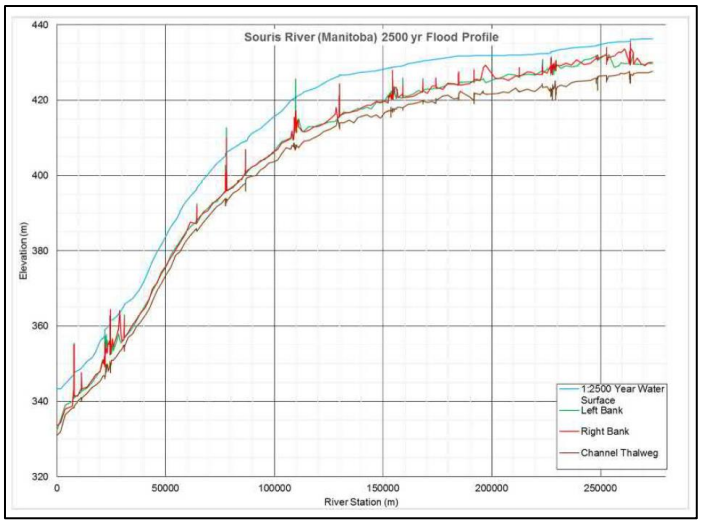

Figure 6.7: Water level profile for the 2500-year flood conditions for the Souris River (Manitoba) case study.

6.6.2 Rafferty and Alameda (Saskatchewan) Model

The same summary statistics were also estimated for this case and reported in the form of MS Excel spreadsheet. Here also, flood wave depth was measured from the channel bank elevation. A profile of the water level along the river for the 2500-year flood condition is shown in Figure 6.8. This profile shows how the elevation and slope of the Souris River changes along the length of the study reach, as well as the relative location of the water surface to the channel banks along the reach. This part of the river has a relatively constant slope throughout the study reach. The downstream boundary condition was modelled as a given water surface elevation at Lake Darling in North Dakota (not included). Station 0 in the model corresponds to the Saskatchewan-North Dakota border, which is essentially the downstream end of the region of interest for this study. All transects that were selected for the study are within Saskatchewan. The high points in the left and right banks reflect elevated channel banks or levees that are in place and protect communities of Estevan and Weyburn.

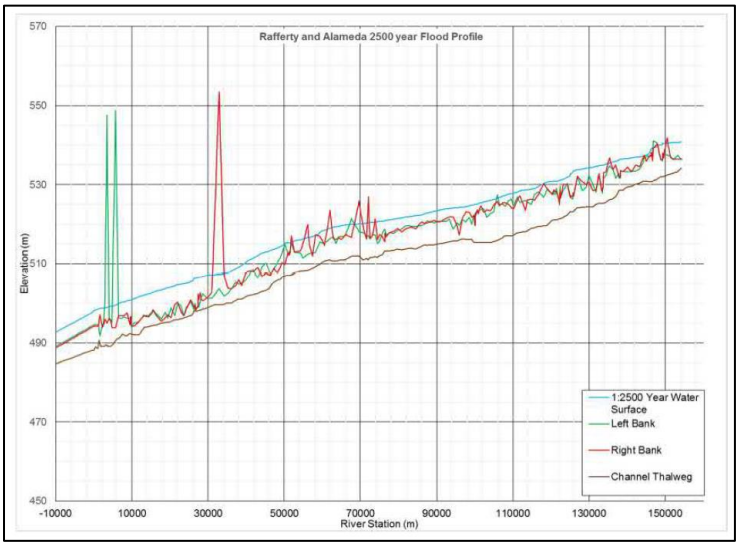

Figure 6.8: Water level profile for the 2500-year flood conditions for the Rafferty and Alameda (Saskatchewan) case study.

6.7 Concluding Discussion

The HEC-RAS hydraulic model for two sections of the Souris River in Manitoba and Saskatchewan was used to simulate a number of flood magnitudes of various return periods, ranging from 10 to 2500 years. Information about flood loading variables (e.g. flood depths and velocities) was compiled in the form of tables and graphics where appropriate. The flood loads data produced in this study can be used to determine potential flood loads on buildings to support NRC's initiative on the design of flood-resistant buildings.

Hatch noted that the procedures developed in this study may be useful for completing similar studies on other rivers across Canada. An evaluation of other modelling approaches apart from

the 1D HEC-RAS modelling may also prove beneficial. While the HEC-RAS model is able to compute velocity across the river cross-section, a 2D model may be able to better calculate the velocity profile across the channel. The 2D modelling method may also provide a more direct benefit in the case of designing a building within a known flood prone area, as it would be beneficial to use the additional computational capabilities to better determine the specific flood loads in different parts of the transects.

7 Ontario – Large Lake Coastal Flooding Case Studies

7.1 Overview

Baird and Associates were contracted to undertake costal flood modelling and flood loads data generation case studies in large lake and northern environments. Two large lake case studies for Lake Erie are covered in this chapter while the one northern case study for Tuktoyaktuk Hamlet, Northwest Territories, is presented in Chapter 9 of this report.

Lake Erie is unique amongst Great Lakes in that the shallow water depths and long SW/NE fetches create a situation where significant storm surge can occur. Additionally, extreme storm systems passing over Lake Erie show a trend of SW winds, putting the NE end of the lake at particular risk to flooding from storm surge. Large storm surges can result in threats to buildings and developments along the Lake Erie shoreline that are typically not found (to the same extent) on the other large lakes in the region.

Under a previous contract with conservation authorities along the north shore of Lake Erie, Baird developed a storm surge and spectral wave model of Lake Erie, as well as datasets that included building footprints and high-resolution elevations around the lake. These datasets, and the ongoing work in the area, led to additional modelling of surge and waves and to characterize nearshore flooding and flood loading conditions to satisfy the requirements of flood loads data generation case studies of the NRC.

Two regions on Lake Erie that have historically experienced significant flooding are the towns of Long Point and Turkey Point, both of which are located in Norfolk County. In the region of Long Point, there are low-lying nearshore developments that see flooding during periods of high lake levels combined with surge events (Figure 7.1). Given that the most extreme winds and waves tend to approach from the SW on Lake Erie, Long Point is particularly exposed. The location of Long Point is close to the central part of the lake, meaning surges are not as extreme as they are at the ends of the lake but are still an important part of the potential damage mechanism at the site.

Turkey Point is located approximately 10 km to the north, in the bay directly north of the geographical feature that forms Long Point. Turkey Point is also a very low-lying area, with many buildings and developments that are exposed to flooding hazards. While close in proximity to Long Point, the flooding hazards at Turkey Point are very different. Long Point provides shelter to Turkey Point from southerly waves, making the region more exposed to easterly winds and waves. However, the alignment of Lake Erie and major storm patterns often result in set-down at the SW end of the lake and set-up at the NE corner of the lake. This means that while Turkey Point may be sheltered from waves during these extreme storm conditions, it is still susceptible to flooding. In contrast, Long Point is typically at risk to large surge and wave events

occurring simultaneously, while Turkey Point is more at risk to large surge events with reduced southerly wave action, or smaller surge events with larger easterly wave action.

The material included in this chapter is directly extracted from the case study report prepared by Baird and Associates (Baird, 2021a). Detailed information on the modelling procedures, assumptions made, compromises on data availability, and data preparation procedures is available in this reference.

Figure 7.1: Long Point and Turkey Point study sites. Inset shows Lake Erie and location of the study sites.

7.2 Data

Various datasets were required to accomplish the coastal flood modelling case studies. A brief description of these datasets is provided below for contextual reasons.

7.2.1 Aerial Imagery

The 20 cm resolution aerial imagery used in this project was acquired by Land Information Ontario (LIO) for southern Ontario within the 2015 Southwestern Ontario Orthophotography Project. This imagery provides a visual reference for ground features such as the delineation of shore protection structures, indications of shoreline substrate, and was used as a base layer for the 1:2000-scale mapping developed for this study.

7.2.2 Elevation

The elevation data utilized for this study is the 2017 Lake Erie Watershed LiDAR dataset, collected as part of the Ontario Government's LiDAR Digital Terrain Model (2016-2018) LIO Dataset. This dataset is a 50 cm resolution raster representing the bare-earth terrain derived from

a classified LiDAR point cloud, which was hydro-flattened using water body breaklines. This dataset provided complete coverage of the study limits of the Norfolk County Lake Erie flood hazard mapping.

7.2.3 Bathymetry

Bathymetry data from various sources was assembled to develop the best available combined dataset for the study area. In the area north of Long Point, the Government of Canada Department of Fisheries and Oceans (DFO) collected bathymetry using an airborne bathymetry sensor. The survey was completed between 19 April and 19 June 2018. However, as a result of water clarity issues during the acquisition flights, this dataset did not extend further south. For the areas south and west of Long Point, a dataset compiled by the US National Oceanographic and Atmospheric Administration (NOAA) National Geophysical Data Center's Marine Geology and Geophysics Division, the NOAA Great Lakes Environmental Research Laboratory and the Canadian Hydrographic Service was used. All datasets were reduced to NAD83 UTM Zone 17 horizontal datum and IGLD1985 vertical datum.

7.2.4 Water Level Stations

Lake Erie water levels were obtained from the DFO's Marine Environmental Data Service. Permanent gauging stations are maintained at Port Stanley (to the west) and Port Dover (east side) of Norfolk County. A third gauging station at Port Colborne was also utilized as part of the modelling effort.

7.2.5 Static Water Levels

In the Ministry of Natural Resources (1989) study, the historical monthly mean lake levels from 1900 to 1988 were adjusted to the constant set of conditions existing after about 1960 (regulation conditions, diversions, etc.) to form a consistent basis of comparison. Considering that an additional 30 years of data was available since 1988, and recognizing the 1970s to 1990s as a period of higher water levels in the Great Lakes, Baird updated the static water level–return period relationships for Port Dover and Port Stanley using only the measured data corresponding to the period of hourly water level measurements (January 1962 to June 2019). This is a conservative approach (i.e. it errs on the side of higher extreme lake levels) because, in June 2019, Lake Erie reached its highest monthly mean lake level ever recorded. The preliminary mean monthly water level for June 2019 (175.14 m IGLD85) was also included in the extreme value analysis. The dataset included 58 years of water level measurements under conditions (i.e. flow regulation, diversions, dredging, etc.) similar to the present.

7.2.6 Surge Levels

Storm surge (or wind setup) was calculated in Ministry of Natural Resources (1989) by subtracting the mean monthly water level from the hourly water level measurements. A computer

model was used to estimate storm surges for locations between gauging stations. Baird updated the storm surge analysis using the 58 years of hourly water level data (1962-2019). In the analysis, static water levels were calculated using a Gaussian-weighted 30-day moving average filter to eliminate the stairstep effect between months. Surge was calculated by subtracting the hourly water level measurements from the "smoothed" static water level. Hourly water levels, calculated static levels, and calculated surges for Port Dover over this timeframe are shown in Figure 7.2.

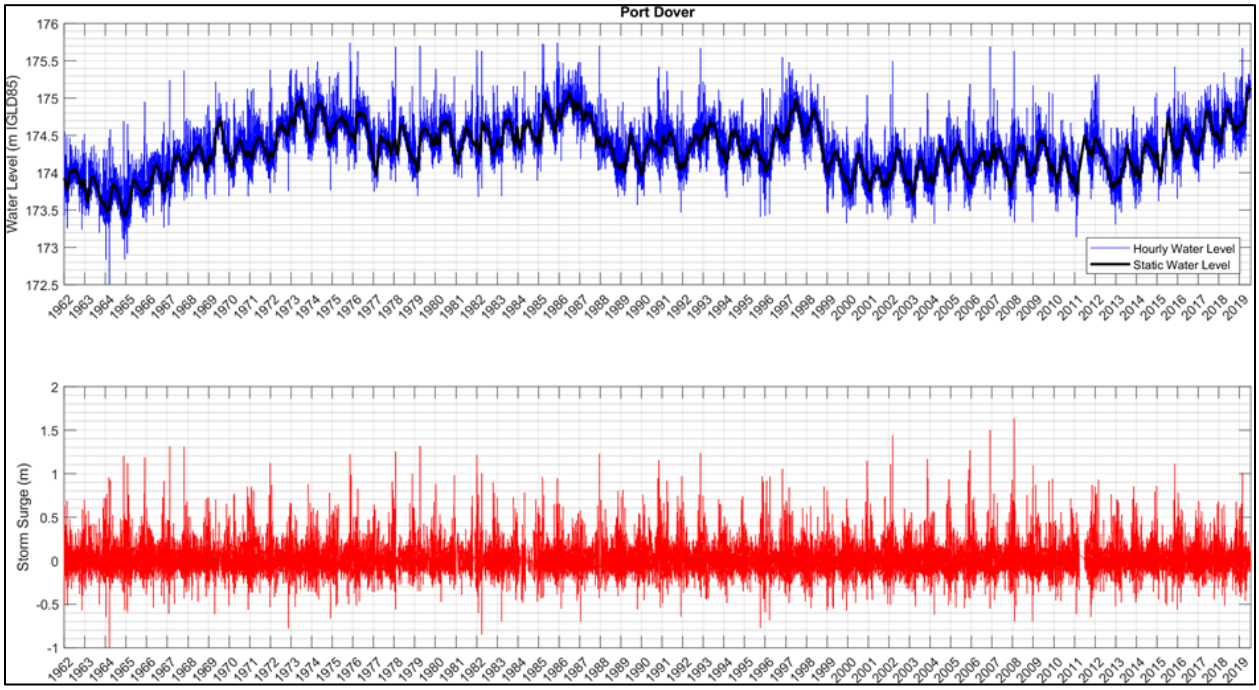

Figure 7.2: Hourly and static water levels and calculated surge at Port Dover from January 1962 to July 2019.

Considering that surges are driven by independent storm events, a peaks-over-threshold analysis was used to identify the largest surge events from the dataset. Using this method, it is very likely that more than one surge event can be from the same year.

7.2.7 Return Period Water Levels

To produce large return period events, a combined probability analysis approach was used to assess the combined occurrence of high mean water levels and high surge events. This analysis was based on the procedures that were used in the HYDSTAT software package (Ministry of Natural Resources, 1982); however, the package routines were extended to produce longer return periods. This analysis was completed for return periods ranging from 1.05-year to 2500-year events and followed the procedure of the Ontario Technical Guide (Ministry of Natural Resources, 2001). Long term water level distributions were assessed by tabulating the maximum monthly water level from each year and developing a cumulative probability distribution function. The Log-Pearson Type 3 (LP3) distribution was fitted to the water levels.

Storm surges were assessed from the recorded data based on the difference between the hourly water levels and a 30-day running average of the lake level. Because multiple storm events could happen in any given year, a peaks-over-threshold approach was used to identify the large surge events. This analysis also used the LP3 distribution, which was found slightly better than the Weibull distribution in fitting the data. The LP3 distribution had the best fit for the monthly water levels and the combined water levels and was therefore selected to represent the surge level as well. It is important to note that there could be a number of possibilities that can create a combined probability water level based on various combinations of static lake and surge levels.

7.2.8 Waves

At Long Point, the same processes that cause high surge levels will also cause the largest wave conditions: strong, sustained onshore winds. With the shallow water depths that exist in front of both sites, there is little chance of having wave damage along the shoreline when there is a lower water level condition (i.e. when the mean lake level is low). Therefore, identification of the highest water levels, which require both high mean lake levels and surge, also involved identification of large wave events and the most damaging conditions at Long Point. Therefore, the wave heights were determined based on numerical modelling of specific storm events. Comparisons between measured and modelled wave heights were possible in some circumstances, but typically in a central part of the lake, rather than close to the site. Additionally, the most extreme storms on Lake Erie tend to happen in winter months; wave buoys are typically decommissioned each winter, and re-deployed when lake conditions open up in spring. This practice causes lack of data for most extreme wave conditions.

The two sites on Lake Erie have different exposures and therefore the processes that affect the two locations are also different. The largest surge and wave conditions at the Long Point site occur when strong winds blow from the southwest. During such an event, the water levels may be fairly high at Turkey Point (and throughout much of eastern Lake Erie); however, the waves will not be strong with this cross-offshore wind direction.

To identify large wave events at Turkey Point, the wave history from the USACE WIS hindcast was assessed to identify higher storm conditions. These typically coincide with easterly winds, which may create a localized surge north of Long Point, which is impacted by regional negative surge at the east end of Lake Erie (see Figure 7.3).

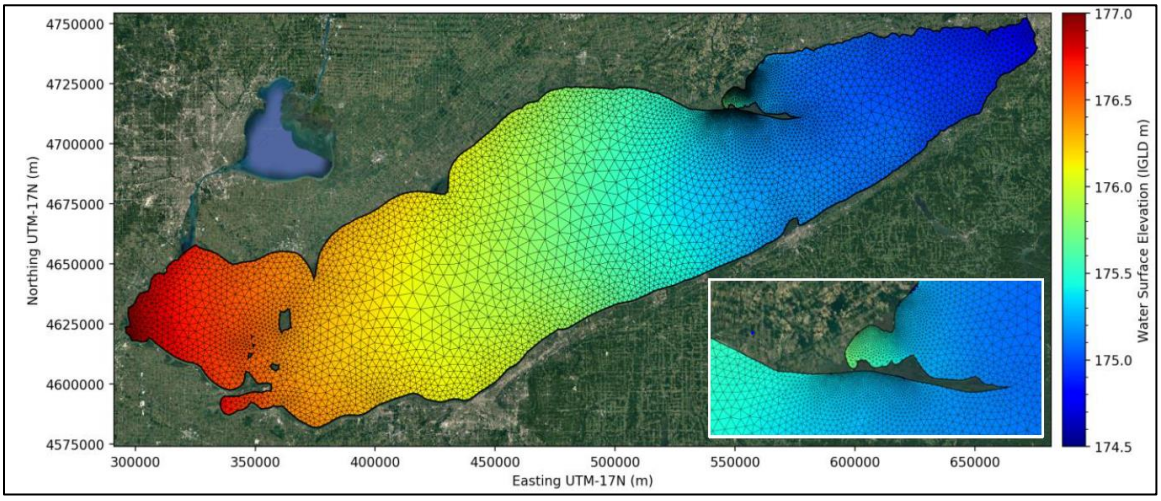

Figure 7.3: Lake Erie surge from easterly winds at 175.75 m IGLD static water level

7.2.9 Climate Change

The Ontario Climate Consortium and Ontario Ministry of Natural Resources and Forestry published a climate change synthesis report for the Great Lakes basin in 2015 (McDermid et al., 2015). The report draws on over 70 water level and surface hydrology studies published since 2010 for the Great Lakes basin. The report outlines the anticipated climate change impacts, evidence, uncertainty, and agreement between studies in a language that is accessible to the general public. The following observations are based on this synthesis report.

Water Levels

Future lake water levels will be most affected by changes in air temperature and precipitation. Over the past 60 years, average annual air temperatures have increased and are predicted to continue increasing. The increase in air temperatures is expected to result in lower water levels due to increased evapotranspiration. The past 60 years have also been slightly wetter than the historical average and annual precipitation is also predicted to increase over the next century. However, the increase in air temperature is predicted to be more significant than the increase in precipitation, resulting in drier conditions and lower lake levels (McDermid et al., 2015).

The natural variability in water supplies is likely more significant than the anticipated climate change impacts on water levels in the Great Lakes. Based on this premise, consideration of climate change impacts on water levels was not considered in this project.

Waves and Surge

The impacts of climate change on waves and surges in the Great Lakes were assessed by Baird in a recent study for Natural Resources Canada and are described below. Wave and hydrodynamic

models were developed for Lake Ontario and Lake Erie as part of an effort to examine the impact of future wind scenarios and ice regimes on wave climatology.

Initially, the MIKE modelling system was used to simulate wave and hydrodynamic conditions on both lakes for fifteen storm events under baseline and projected future climate conditions. The USACE WIS wave hindcast dataset, which provides continuous hourly wave climatology on the Great Lakes from 1979 to 2014, was used to select the fifteen storm events. An assessment of the wind datasets showed that the future scenario considered in this study was not significantly different from the baseline conditions suggesting the strength of storms (i.e. wind speed) may not increase significantly in the future.

Baird expects that while the total wave energy reaching the shoreline may be increased, extreme water levels and waves from winter storms that may cause flooding may be mitigated by the generally lower water levels in the winter months. Therefore, the results of this study should be considered representative until more certainty in climate change impacts is available.

7.3 Modelling Approach

Hydrodynamic modelling for the two sites was undertaken using the MIKE21 Flexible Mesh (M21FM) hydrodynamic and spectral wave models. These models are designed to work together and both use the same computational grid to simulate surges on the lake resulting from strong winds and the generation and propagation of waves. For this study, flood risks were required for a wider range of flood events, including the 1000- and 2500-year longer return period events. This was accomplished by expanding the computational grid to cover all of Lake Erie (Figure 7.4). However, existing modelling was undertaken to mapping only the 100-year floodplain, among other things. A close-up of the region near Long Point and Turkey Point is also shown in the inset.

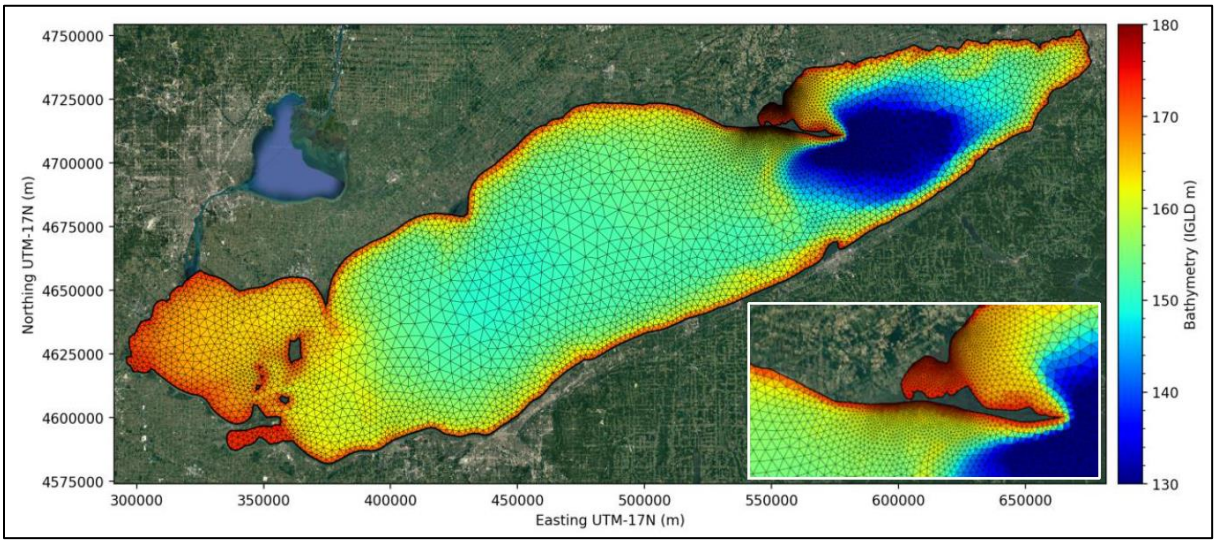

Figure 7.4: MIKE21 Lake Erie model mesh, inset shows a close-up of Long Point and Turkey Point.

The nearshore area at the study sites is resolved in the mesh to approximately 200 m along the shoreline, while the central part of the lake gradually increases in size to a resolution of approximately 5 km. Though this varied grid spacing provided modelling efficiencies, the 200 m grid spacing is still very coarse relative to the processes that occur along the shoreline (e.g. wave refraction, breaking, runup, etc.). Also, the model mesh does not extend into the overland area where roads and houses may be flooded in an extreme event. In general, in coastal modelling applications for large sections of the shoreline, it is not practical to simulate the runup and overtopping processes that occur using a large-scale two-dimensional model. Thus, extending mesh into overland areas is of little use and modelling of runup and overtopping is completed with profile models that simulate the transition of waves from the nearshore area (perhaps 5 m water depth), up the shore face and into the backshore area. Many profiles can be effectively run to simulate the varied conditions and structures along the shoreline. For these sites, CSHORE model, developed by the US Army Corps of Engineers and the University of Delaware, was used to simulate runup and overtopping along profiles that were cut through both project sites.

Surge Modelling

Surge modelling was simulated with the M21FM model using a representative still water lake level, and then applying wind fields across the numerical domain. Historical events were used for the calibration of the model and winds were applied based on the Climate Forecast System Reanalysis (CFSR) dataset. The CFSR data includes winds at a 10 m elevation over the lake at a grid spacing of about 0.2 degrees (~22 km); these winds are available at an hourly time step from 1979 to the present time. Using a realistic wind field is important for comparisons of modelled and measured water levels since spatial differences throughout the lake (almost 400 km in length) can be important.

An example of a storm surge simulation is shown in Figure 7.5. The mean water level in this simulation is shown as a light green colour (centre of the lake), while opposite ends of the lake are higher and lower by over 2 m. Surge in the project areas is less than that at either end but is still significant. Calibration of the model was undertaken by comparing modelled and measured water levels for a series of historical storm events.

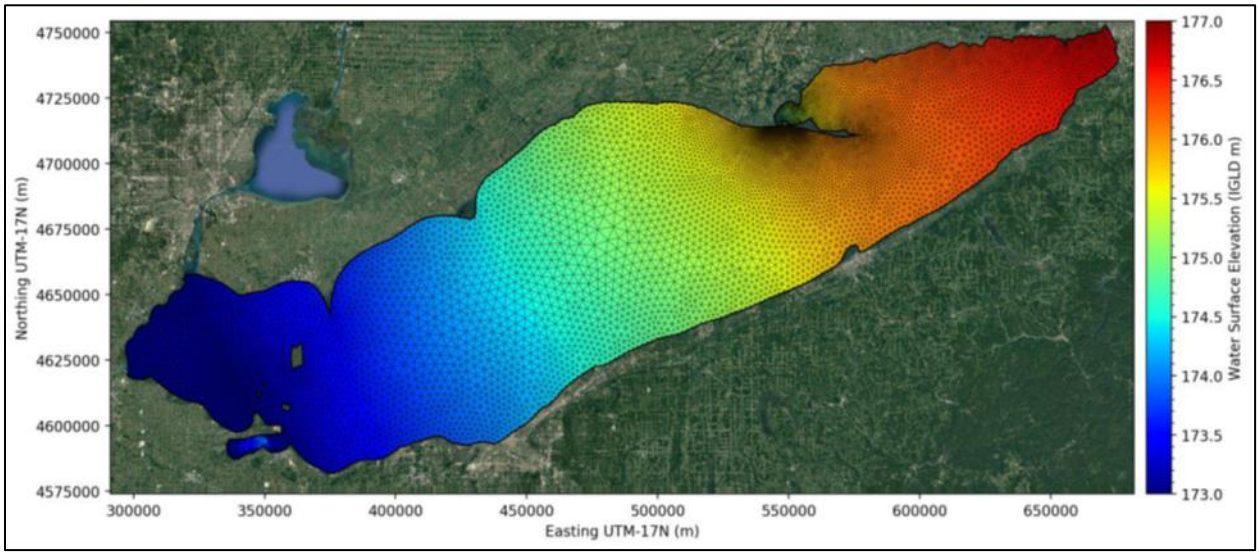

Figure 7.5: Storm surge simulation for the December 1985 event on Lake Erie.

Wave Modelling

Waves were simulated with the MIKE21 Spectral Wave model, using the same mesh as used for surge modelling. Waves were simulated using the fully spectral option in the model and typically covered a period of about four days centered on the peak of the storm.

CSHORE Modelling

CSHORE is a non-linear time-averaged nearshore profile model that simulates wave processes on beach and stone slopes to the extent of wave runup or overtopping. CSHORE is a stable and fast model that is recommended by FEMA for flood hazard mapping. CSHORE allows for nearshore propagation of wave conditions, while capturing the processes that occur along the shoreline (i.e. wave setup, run-up, overtopping, etc.). This approach was used to bridge the gap between the comparably coarse lake-wide MIKE21 model, and the detail required at and around structures affected by flooding. This model allowed for calculation of water levels, wave heights and velocities, and other parameters of interest along each profile that can be used to assess flood loads on structures.

Baird also experimented with the EurOtop model (EurOtop, 2018), which is an empirical Machine Learning type formulation to estimate the runup and overtopping performance of coastal structures. EurOtop is best suited for structures such as dykes, revetments, or relatively high sloped beaches, which reflect the empirical datasets from which the method was derived. Compared to the EurOtop model, the advantage of the CSHORE model is that it can be run directly on the profiles cut through the shore, rather than on a schematized cross-section, and directly computes the wave characteristics.

The locations of the profile extractions are shown in Figure 7.6 and Figure 7.7 for Long Point and Turkey Point, respectively. Each profile was placed 100 m apart along the shoreline, for a total of 53 profiles at Long Point and 35 at Turkey Point. For each profile, model output was extracted from 300 m to 350 m along the profile, in 5 m increments. The total length of each profile was 600 m, with 300 m landward and 300 m lakeward of the average waterline.

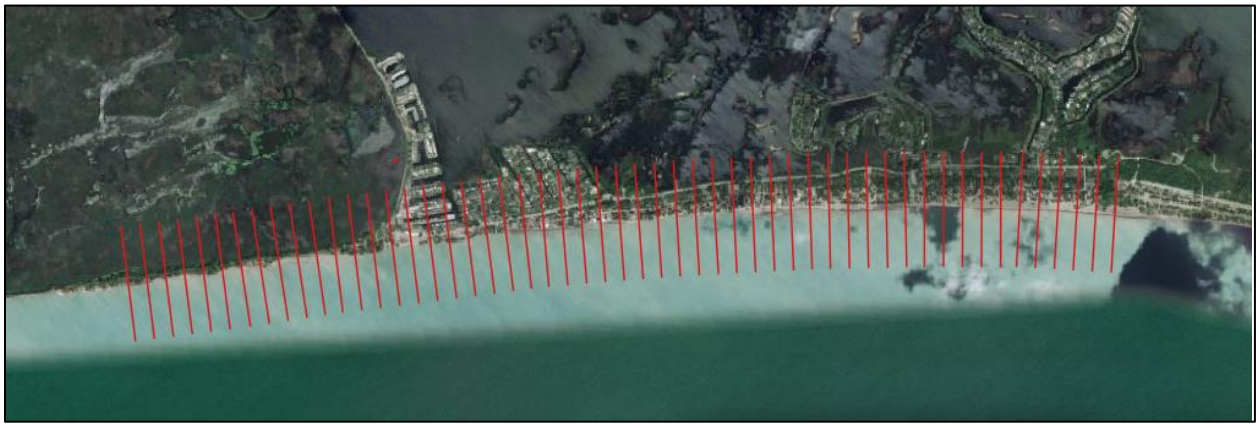

Figure 7.6: CSHORE profiles at the Long Point site.

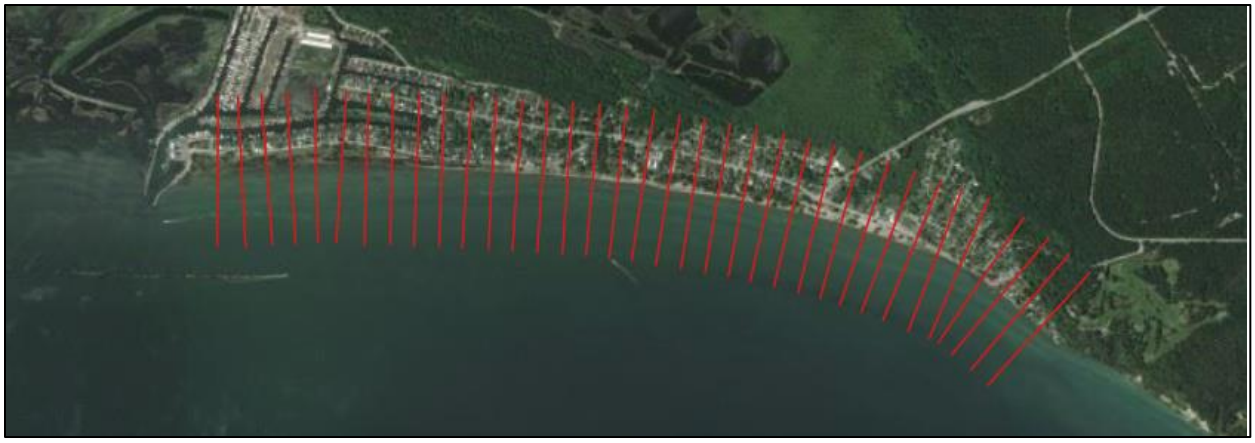

Figure 7.7: CSHORE profiles at Turkey Point.

The CSHORE model can result in one of the following three scenarios: (1) the runup does not reach the highest point of the profile and is contained on the beach slope; (2) the runup exceeds the crest of the beach and results in overtopping and inland bore propagation; or (3) the water level is so elevated that the entire profile is submerged.

7.4 Considerations for Storm Simulations and Flood Loads Data

Simulation of water levels corresponding to longer return period events such as 2500-year event is often difficult to define given the typical data record lengths, but is somewhat more feasible on the Great Lakes using the combined probability approach. In order to provide realistic storm

conditions for Lake Erie, historical storm events were used as much as possible, rather than using a static (constant) wind field blowing over the lake.

Long Point Simulations:

For the purpose of this study, various return periods were associated with combined lake levels, i.e. the 2500-year event was a storm event resulting in a 2500-year combined lake levels at the region of interest. Furthermore, estimates of return periods were based on water levels occurring in simulations at Port Dover, which is the closest known location with adequate data to support an extreme value analysis for determining water levels corresponding to various return periods.

By selecting historical storm wind fields and adjusting the mean water level, a wide number of events were developed that met the criteria of the study. At Long Point, a strong correlation was found between surge and wave height, suggesting it was not necessary to select storms based on wave height as selection based on surge level led to the same result.

For developing 11 different return period storm scenarios (combined lake levels) required for this study, five different historical storm events were applied at different mean lake levels. For example, the 500-year event was developed by simulating the storm of January 30, 2008, but applying it at the 5-year static water level. For certain scenarios, historical storms were considered without any alteration, e.g. the March 10, 2002 and December 2, 1985 events. These cases corresponded to combined water levels with return periods of 1.05 years and 10 years, respectively.

It was found that the wave conditions at Long Point were much higher than those at Turkey Point. The increased water level at Turkey Point was more a function of how storms were selected to generate the worst overtopping, rather than an indication of water level differences between the sites.

Turkey Point Simulations:

Storm simulations for Turkey Point revealed that the largest surges in the Turkey Point area were associated with very strong winds from the SW that resulted in a lake-wide surge event (e.g. the storm conditions chosen for the Long Point runs). The lake-wide surge caused an increase in the water level at the east end of Long Point; however, the water level on the north side of Long Point was reduced somewhat in areas to the west (near Turkey Point) as a result of SW winds. At the same time, the waves were quite small as the winds were mostly in an offshore direction. This was fundamentally different than the strong surge and wave correlation observed at Long Point. The largest waves at Turkey Point occurred during winds from the east, which also caused a localized storm surge on the north side of Long Point.

Data for Flood Load Calculations:

Outputs from the CSHORE model simulations were converted in tabular formats. One table was assembled to summarize the offshore input conditions at each of the profiles, and another for save points along the profile beyond the typical water line (from 300 m to 350 m along each profile in 5 m increments). The following flood loads related variables and parameters were compiled in tables:

- Ru2% IGLD85 (m): The 2% run-up elevation in meters IGLD85 vertical datum.
- h0 (m): The initial overtopping wave bore depth at the profile crest in meters.
- v0 (m/s): The initial overtopping wave bore velocity at the profile crest in meters.
- Ls (m): The landward extent of the overtopping wave bore from the profile crest in meters.
- 2% Wave Height (m): The 2% wave height corresponding to the coordinates of the profiles and save points.
- 2% Water Depth (m): The 2% water depth corresponding to the coordinates of the profiles and save points.
- 2% Velocity (m/s): The 2% velocity corresponding to the coordinates of the profiles and save points.

Figure 7.8 shows an overview of CSHORE modelling results for all storm conditions, at all profiles, for both Long Point and Turkey Point. The 2% runup height is shown as a representation of the flooding and overtopping conditions at each profile, plotted against the crest elevation of each profile. It can be noted from this figure that there were significant variations across the two sites for all storms. This speaks to the highly localized nature of flood loading conditions due to differences in the profile geometry, as well as variations in the offshore water surface and wave conditions from different storm tracks.

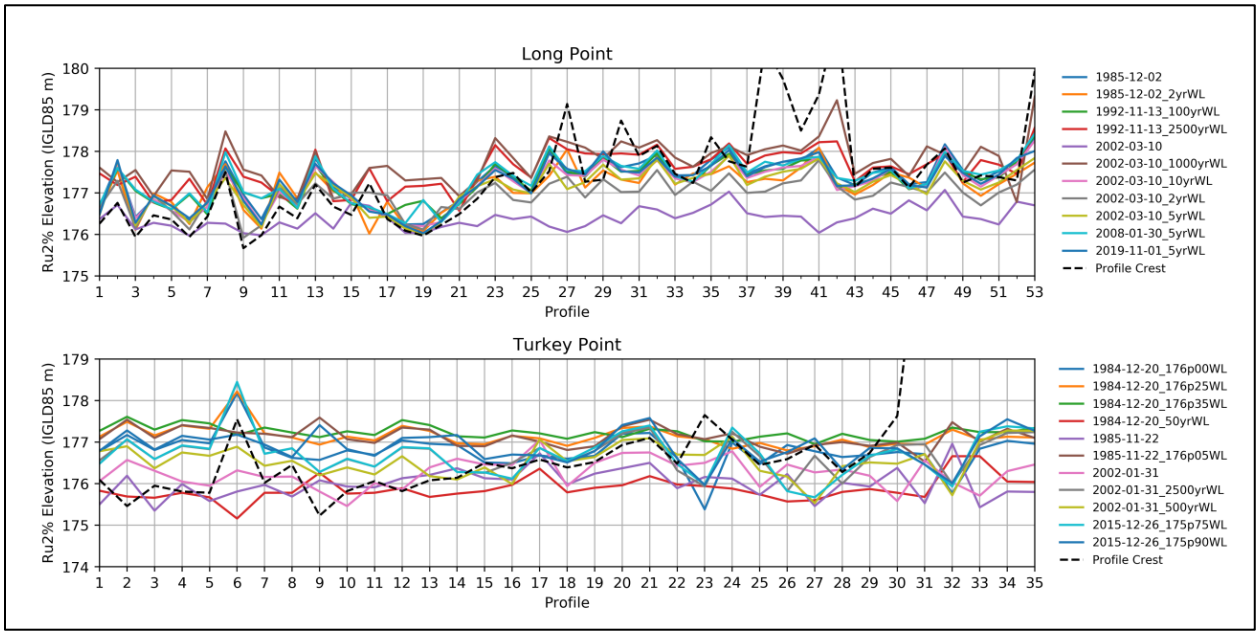

Figure 7.8: 2% Runup elevation for all profiles and storms versus profile crest elevation.

7.5 Concluding Remarks

For the two locations, despite being on the same lake and in general proximity to each other, the surge processes on Lake Erie required different approaches for both Long Point and Turkey Point sites. Long Point represents more of a traditional coastal setting where both large waves and surge are coincident, since they are produced by very similar processes. Turkey Point is quite different since a strong onshore wind (easterly) can result in little (if any) storm surge that accompany incoming waves.

The process that was used to select severe storms at Long Point relied on the coincident nature of the waves and surges, and considered the random distribution of storm conditions against the long term fluctuations in the lake levels. Using the combined probability approach (large storms at high water levels), it was possible to define much longer return period events than were possible through conventional statistical frequency analysis approaches.

For Turkey Point, large storm events were defined by the coincident occurrence of high mean lake levels and large easterly wave events. Here, again a combined probability approach was used to define longer return period events; however, it was not simple to determine the severity of storm events. For Long Point, two types of water levels (mean and surge) were combined to produce a total water level, but the waves were depth limited for large storm events. For Turkey Point, the combination of wave height and water level was more complex as it involved determining the relative influence of two different variables.

The parameters such as flooding, runup and even wave height can vary rapidly along the shoreline in response to nearshore bathymetry. This suggests that defining return period levels can realistically be done on a profile by profile basis, rather than regionally with a similar value. It was also demonstrated that the overtopping volume is not a simple well-behaved pattern as a function of water level and wave height. Processes that involve waves are much more complicated than still-water flooding since in addition to wave height, factors such as wave period, wave direction, wind action and the nearshore bathymetry/structure shape all play an important role. Finally, Baird alarmed that the results from coastal flooding assessments for building design purposes should be treated as approximate only, since the numerical models that were used provide an order of magnitude values for some variables such as overtopping rates.

8 Quebec – Riverine and Urban Flooding Case Studies

8.1 General

LaSalle | NHC (LaSalle hereafter) Montreal were contracted to undertake riverine flood modelling and flood loads data generation case studies in Quebec. Two representative riverine floodplain mapping studies were selected where most of the required supporting datasets and models were already available. The first case study was of the Beauport River (Quebec urban community) and the second was of the Clair Creek, Mont Tremblant. For these case studies, LaSalle already had completed detailed floodplain mapping studies. By selecting these locations where previous detailed studies existed, considerable efficiencies were realized as much of the background data sources were already compiled and the models were already set up. There were also considerable gains in terms of data pre-processing and modelling experience. LaSalle extended these existing studies to satisfy the requirements of flood loads data generation initiative of the NRC.

The information included in this chapter is extracted directly from the report prepared by LaSalle (LaSalle | NHC, 2021). Detailed information on the modelling procedures, assumptions made, data sources, and data preparation and modelling procedures is available in this reference and also in the original studies (i.e. LaSalle | NHC, 2018, 2019).

8.2 Project Areas and Representative Cross-sections

The first case study pertains to the Beauport River, which passes through the Quebec urban community and discharges into the St. Lawrence River. The associated catchment is highly urbanized with a contributing area of approximately 29.1 km^2. The study area for the Beauport River is shown in Figure 8.1.

The Clair Creek runs through the community of Mont-Tremblant, located within the Laurentian Mountains, and discharges into the Devil's River. The upstream catchment is primarily forested with some urbanized areas. The total catchment area of the Clair Creek, considered for this study, is 34.5 km^2. The study area is shown in Figure 8.2.

For each study site, 10 river cross-sections were selected to provide a representation of flooding conditions within the project area. These cross-sections are shown in Figure 8.3 for the Beauport River and in Figure 8.4 for the Clair Creek. Flood extents corresponding the 100-year flood are also provided in these figures.

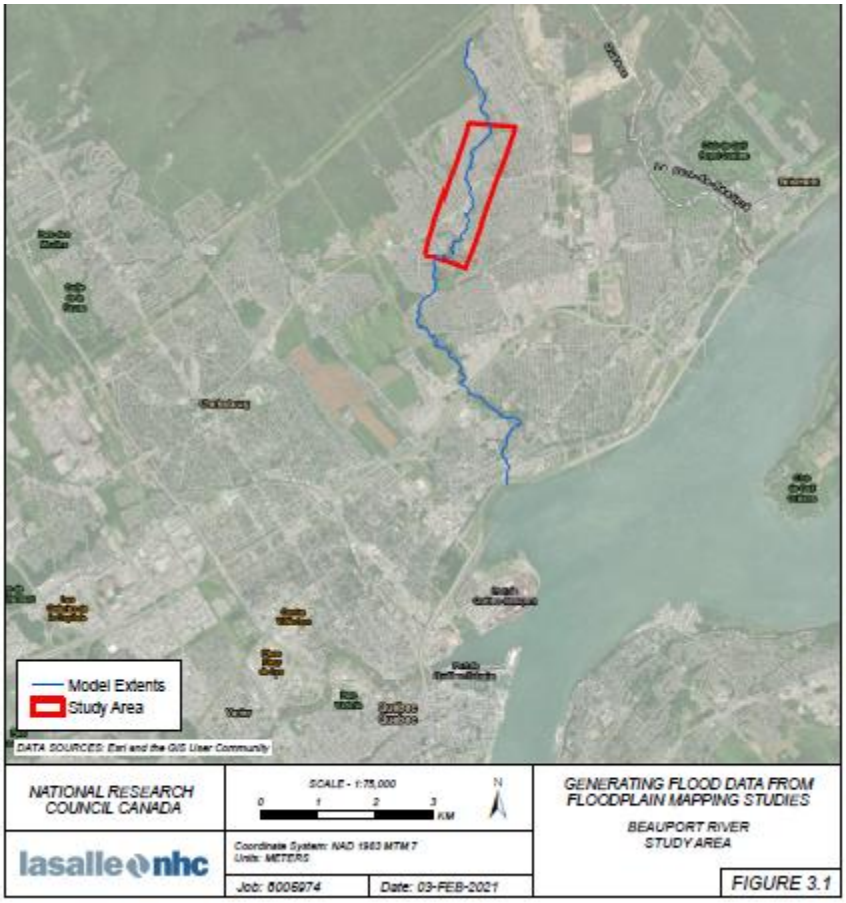

Figure 8.1: Study area for the Beauport River, Quebec urban community.

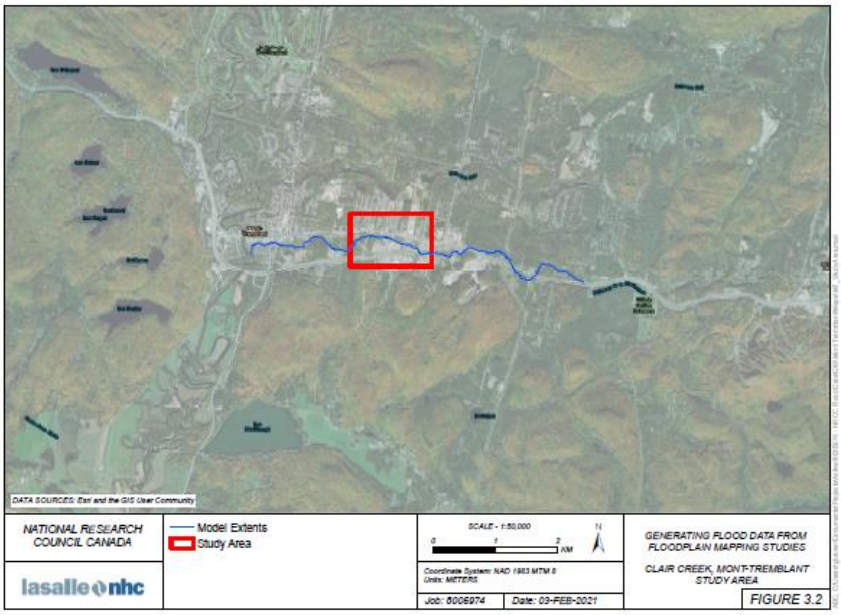

Figure 8.2: Study area of the Clair Creek, Mont Tremblant.

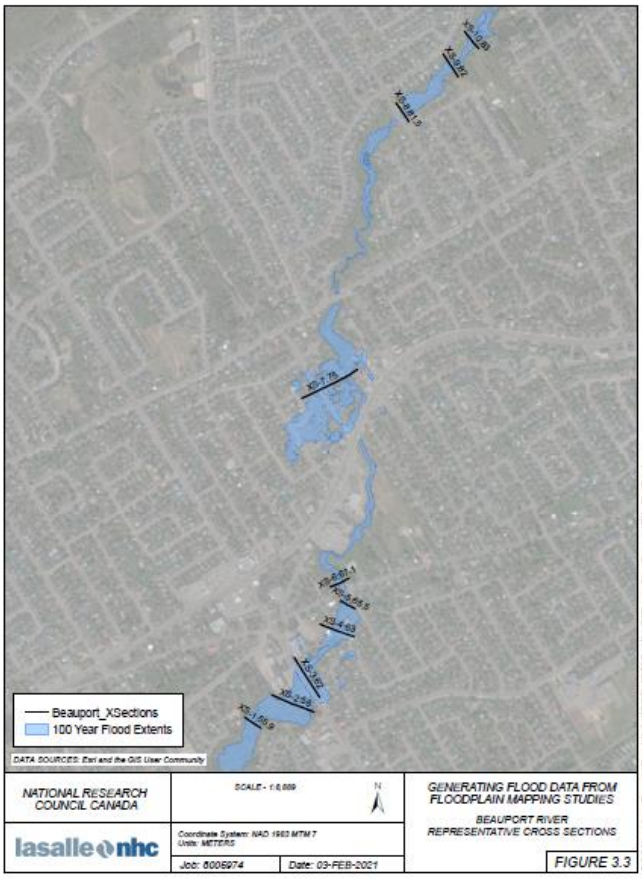

Figure 8.3: Representative river cross-sections along with the 100-year flood extents for the Beauport River.

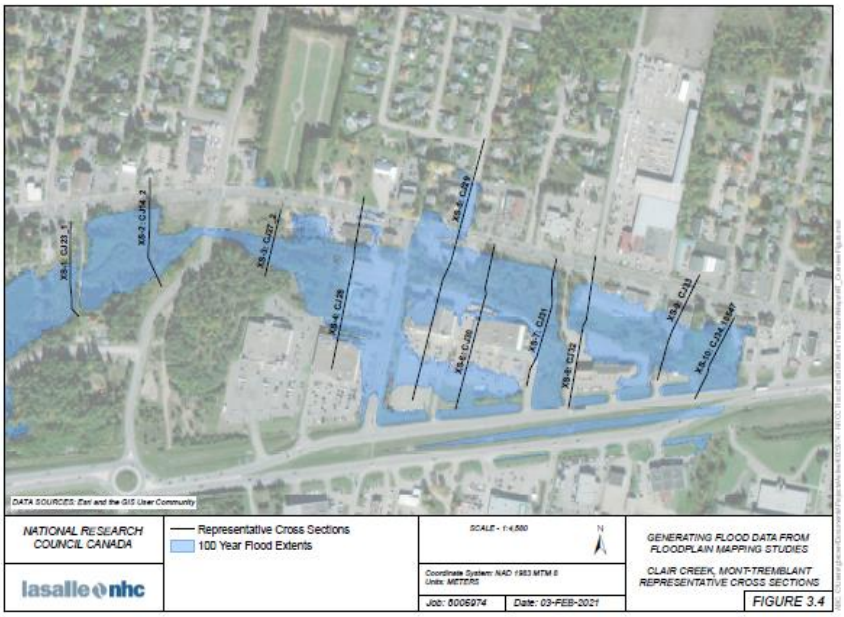

Figure 8.4: Representative river cross-sections along with the 100-year flood extents for the Clair Creek.

Each cross-section was divided into a number of panels (or save points) which cover the left overbank, main channel, and right overbank portions of the river cross-section. The information at the midpoint of each panel was considered as representative of the save point location. For each cross-section, two sets of panel widths were used. The channel section was divided into 3 panels of equal width. The panel width for the overbank sections was determined based on the channel topography and by maintaining a similar number of panels for all cross-sections. The panel topography was considered to avoid large changes in elevation across an individual panel. This strategy led to 17-20 overbank panels, with 20-23 total number of panels for both sites. Depending upon the cross-sectional geometry, the width for both the far left overbank panel and the far right overbank panel was smaller than the width of other panels.

Four selected cross-sections (out of 10) for the Beauport River are shown in Figure 8.5 and those for the Clair Creek in Figure 8.6. In these figures, the maximum water levels corresponding to 20-, 100-, 200-, and 2500-year return periods are also shown.

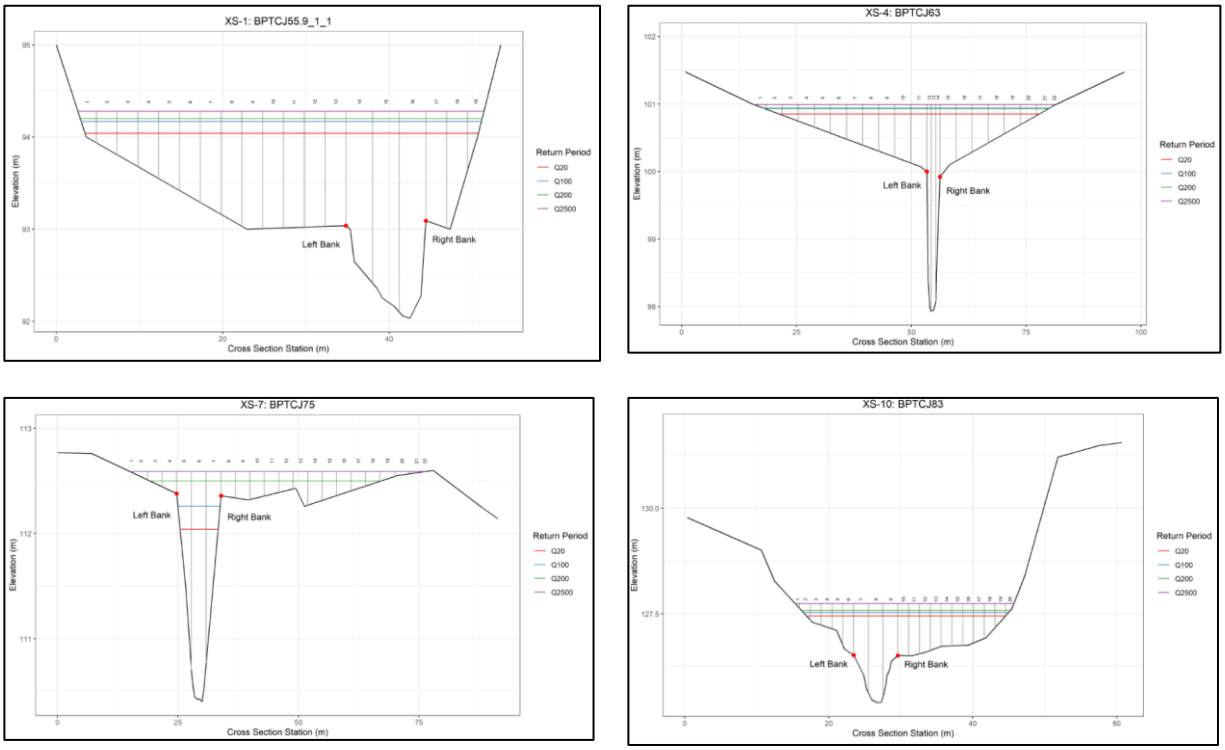

Figure 8.5: Selected cross-sections and the maximum water levels for the 20-, 100-, 200-, and 2500-year return periods for the Beauport River.

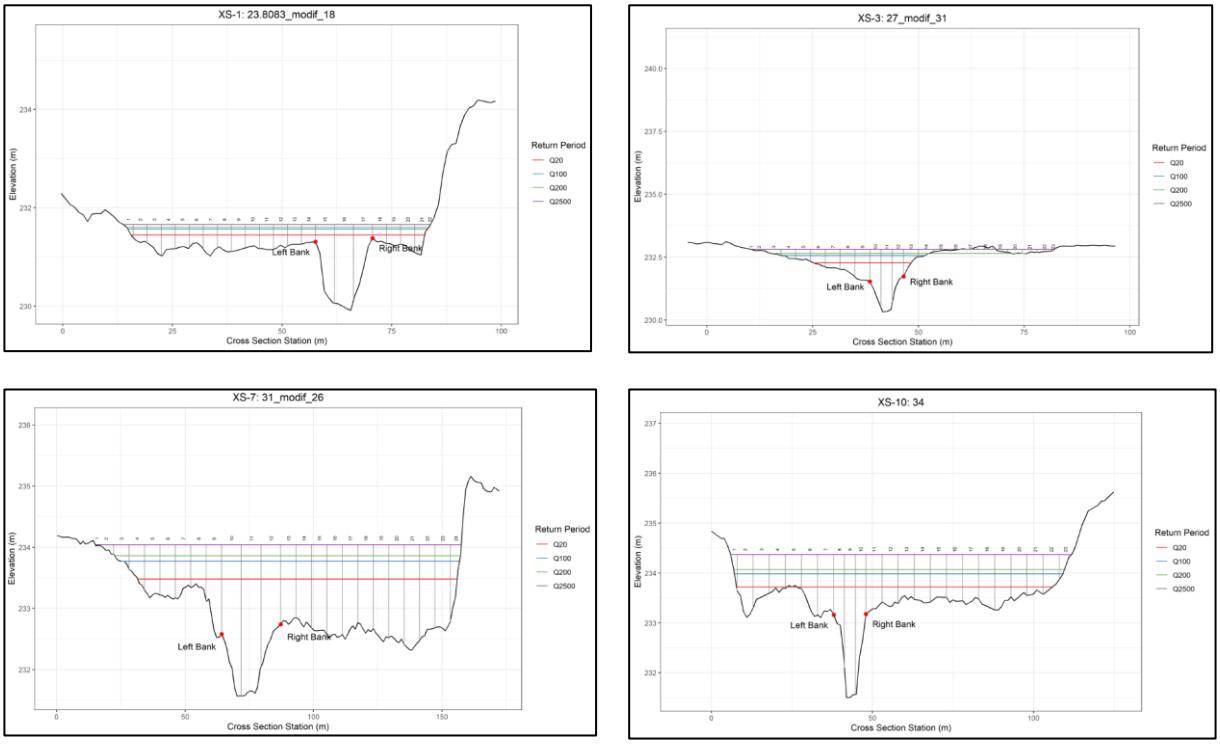

Figure 8.6: Selected cross-sections and the maximum water levels for the 20-, 100-, 200-, and 2500-year return periods for the Clair Creek.

8.3 Hydrologic Considerations

The existing studies for the Beauport River (LaSalle | NHC, 2019) and for the Clair Creek (LaSalle | NHC, 2018) were based on the 100-year design events. Information on the lower return period (i.e. 10-, 20-, 50-, and 100-year) floods was already available through these studies and that for the larger than the 100-year level were generated from the existing flood frequency relationships. However, it was cautioned that the flood magnitudes corresponding to larger return periods (e.g. 1000-year or 2500-year) are associated with considerable uncertainties due to limited at-site observations that were used in the development of flood frequency relationships.

8.3.1 Beauport River

In the original study for the Beauport River, 1D hydrologic-hydraulic model (i.e. PCSWMM) was used and the design flood was calculated based on the 24-hour storm following the Soil Conservation Service (SCS) approach. Intensity duration frequency (IDF) estimates were obtained from 57 years of data available at Environment and Climate Change Canada's Quebec Lesage International Airport station. The HyfranPlus software (Bobee and El Adlouni, 2015) was used for the development of IDF relationships based on the Gumbel distribution, fitted using the method of moments. Total precipitation amounts from the IDF analysis were used to develop synthetic hyetographs (24-hour SCS design storms) for each return period. These hyetographs

were applied to the contributing catchments within the PCSWMM to generate design flows for the Beauport River at the upper limit of the study area.

8.3.2 Clair Creek

In the original study for the Clair Creek, the same 1D hydrologic-hydraulic model, which was used for the Beauport River, was also used in this study. In this case synthetic hydrograph approach was used and that was designed to provide specified peak flows and volumes at the upper limit of the modelling domain for spring snowmelt events. In the absence of streamflow records for this river, design flows were scaled from those estimated from a nearby gauge, Saint-Louis (02LC043), with similar hydrologic regimes. Annual maximum flows and volumes for the springtime were analysed for Saint-Louis from 1969 to 2017 using the HyfranPlus software. The log-normal distribution was used for modelling flows and the generalized extreme value distribution for flow volumes. The resulting flows and volumes for Saint-Louis were scaled for the Clair Creek based on the ratio of the contributing catchment areas and a representative hydrograph, which maintained the desired design flows and volumes and represented the duration of a typical flooding event for the region, was developed. This was then integrated with the PCSWMM to generate flood levels for the Clair Creek.

8.4 Hydraulic Models

8.4.1 Beauport River

The PCSWMM setup was originally developed by Aquapraxis (2011) from the HEC-RAS setup, which was undertaken by the Centre d'Expertise Hydrique du Quebec (CEHQ, 2015). The PCSWMM and HEC-RAS models were compared by LaSalle in 2019 (LaSalle | NHC, 2019), who noted that the HEC-RAS model was not setup to deal with pressurized flows and submerged culverts. This was made possible in the PCSWMM setup and that led to a more physically realistic hydraulic model. In the PCSWMM based model, the same Manning's roughness coefficients and transects as used in the original HEC-RAS model were retained. However, the surrounding storm system which discharges into the Beauport River was also incorporated in the PCSWMM. This existing model was used, without any modification, for flood loads data generation. Two sample flood maps are shown in Figure 8.7 and Figure 8.8.

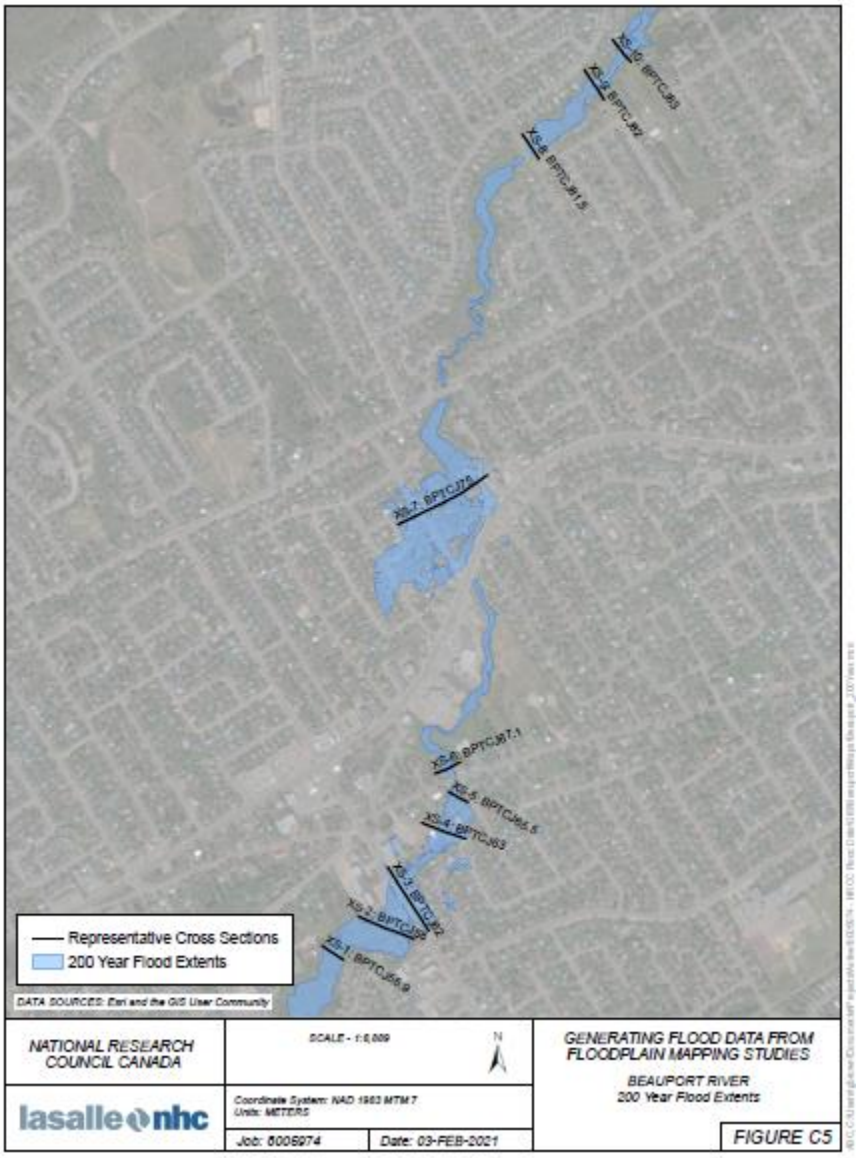

Figure 8.7: Flood inundation extents for the 200-year event.

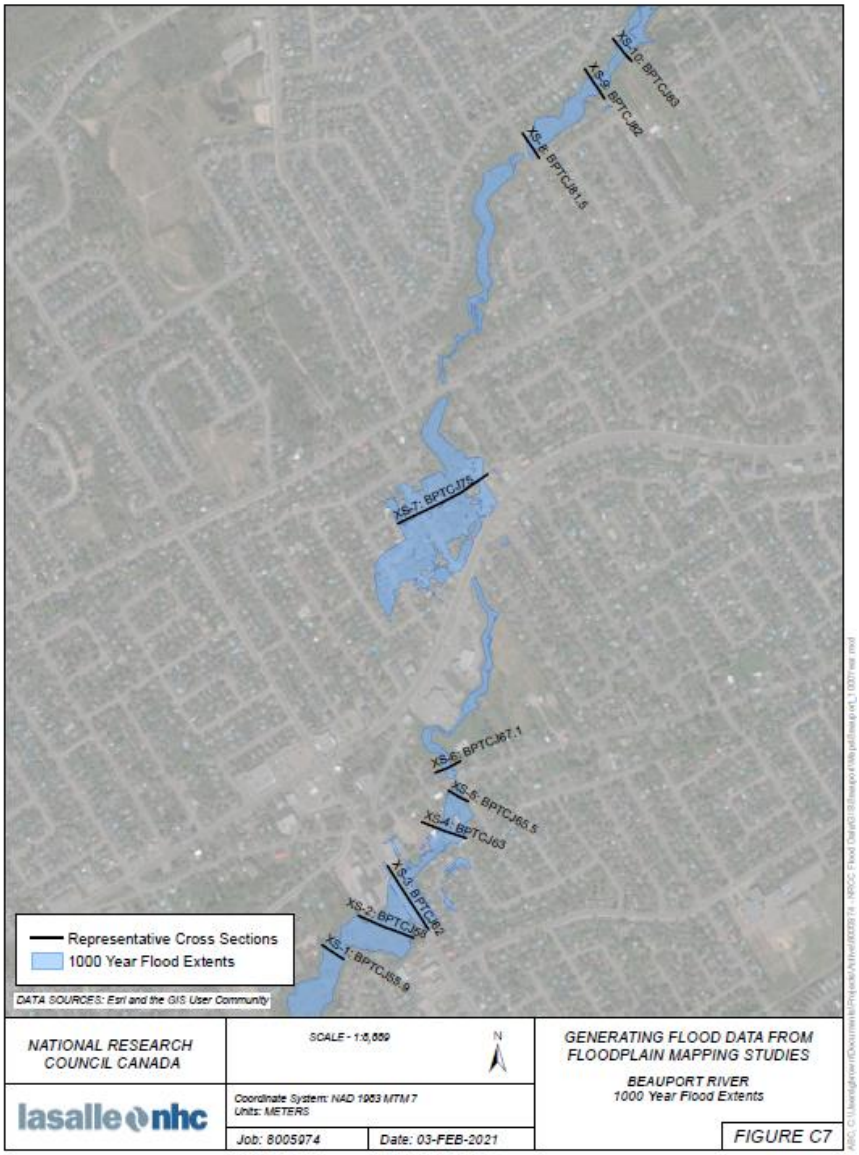

Figure 8.8: Flood inundation extents for the 1000-year event.

8.4.2 Clair Creek

The PCSWMM based hydraulic model for the Clair Creek was developed by LaSalle in 2018 (LaSalle | NHC, 2018). For the model development, an existing HEC-RAS model, which was developed by JFSA in 2015 (JFSA, 2015), was adopted as the starting point. In the new model, simulation of unsteady flow, inclusion of hydraulic structures located along the stream, and revised cross-sections based on LiDAR data were considered. The storm system of Mont Tremblant was not considered in the model. However, some minor ditches within the vicinity of the creek were included. This existing modelling system, without any modification, was used for flood loads data generation. Two sample flood maps are shown in Figure 8.9 and Figure 8.10.

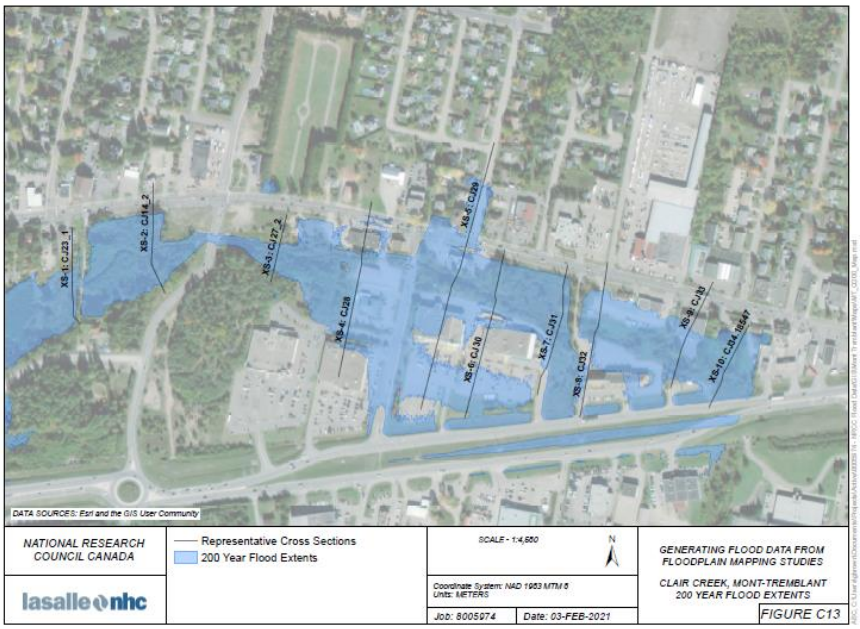

Figure 8.9: Flood inundation extents for the 200-year event.

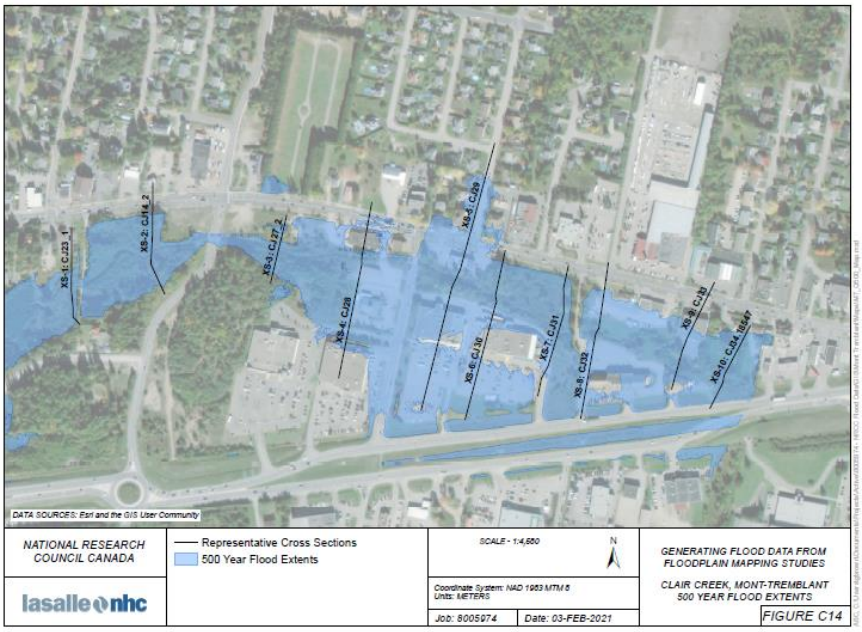

Figure 8.10: Flood inundation extents for the 500-year event.

8.5 Flood Characteristics

8.5.1 Cross-Section Characteristics

For each cross-section and return period, the following information was compiled:

- Cross-section location (latitude and longitude);
- Longitudinal location of cross-section from a downstream point;
- River discharge;
- Total cross-sectional flow area (including left overbank, main channel, and right overbank areas);
- Water level at the time of maximum flood (from a common datum);
- Mean flow velocity at the time of maximum flood (for the left overbank, main channel, and right overbank areas); and
- Kinetic energy coefficient alpha.

The discharge and water levels were extracted directly from the PCSWMM outputs at each junction corresponding to the transect location. The cross-sectional area was calculated based on the transect bathymetry and water level. The kinetic energy coefficient alpha was calculated using the methodology outlined in the HEC-RAS reference manual (Brunner, 2016). Ineffective flow areas were identified in some cross-sections for the Mont-Tremblant site. Ineffective flow areas are areas within the river cross-section that contain water but do not actively convey any flow. They are typically areas where water is expected to pond but will have a velocity close to zero. For such instances, the ineffective flow area was excluded from the transect velocity calculations.

8.5.2 Save Point Characteristics

For each save point and return period the following data was compiled:

- Locations of the save points along the transect with respect to the left limit of the transect;
- Latitude and longitude of each save point;
- Ground elevation of the panel centroid (taken to be the midpoint of each panel);
- Water level at the time of maximum flood (from a common datum);
- Local flood depth at the time of maximum flood (panel averaged depth and maximum depth);
- Local flow velocity at the time of maximum flood (section averaged velocity);
- Cross-sectional area of each panel;
- Manning's roughness coefficient;
- Panel width; and
- Relative conveyance.

Local velocity was calculated based on the effective conveyance of each panel within a transect. Using smaller subdivisions resulted in a slight increase in the overall hydraulic radius and thus the conveyance. This issue has also been discussed in the HEC-RAS manual (Brunner, 2016). Consequently, correction factors were required to be applied to ensure that the flows and conveyance in the left overbank, channel section, and right overbank match between the save point characteristics and the cross-section characteristics. Ineffective flow areas were noted in

some cross-sections for the Clair Creek site. For these areas local flood depths were obtained, but local flow velocities were set to zero.

8.6 Statistics for Flood Loads

Mean and standard deviation of the average flood depth, maximum flood depth, and local velocity for all save points were calculated corresponding to each return period. Similarly, at each site, a large sample was created for individual return periods and together for all return periods, considering all save points for all transects. The following summary statistics were obtained: mean and standard deviation of average flood depth, maximum flood depth, and flood velocity. These statistics were calculated for the left overbank, main channel section, right overbank, combined overbanks, and considering all locations.

8.7 Concluding Discussion

LaSalle conducted two case studies from Quebec to generate flood loads data: the Beauport River and the Clair Creek. For each case study, 10 representative cross-sections were selected with each cross-section being divided into a number of panels or save points. The existing hydrologic analyses and hydraulic models were expanded to accommodate calculations for larger than 100-year return periods, while noting that the flood parameters corresponding to larger return periods are associated with considerable uncertainties. Given the level of uncertainties, LaSalle cautioned on the application of data generated for larger return periods.

In the case of Clair Creek, a physical constraint was experienced within the selected reach of the stream, i.e. a reduction of flow in the downstream direction for return periods greater than the 500-year event. This decrease was associated with inadequate capacity of a bridge opening and as a result of this phenomenon, the flow backed up a ditch located perpendicular to the channel. LaSalle cautioned that the depth and velocity estimates for the impacted cross-sections 1 through 4 should be used cautiously.

LaSalle also conducted a sensitivity analysis by changing the number of panels for the Beauport River from 20 to approximately 50, 200, 1000 and 5000 panels for each transect. It was found that as the number of panels increased the flood depths converged to a single value because the cross-section was more finely discretized. The average flood depth was found to be relatively insensitive, while the maximum flood depth was found to be more sensitive to the number of panels. Future studies may shed additional light on these aspects.

9 Northwest Territories – Coastal Flooding Case Study

9.1 Overview

Baird and Associates were contracted to undertake coastal flood modelling and flood loads data generation case studies in large lake and northern environments. Two large lake case studies are presented in Chapter 7. In this chapter, the northern case study for the Tuktoyaktuk Hamlet, Northwest Territories, is presented. Baird has been undertaking coastal flood modelling studies at these sites for their regional clients. By selecting these sites where there were ongoing studies, considerable efficiencies were realized as much of the background data sources were already compiled and the models were already set up or some preliminary framework was already in place. There were also considerable gains in terms of data pre-processing and modelling experiences. The existing studies were extended to satisfy the requirements of flood loads data generation case studies of the NRC. This also involved establishing agreements with other clients for sharing of data.

Tuktoyaktuk is located on the Beaufort Sea at the eastern edge of the Mackenzie River delta (Figure 9.1). The delta setting means that water depths in the area are quite shallow over a broad offshore distance; it is approximately 30 km until a 10 m water depth is found in this area. This shallow nearshore area experienced significant storm surges when strong onshore winds occur.

The long period of seasonal ice cover also plays an important role in defining how flooding occurs at the site. Surges are mostly absent when the area is covered in a solid ice sheet since the wind stress acts on a shore-fast (mostly fixed) ice sheet, rather than the water. There is typically less than five months of open water at the site. Tides in the area are very small and therefore the surges become very important in defining the flooding potential at the site. The region is also faced with a land subsidence issue, which is in the range of 1.3 mm/yr. When combined with sea level rise of about 2.4 mm/year (over the past 50 years), this results in an effective sea level rise of 3.7 mm/year (Ford et al., 2016).

Topography in the Tuktoyaktuk area is extremely different from many other regions in central and southern Canada. The large amount of ice content in the ground results in formations such as thermokarst lakes and pingos and a very irregular shoreline. There is no bedrock in the Tuktoyaktuk region, meaning that most of the shoreline is very prone to erosion. Baird's ongoing work for the village of Tuktoyaktuk focused on both the village and the island that protects the harbour. For this study, the focus was on the village, which is located on the peninsula (see Figure 9.2).

The information included in this chapter is directly extracted from the case study report prepared by Baird and Associates (Baird, 2021b). Detailed information on the modelling procedures,

assumptions made, compromises on data availability, data sources, and data preparation and modelling procedures is available in this reference.

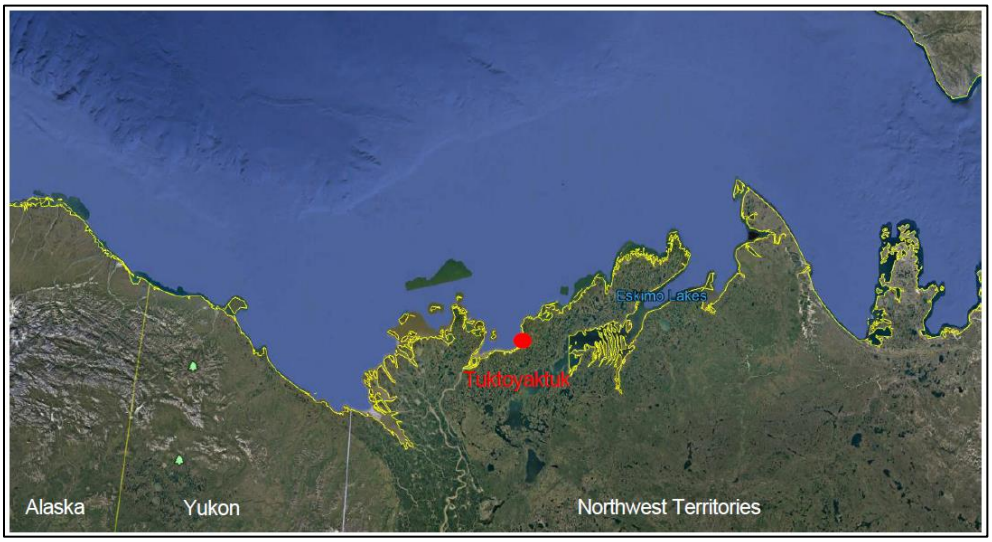

Figure 9.1: Tuktoyaktuk study site, Northwest Territories.

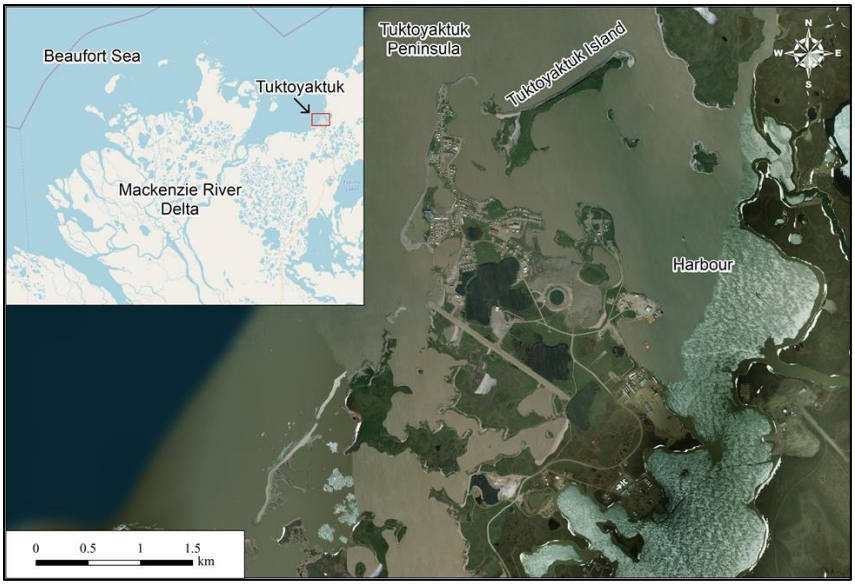

Figure 9.2: Tuktoyaktuk study aerial imagery, showing Tuktoyaktuk Peninsula, Island, and the Harbour. Inset shows Mackenzie River delta.

9.2 Data

Various datasets were required to accomplish the coastal flood modelling case study. A brief description of these datasets is provided below for contextual purposes. In addition, some information on the impacts of climate change on coastal flood risks is also discussed.

9.2.1 Topography and Bathymetry Data

A LiDAR topographic survey of the Tuktoyaktuk area was conducted by Airborne Imaging Inc., from July 19 to August 9, 2004. This data was available through the Geological Survey of Canada and was used in this project to delineate various topographic features.

9.2.2 Shoreline Erosion and Protection

Over the past 45 years there have been a range of shoreline protection measures put in place to protect the Tuktoyaktuk site. Most of these have been about mitigating erosion hazards, rather than preventing flooding and its consequences. Therefore, all erosion protection measures were undertaken in isolation.

9.2.3 Wind Data

Wind data from the Tuktoyaktuk Airport were obtained from Environment and Climate Change Canada. The wind rose shown in Figure 9.3 indicates that winds were predominantly from the east to southeast and from the west to northwest in this region. The peaks-over-threshold extreme value analysis of wind speeds at Tuktoyaktuk Airport was completed to estimate wind speeds corresponding to various return periods for storm surge analysis. In this analysis, all wind directions and data from the full year were considered. The Meteorological Service of Canada (MSC) hindcast was also valuable as a source of wind data for this site. This provided a gap-free hourly wind record from 1970 until 2015, which was extended by Baird until 2018.

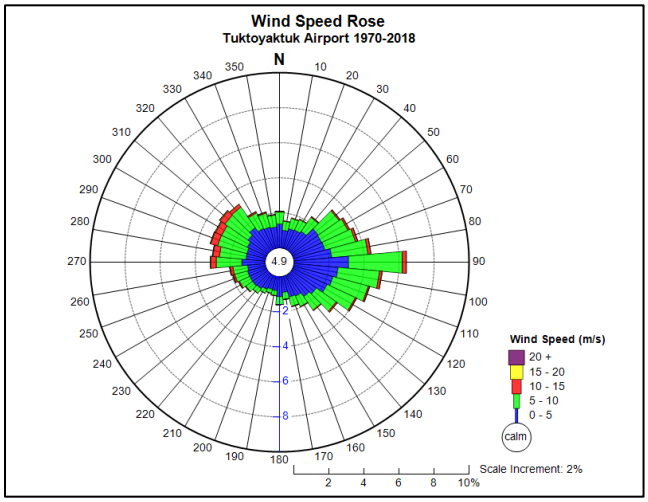

Figure 9.3: Wind speed rose for Tuktoyaktuk airport for the period 1970-2018.

9.2.4 Sea Ice Conditions

Sea ice conditions were classified by means of ice charts, developed by the Canadian Ice Service from remote sensing data. For this study, ice extents were acquired for the Western Arctic, in which Tuktoyaktuk is located. Weekly ice data is available from 1968 to the present time.

A review of the ice data indicated that the open water season is typically from some time point in July until November, although there is some variability in the start/end dates. To avoid such uncertainties, August through October period was considered more reliably open and therefore was selected as true “open water” months for this study.

9.2.5 Wave Data

Hindcast wave data offshore of Tuktoyaktuk was obtained from the MSC Beaufort Sea hindcast (Swail et al., 2007; Wang et al., 2015). The hindcast is a computer model simulation of wave conditions developed from wind, atmospheric pressure forcing and open-water extents. The model covers a 46-year period from 1970 to 2015.

9.2.6 Water Levels

Water levels at Tuktoyaktuk are modulated by tides and surges. Tuktoyaktuk is microtidal, meaning tides are small with a spring tide range of approximately 0.3 m. Recorded water levels at Tuktoyaktuk Harbour (Station Number 6485) were obtained from the Department of Fisheries and Oceans Marine Environmental Data Service. Hourly water level data were available from November 1961 to the present with several large data gaps.

9.2.7 Tidal Water Levels

During storm events, surge can be significant due to the wide, shallow offshore shelf. Surges of up to 2.5 m have been documented. This is of concern, due to the low topography. Surge is a function of wind speed, direction and duration, fetch and ice cover, which may limit the fetch. Predicted tide levels were generated for Tuktoyaktuk using established tidal constituents from the Canadian Hydrographic Society. The tide range at Tuktoyaktuk was found to be about 0.3 m. Mean tide water level is about 0.44 m above Chart Datum. A time series of hourly water levels at Tuktoyaktuk was predicted from the tidal constituents using the MIKE21 software package. The predicted tides for 2019 are shown in Figure 9.4. All water levels are referenced to Chart Datum.

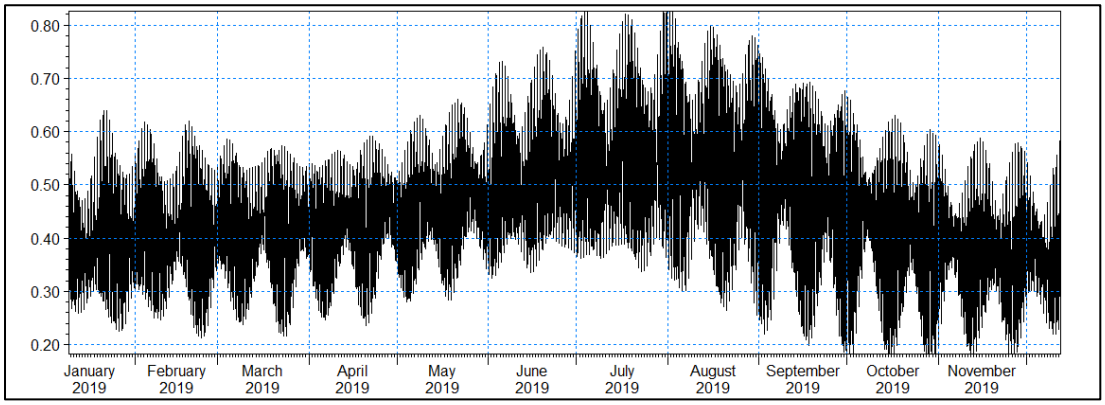

Figure 9.4: Predicted tide levels at Tuktoyaktuk (referenced to Chart Datum).

The “bulge” in the predicted tide levels during the summer months could be the result of non-astronomical forcing such as meteorological effects, ice cover, and/or flow from the Mackenzie River. The envelope of predicted tide levels by season is shown in Figure 9.5. This figure shows that mean water levels in late July and early August are approximately 11 cm above the mean water level for the year. This coincides with the open water season, when surge may occur causing the Tuktoyaktuk shoreline to be exposed to erosion and flooding risks.

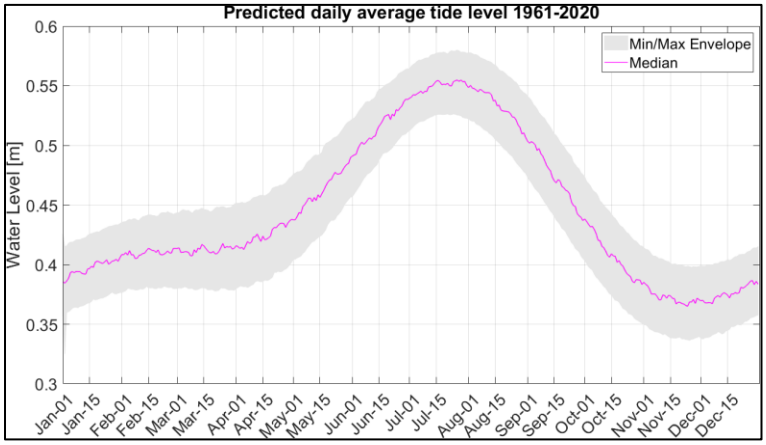

Figure 9.5: Envelope of predicted tide levels by season for Tuktoyaktuk.

9.3 Storm Surge

Storm surge is a primary concern at Tuktoyaktuk due to flooding and shoreline erosion. The elevated water levels allow larger waves to propagate to the shoreline which increases the damage potential. Additionally, flooding may cut off parts of the community putting lives and property at risk. When assessing measured data, storm surge was defined as being the departure of the water level from the predicted water level. The predicted water level was defined by tidal constituents; however, there are also other factors that can affect the mean water level in the area that cannot be reliably defined in the historical data. Flows in the Mackenzie River and nearby ice can impact water levels, as is the atmospheric pressure. Therefore, the historical storm surges were assessed by examining recorded water levels and developing a correlation between the surge level and the wind speed. The overall threat of flooding at the site is largely a function of storm surge, but also whether that surge happens at a high vs. low tide, spring vs. neap tide. The threat is also affected by whether there is a general increase or decrease in the mean water level over the surrounding few days, as these departures from the mean level play an important role in defining the overall water level.

9.3.1 Storm Surge from Measured Water Level Data

Hourly water level data from 1961 to 2018 were obtained for the tide gauge at Tuktoyaktuk. Storm surge was estimated by subtracting the predicted tide level from the measured water level.

An example of the estimated surge levels at Tuktoyaktuk is shown in Figure 9.6 for the August 16-18, 2018 storm event (water levels are reported in Chart Datum).

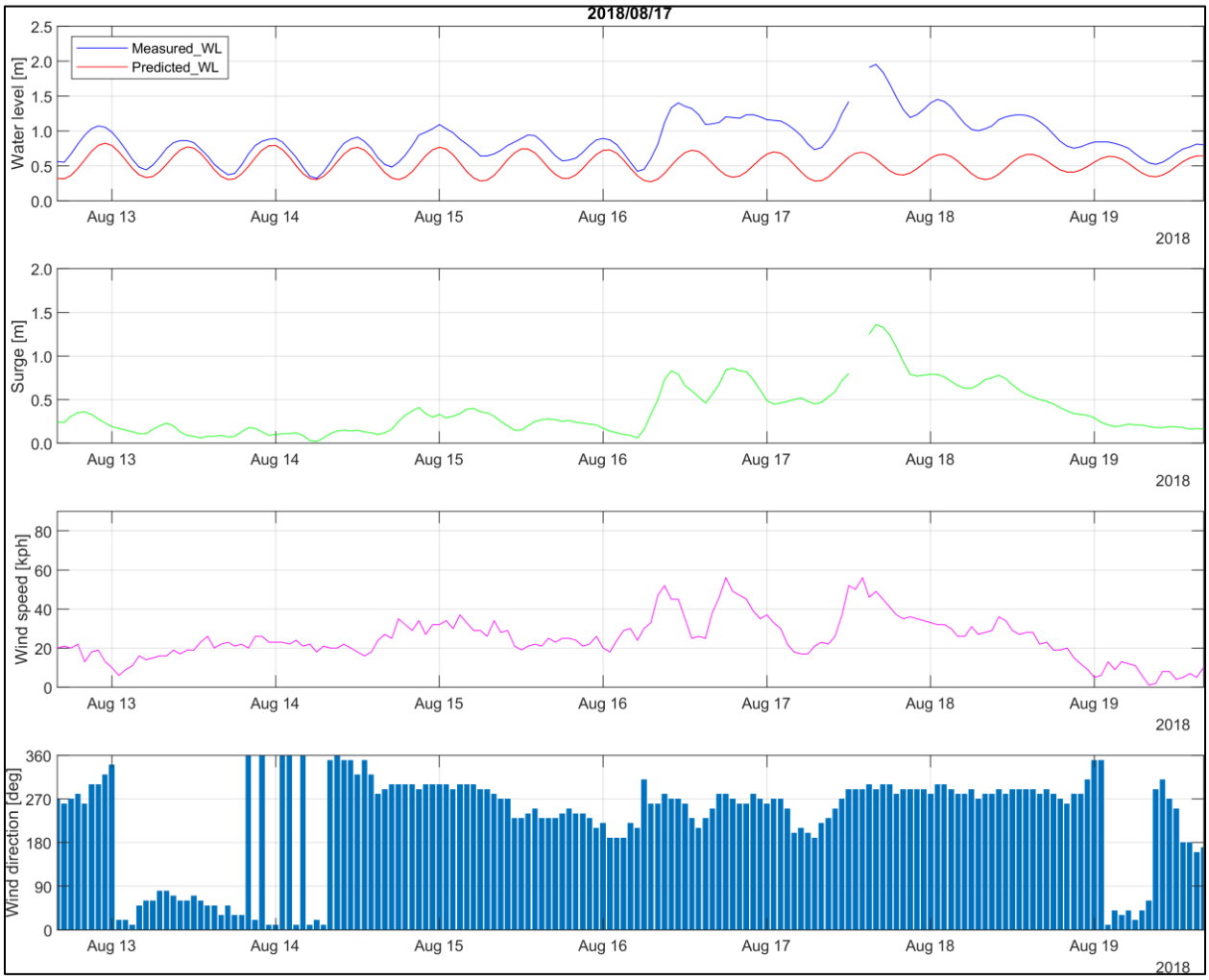

Figure 9.6: Water levels, estimated surge and wind data (both magnitude and direction) from August 2018 storm.

A peaks-over-threshold analysis was conducted on the data from 1961 to 2018 to identify independent storm surge events. The peak storm surge within 12 hours of the peak water level, and peak wind speed within 2 days of the peak water level were identified for the analysis.

9.3.2 Storm Surge versus Onshore Wind Speed

The relationship between storm surge and wind speed was analyzed for the open water months only, with July being excluded as it is often a smaller region close to shore that is open. A few things became evident from this analysis, i.e. (1) The storm surge to wind relationship was found to be concave upwards; (2) The theoretical value was found to be generally lower than the measured events; and (3) Lot of variability was noted in the measured data; for example, a wind speed of 14 m/s could result in a surge from 0.9 to 1.5 m. The last point was critical as it

indicated that there were other processes occurring at the site that affected the surge magnitude and also the background (baseline) water level that was used to define the surge (a deviation from the predicted tide level). The fitted polynomial relationship (i.e. Surge = $0.0017 \times Wind^2 + 0.0264 \times Wind + 0.083$) showed the correct slope and upward curvature. However, the scatter in the data was quite large, i.e. the scatter was larger at the higher wind speeds than the lower wind speeds.

9.3.3 Random Event Simulations

By recreating the surge-wind speed scatter, it was possible to create many random realizations. This was important because a strong wind event could randomly occur at any tide level and also at any other "residual level" (variation from the expected mean water level not attributed to strong onshore winds). The next step in the process was to assess the historical storms from the MSC hindcast. This source was chosen as it provided continuous hourly data coverage with no gaps and was shown to be statistically very similar to the measured data (including at extreme levels). Storms within the open water season were identified and the component of the onshore wind was used to assign a surge value based on surge-wind speed polynomial relationship.

9.4 Climate Change

An assessment of climate change impacts was undertaken by the University of Toronto in support of design criteria development for the project. A conservative high-end estimate of sea level rise at Tuktoyaktuk was found to be about 0.4 m by mid-century and just over a metre by the end of the century. Increases in the length of the open-water season could lead to two months (by 2040-2060) and three to four months (by 2080-2100) longer ice-free season at Tuktoyaktuk, with accompanying sea ice thinning, reduction in freezing days, and general warming. For Tuktoyaktuk, changes in winds are uncertain, but recent evidence suggests that mean winds will strengthen and extreme winds might greatly increase owing to climate change. This assessment will need to be updated as new model simulations and observations become available.

9.4.1 Sea Level Rise

Global mean sea level rise from climate change, relative to the Earth's centre, is anticipated to be up to a metre or more by the end of the century, owing to the combined effects of land-ice melt (which provides direct input of meltwater into the global ocean) and thermal expansion of the global ocean from enhanced energy input (the steric effect). Over the past roughly 50 years at Tuktoyaktuk, sea level has risen about 2.4 mm/year (Ford et al., 2016). Tuktoyaktuk and much of the Beaufort Sea coast have had modest crustal subsidence contributing to relative sea level rise. James et al. (2014) report that the apparent sea level rise from vertical crustal motion for Tuktoyaktuk is approximately an additional 1.3 mm/year, for a total of 3.7 mm/year of sea level rise. For the design of a coastal structure in Tuktoyaktuk, it will be necessary to consider future water levels. The selected future change to the water level will need to consider the expected

design life of the structure as well as the emissions scenario the designer believes is the most appropriate (this may depend on risk tolerance and many other aspects).

9.4.2 Changes to Sea Ice

The University of Toronto (Kushner et al., 2018) undertook data analysis on projected changes for the sea ice environment. Projections were developed for the 2040-2060 and 2080-2100 period. Recognizing that future projections of sea ice changes are highly uncertain on regional scales, model sub-selection was used to develop site specific projections for the project area.

9.4.3 Changes to Wind Environment

The strongest wind events at Tuktoyaktuk, which drive strong storm surge events causing coastal erosion, are northwesterly winds along the fetch during the open-water season and conditions of low static stability (Small et al., 2011). Traditional knowledge sources indicated that recent changes in wind velocity, direction, frequency, and increased frequency of extreme weather events and storm surges are also occurring. However, the relationship between wind, open-water season, and storm surges and other extreme events remains challenging to assess. Based on the Baird's investigation, there was insufficient information to draw strong conclusions about the magnitude of these changes, which increases the level of uncertainty for assessing flood risks in the future.

9.5 Modelling Approach

9.5.1 Surge Modelling

The modelling approach for Tuktoyaktuk was similar to the approach that was used for deriving statistics for the site. Historical storms were selected from the record based on the intensity of their onshore wind speed, and the approximate surge at the site was calculated based on the relationship described by the surge-wind speed polynomial relationship, discussed above. A shift in the water level was applied, representing a combination of the tide level and a random value for the departure of the mean water level from the normal mean value. The flooding potential at the site was found to be linked to the combined occurrence of high water levels and large waves. These two processes were created by the same factors (strong sustained onshore winds) and the wave height at the site, which was depth-limited in the nearshore (the waves will be as large as the water depths permit). Therefore, the flooding potential at the site can be directly linked to the water level.

A numerical model of the region was developed using the MIKE21 Flexible Mesh (M21SW) hydrodynamic model. The model covered the region from the deep water (~1000 m deep) to the site. The offshore boundary was defined as the tide level at the site (plus any deviation from the mean), with lateral boundaries (SW and NE sides) as closed boundaries. A view of the mesh in

the region close to the site is shown in Figure 9.7. In the region close to the site, the mesh reduces to a spacing of about 10 m, which allows for details of wave breaking over the nearshore areas to be properly represented.

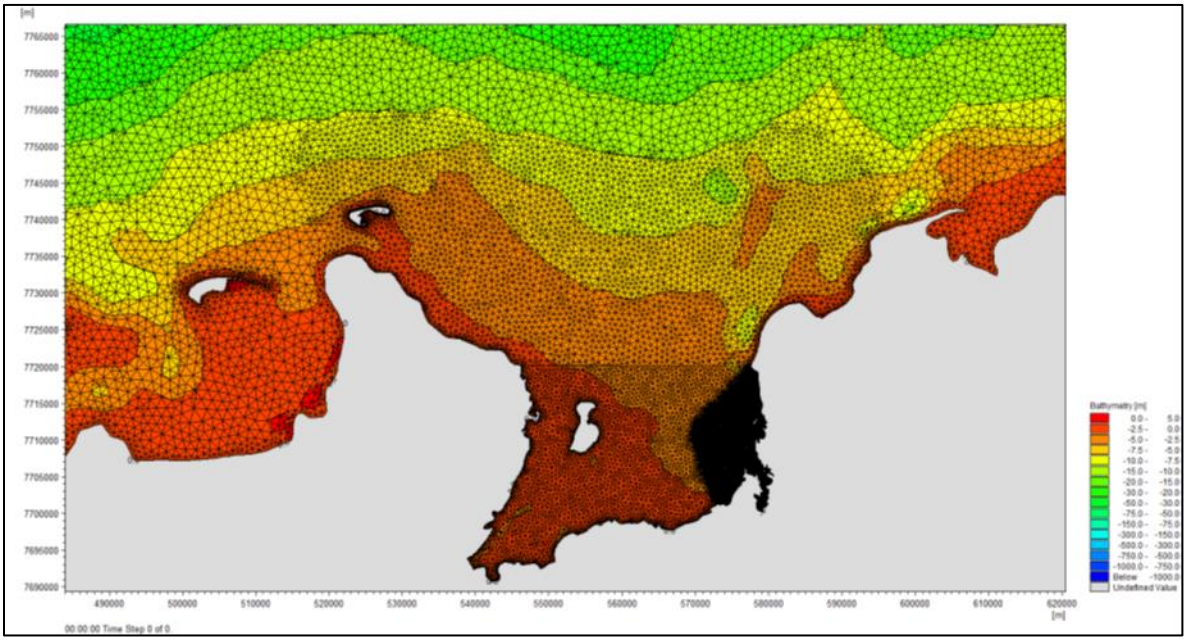

Figure 9.7: A close-up view of the numerical mesh near the study site.

Also, the model mesh does not extend into the overland area where roads and houses may be flooded during an extreme event. In general, in coastal modelling applications for large sections of the shoreline, it is not practical to simulate the runup and overtopping processes that occur using a large scale two-dimensional model. Instead, this type of modelling is accomplished with profile models that simulate the transition of waves from the nearshore area (perhaps 5 m water depth), up the shore face and into the backshore area.

9.5.2 Selection of Events

The events that were modelled were selected based on specific wind events that occurred at the site, as defined by the MSC hindcast. The most extreme open water storm of 1970 was used for the higher events, including a scaling of the wind speed for the 500- and 1000-year events. Storm conditions were selected independent of whether or not open broad areas of water existed at the time of the storm. The focus was on using realistic wind fields rather than on calibration to measured water levels (not available for most of the large storms). An example of the water level during the scaled 1979 event (representing the 1000-year event) is shown in Figure 9.8.

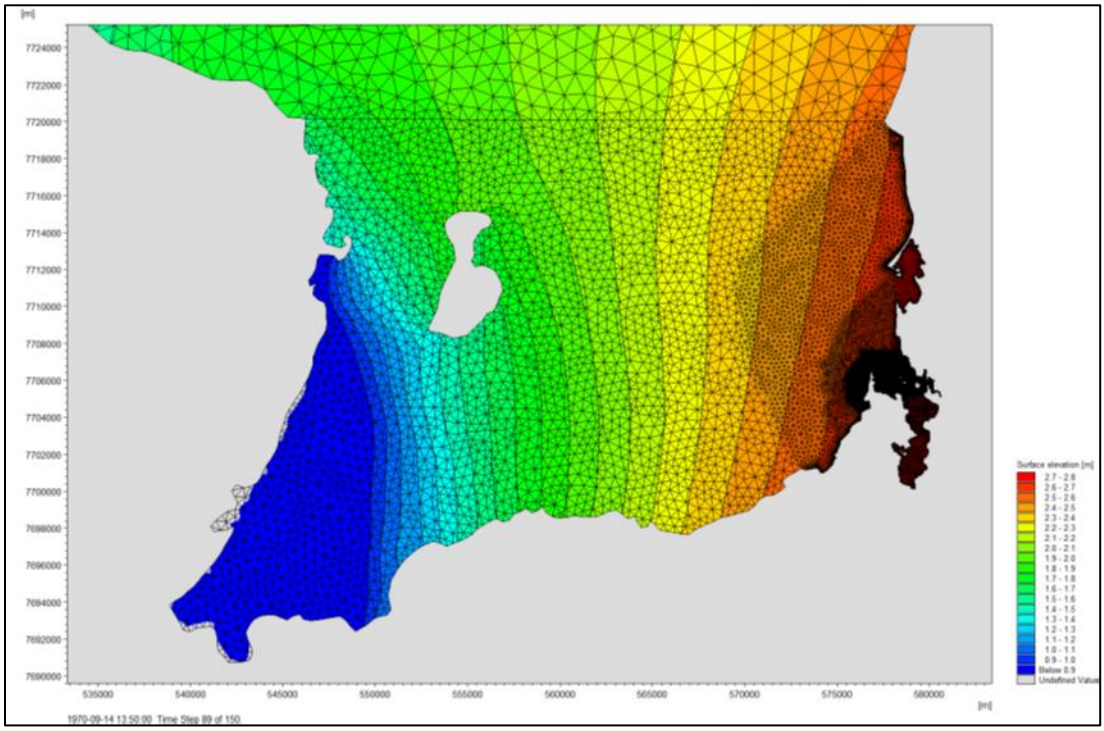

Figure 9.8: Water level during the scaled 1979 storm (1000-year event).

9.5.3 Wave Modelling

Wave modelling was completed using the M21SW model with the same bathymetric mesh as that used for surge modelling. The model uses fully spectral wave equations and has an advanced wave breaking formulation in shallow waters, which is important for the site. The wave simulations covered about 18 hours before the peak of the surge, and about 6 hours after the peak. The final process of determining the wave height at the shoreline relied on the equation of Goda (2010). Goda's method is well-accepted for determining the significant and maximum breaking wave height at the toe of the structure, as a function of nearshore bed slope, water depth, wave height, and wave period. Profile measurements from the bathymetric survey were examined to categorize the slope leading to the base of each shoreline profile. Shoreline slopes were typically in the range of 10:1 to 100:1; a few of the nearshore areas were essentially flat.

9.5.4 EurOtop Modelling

The CSHORE model, used for the Lake Erie sites, is really intended for beaches and not for semi-armoured shorelines at Tuktoyaktuk, which required a different approach. Empirical methods described in the EurOtop overtopping manual (EurOtop, 2018) were used to estimate wave runup and overtopping of the Tuktoyaktuk hamlet shoreline. Guidance in the manual is largely based on physical model experiments carried out for standard configurations for coastal dikes, embankment seawalls, rubblemound slopes, and vertical sea walls found in Europe.

Because these data are obtained from physical model tests, processes such as wave setup are inherently included in the approach, as well as the various modes of overtopping that occur.

Wave Runup

- Wave runup is the maximum vertical height a wave can reach on a shoreline or structure above the still water level.
- Wave runup does not result in any flooding landward of the slope as the water simply runs up the slope and then back down into the sea.
- While runup does not cause flooding, the up rushing wave can still cause damage to structures in this zone.
- The zone of wave runup and rundown can be rather large and may vary between 1 and 4 times the wave height at the toe of the slope.

Wave Overtopping

- Wave overtopping occurs when the crest height of the shoreline or structure is lower than the runup elevation, resulting in water flowing over the crest and causing flooding of the back shore area.
- Wave overtopping is generally expressed as a flow rate per meter length of the structure (L/s/m).
- The height of the water as it flows over the crest of the structure is referred to as the overtopping height.
- Wave overtopping results in flooding that may range from mild to severe. A lower crest elevation leads to lower overtopping elevations but higher overtopping rates. In layman's terms: "more water flowing over but at a lower level".

Determination of Wave Runup and Overtopping

The EurOtop model was applied to 18 profiles along the shoreline of Tuktoyaktuk, as shown in Figure 9.9. Profiles P0000 through P1110 were simulated, with the exception of P0950 due to the low lying nature of the profile and conditions beyond the crest being open water.

Figure 9.9: Positions of 21 shoreline profiles in Tuktoyaktuk, identified for collecting flood loads data.

The empirical methods in EurOtop require that the shoreline profiles be schematized using 14 parameters describing relative elevations, widths, slopes, armour size, and roughness. The user must select the relevant empirical equations according to the shoreline/structure type, influence of the foreshore, and structure slope. Following this, the user then applies a series of influence factors to account for composite slopes and berms, roughness, angle of wave attack, currents, and the presence of promenades and storm walls at the slope crest. A flow chart is provided in the EurOtop manual to assist with this process. The EurOtop is a Machine Learning based overtopping prediction tool and contains a database of over 13,000 wave overtopping experiments. The tool is provided online as a companion to the manual and automatically selects the physical model experiments that are most similar to the parameterized data. The EurOtop model was used to verify the results of empirical calculations as a quality control.

Runup and Overtopping Estimates

Wave runup elevations and overtopping rates were estimated at the 18 shoreline profiles for various events, representing offshore conditions (i.e. onshore wind and total surge corresponding to 20-, 50-, 100-, 200-, 500-, and 1000-year return periods) and wave conditions based on three historical events (scaled and unscaled). Water level and wave data were obtained from the M21SW and Hydrodynamic models at the end of each profile on an hourly time step. Because the EurOtop model is not a physically based model it is not possible to extract data at different locations along the slope of the profile. This does not create a problem for assessing structural impacts since there are rarely (never in Tuktoyaktuk) structures along the seaward slope of the revetment or rubble slope. At the crest of the structure the volume of overtopping and the height

of the wave are defined by the EurOtop tool. The landward extent of overtopping flow (past the end of the profile) is calculated using a modified form of the Cox-Machemehl equation (Cox and Machemehl, 1986), which relates the decrease in flow depth with distance from the structure crest.

Wave Impacts on Buildings

Depending on the position of an asset, there could be flooding and possibly damage as a result of wave impacts in the nearshore area. Coastal high hazard areas are defined as areas where wave action and/or high velocity water can cause structural damage to buildings during the design storm event.

9.6 Storm Simulations

Storm simulations of Tuktoyaktuk flooding were completed, including the more extreme event, i.e. the 1000-year event. This event was defined based on applying a historical storm wind to a significantly increased mean water level. With all of the uncertainties in the water level, related to tides, Mackenzie River flows, ice effects, etc., this increase in the mean water level was determined to be a more likely scenario than exceptionally strong winds on a more normal mean water level.

9.6.1 Wave Runup Summary

In most instances, the runup was well above the crest level, indicating significant overtopping of the shoreline. EurOtop also provided the overtopping rate (typically in m^3/s per metre of shoreline); however, Baird did not report this value for this study since the geometry inland was not aligned with the way EurOtop methods were developed. EurOtop assumes that the structure is a dyke with a downward sloping inland side. Many of the profiles were truncated on the crest (in front of buildings) before a gentle rise in the topography. This means that the overtopping rate would be an overestimate as much more of the water would reverse and flow down the front face of the structure.

The EurOtop equations were developed from physical model studies where the wind driven elements were not included. This makes the overtopping volume estimates more uncertain for coastal structures compared to beaches; however, overtopping is still a roughly estimated parameter. The results of the six selected storm events (corresponding to 20-, 50-, 100-, 200-, 500-, and 1000-year return periods) were developed and two sample cases are shown in Figure 9.10 and Figure 9.11 that include all profiles.

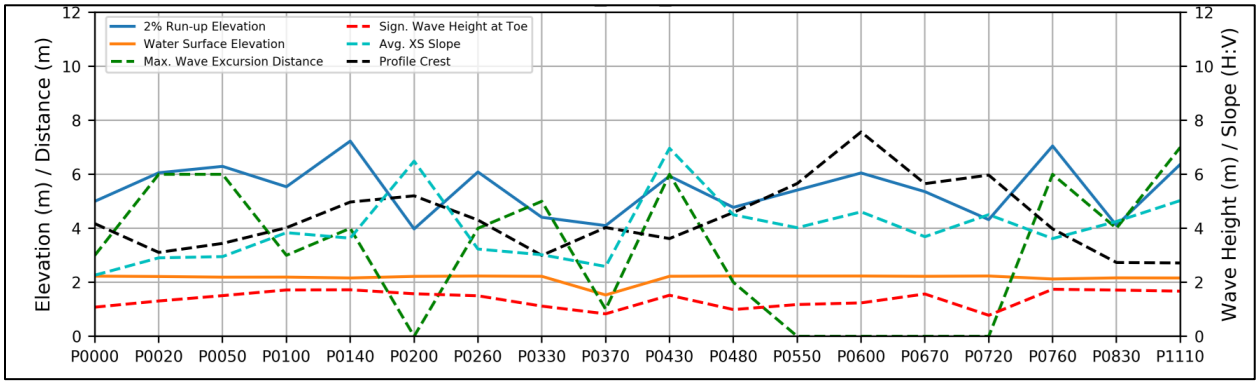

Figure 9.10: Results from the 100-year storm event (September 1970).

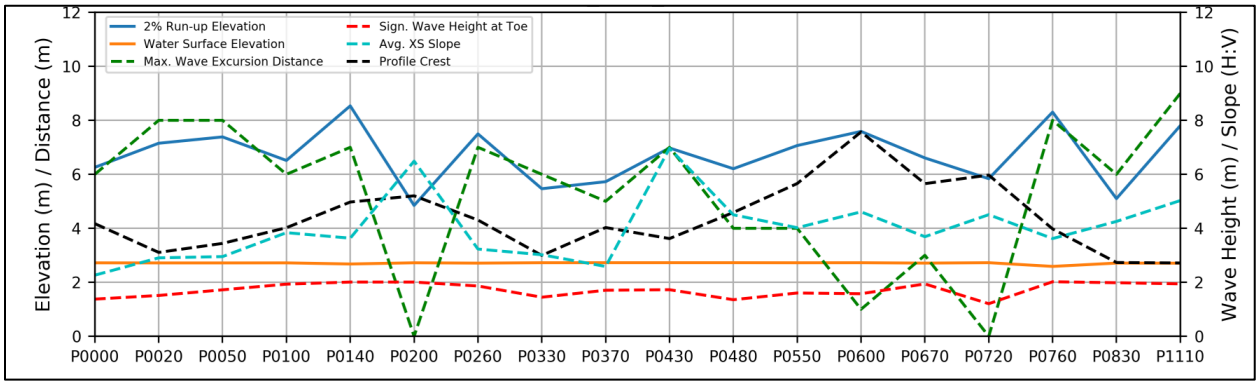

Figure 9.11: Results from the 1000-year storm event (September 1970), with raised water level and scaled wind.

9.6.2 Data for Flood Load Calculations

In this harsh northern environment there were no structures on the steep shoreline slopes and therefore the flooding information from the EurOtop model was not so useful. The distance inland above the structures where wave action generally occurs was also narrow, and therefore the data was extracted with a much tighter spacing (i.e. 1 m) compared to the Lake Erie coastal sites where the spacing was 5 m. One table was assembled to summarize the offshore conditions at all profiles, and another for save points along each profile. The following flood loading related variables and parameters were compiled and included in tables:

- WL (m): The water level in meters corresponding to the coordinates of the profiles and save points;
- Hm0 (m): The offshore significant wave height in meters;
- Tp (s): The offshore peak wave period in seconds;
- Profile Crest (m): The crest of the profile in meters;
- Ground Elevation (m): The ground elevation at each save point in metres;
- Ru2% Elevation (m): The 2% runup elevation;
- h0 (m): The initial overtopping wave bore depth at the profile crest in meters;

- v0 (m/s): The initial overtopping wave bore velocity at the profile crest in meters;
- Ls (m): The landward extent of the overtopping wave bore from the profile crest in meters;
- 2% Water Depth (m): The 2% water depth corresponding to the coordinates of the profiles and save points;
- 2% Velocity (m/s): The 2% velocity corresponding to the coordinates of the profiles and save points; and
- Min. Ponding Elevation (m): Elevation of ponded water on crest based on Profile Crest plus 25% of "(Ru2% Elevation – Profile Crest)".

9.7 Concluding Discussion

The simulation of coastal flooding in the region of Tuktoyaktuk is a complicated process due to the large surges that can occur and other variations in the mean water level from a range of different forces. The strong winds that create the surges also create large waves and these waves break due to limited water depth before they reach the shoreline. Therefore, it is the magnitude of the surge that is the controlling factor in the nearshore wave height, and the surge also determines the magnitude of the flood risk.

An assessment of historical winds and surges was undertaken, and relationships were established to link the surge magnitude to the wind speed. A randomization approach was used to simulate many ensembles of historical surges that were then superimposed upon a random tide level and a randomization of water level variability from other factors. This approach was used to define the surge level for events up to the 1000-year event. Estimation of levels for much longer return periods (e.g. 2500-year) was not undertaken.

A series of storm events were simulated in MIKE21 and the wave height and surge were extracted at the offshore ends of the profiles. These events included historical events, and scaled (wind speed) historical events at higher mean water levels to reach the desired storm surge return periods. The wave heights approaching the shore were calculated and used to simulate overtopping in the EurOtop model. The EurOtop model predicted overtopping on these steep slopes and provided the overtopping water depths at the crest of profiles.

With the steep shorelines at Tuktoyaktuk, there is also the potential for additional overtopping due to wind driven spray. However, this process was not included in the analysis. This type of phenomenon is not expected to cause significant flooding, but could cause some damage, especially during very cold temperatures, causing ice formation on structures.

10Concluding Remarks and Perspectives on Future Work

10.1 Flood Loads Data Generation Initiative

Through the Climate Resilient Buildings and Core Public Infrastructure (CRB-CPI) Project, the National Research Council Canada (NRC) launched a major effort to develop guidelines for the design of flood-resistant buildings and improving flood-resistance for existing buildings in an effort to provide flood provisions in the National Building Code (NBC) of Canada. Currently, like wind, snow and ice loads, the NBC does not contain provisions on flood loads for the design of buildings. Coulbourne Consulting team, which was heavily engaged in the development of similar guidelines in the US, was contracted to lead this effort. To support the development of these guidelines, NRC also started flood loads data generation case studies initiative. For these case studies, five Canadian consulting firms were contracted to carry out 13 different case studies in riverine, urban, large lake and coastal environments across the country. Included in these case studies were two coastal case studies for British Columbia, two riverine case studies in Alberta, one riverine case study in Saskatchewan and another in Manitoba, two large lake case studies in Ontario, two riverine/urban case studies in Quebec, four riverine/urban/coastal case studies in Atlantic Canada, and one northern case study in Northwest Territories.

The design recommendations for flood-resistant buildings are tied with what is shown and could be made available on flood maps in the form of mapped design water levels or flood construction levels (Coulbourne Consulting, 2021a, 2021b). For riverine conditions, the guidelines recommended determining design flood elevations for specified return periods or mean recurrence intervals (MRIs), plus future conditions that affect the water surface elevation. For coastal conditions, the design flood elevation for a specified MRI, plus the wave effect above the storm surge, plus future conditions were recommended. The recommended flood design levels were based on the building occupancy class from the NBC. There are four classes in the NBC: low, normal, high, and post-disaster. Recommended flood design MRI is 100-year for low, 500-year for normal, 750-year for high, and 1000-year for post-disaster buildings.

The normal category of buildings covers most or many residential buildings, whether they are single family, multi-family or apartments. The recommendations are for adopting the 500-year MRI flood protection level than the 100-year level, typically used for flood mapping purposes. High class buildings are typically high occupancy buildings as there are potentially more people involved. Consequently, these buildings need to be designed for higher return periods (i.e. 750-year). Post-disaster buildings are most important to the community, e.g. hospitals, fire stations, police stations, etc. These buildings need to be designed to even a higher MRI (i.e. 1000-year). The MRIs recommended by the guidelines on improving flood-resilience for existing buildings (Coulbourne Consulting, 2021b) are 100-year MRI for low, 250-year MRI for normal, 500-year MRI for high, and 750-year MRI for post-disaster buildings. These recommendations are a little lower than what is recommended for new buildings. Canadian practice on MRIs varies from 100-

year MRI for most of the country to 200-year MRI in British Columbia and 500-year MRI in Saskatchewan. To overcome this issue and to be consistent with the recommendations, a prescriptive method was recommended for scaling up flood levels corresponding to currently mapped MRIs to the recommended larger MRIs. To underpin these recommendations and prescriptive methods, targeted flood loads data generation case studies were designed and undertaken in different parts of the country. This report attempted to document an overview of these diverse case studies in Chapters 3 to 9, by providing information on technical aspects, modelling approaches used, data sources, and generated flood loading information. The information provided in this report is expected to help pave the way forward for improving estimation of flood loading variables and undertaking similar studies in the future.

10.2 Future Outlook

Some observations made over the course of the flood loads data generation case studies project, the status of Canadian flood maps in the light of the recommendations for flood-resistant design of buildings, and future prospects of additional case studies are discussed below.

- Flood loads data generation case studies initiative was a very first effort for undertaking detailed flood modelling and mapping studies with a view to derive information on flood loading related variables from riverine, urban, large lake, and coastal environments. This type of work has never been done before in Canada. Several questions came up during these studies, particularly with respect to the number of panels a transect across the river channel or perpendicular to the coastline be divided into in order to capture variations in velocity and depth of water. Information on flow velocity is used to calculate hydrodynamic loads, while that on water depth is used to calculate hydrostatic loads. Typically, buildings are subjected to these loads when sited in floodplains. In a few sensitivity experiments conducted by Northwest Hydraulics Consultants, velocity was found to be more sensitive to the number of panels compared to the depth of water. In the future, this can further be confirmed through additional case studies, as well as through laboratory experiments, in order to improve the quality of flood loads data.
- Another important question that has come up repeatedly is regarding the derivation of flood magnitudes and extreme rainfall amounts corresponding to return periods or MRIs beyond the 200-year mark, especially the 1000-year and 2500-year return periods. The corresponding return values are associated with large uncertainties since the original relationships that were used in extrapolation were basically developed from short samples, comprising merely 30-40 years of data. Since the flood-resistant design recommendations are towards adopting longer return period events for different categories of buildings (i.e. low, normal, high, and post-disaster), concerted research efforts need to be conducted to investigate how robustly such return values can be estimated from short historical samples.

- The prescriptive guidance for the design of flood-resistant buildings to withstand flood loads originating from longer return period events was validated on data derived from a small number of case studies. It will be important to enrich this database with additional case studies from riverine, urban and coastal environments using multiple modelling tools and improved datasets, especially using high quality bathymetry data and fine resolution topographic surveys.
- In critical cases, e.g. when siting a new hospital or an emergency centre, it is anticipated that the project engineers will likely recommend a more detailed flood modelling and mapping study than just using the proposed prescriptive guidance in order to derive various flood loads and load combinations, expected on structural components of such buildings. To facilitate this process based on best practice guidelines, it would be sensible to support additional research and to develop a standards document containing information on best practice guidelines for deriving and evaluating various types of flood loads for designing flood-resistant buildings in the future.
- In 1976, the federal government started a nation-wide flood protection program, the Flood Damage Reduction Program (FDRP), to protect Canadian communities and their assets from flood hazards by mapping flood-prone areas. In 1995/96, when the FDRP ended, most of the flood-prone areas and vulnerable major population centres across the country were flood risk mapped. Majority of the flood maps produced within the FDRP were targeted to show flood extents following the two zone concept, i.e. floodway and flood fringe. The floodway is the portion of the floodplain where flood velocities are expected to equal or exceed 1 m/s and/or water depths equal or exceed 1 m. The flood fringe is the remainder of the flood zone where the flood velocities are under 1 m/s and the water depth is below 1 m. The new maps which were developed or updated from existing maps under the Public Safety of Canada's funded National Disaster Mitigation Program (NDMP) also followed the same practice, with some locations now showing additional information in terms of future floodlines and additional higher return period scenarios. Detailed spatial information about flood depths and velocities is available only for a few west and east coast communities, where new mapping initiatives were recently undertaken. Most of the flood maps show inundation extents and spatial distribution of flood depths in terms of floodway and flood fringe and rarely any information on velocities. Detailed information on flood depths and velocities is absolutely required if design specifications and flood-resilience is required at the building footprint level in flood-prone areas. Going forward, detailed floodplain modelling and mapping studies should be encouraged for all new flood mapping efforts being supported through federal and provincial initiatives.

11References

Aquapraxis D, 2011. Mise à jour du Plan directeur de gestion des eaux pluviales – Rivière Beauport. Rapport d'étude 085-P027473-0104-CI-0001-00, pp 193.

ASCE/SEI 7-16, 2017. Minimum Design Loads and Associated Criteria for Buildings and Other Structures. Standards ASCE/SEI 7-16, American Society of Civil Engineers, Reston, Virginia.

Ausenco Sandwell, 2011. Sea Dike Guidelines. Technical Report, BC Ministry of Environment.

Baird, 2021a. Coastal Flood Case Studies: Lake Erie Sites Summary Report. Baird and Associates, Ottawa, ON.

Baird, 2021b. Coastal Flood Case Studies: Tuktoyaktuk Summary Report. Baird and Associates, Ottawa, ON.

Bobee B, El Adlouni S, 2015. HyfranPlus. University of Quebec, Quebec, Canada.

Brunner GW, 2016. HEC-RAS, River Analysis System Hydraulic Reference Manual. User Manual. US Army Corps of Engineers Hydrologic Engineering Center, Davis, CA, pp 547.

CBCL, 2021. Generation of Data from Floodplain Studies for Deriving Flood Loads to Support Building Design. Final Report. Halifax, NS.

CEHQ, 2015. Détermination des cotes de cures – Rivière Beauport (Rapport d'étude CEHQ 4132-0540-05-9944), pp 46.

Coulbourne Consulting, 2021a. Design of Flood-Resistant Buildings. NRC Contract No. 930582, Coulbourne Consulting, Annapolis, MD, USA.

Coulbourne Consulting, 2021b. Guidelines for Improving Flood-Resistance for Existing Buildings. NRC Contract No. 930582, Coulbourne Consulting, Annapolis, MD, USA.

Cox J, Machemehl J, 1986. Overload bore propagation due to an overtopping wave. Journal of Waterway, Port, Coastal and Ocean Engineering 112 (1), 161–163.

Environment and Climate Change Canada, 2016. Flood Damage Reduction Program. Retrieved from: https://www.ec.gc.ca/eau-water/default.asp?lang=En&n=714F6E0D-1.

EurOtop, 2018. Manual on Wave Overtopping of Sea Defences and Related Structures. Authors: Van der Meer JW, Allsop NWH, Bruce T, De Rouck J, Kortenhaus A, Pullen T, Schüttrumpf H, Troch P, Zanuttigh B. Available at: www.overtopping-manual.com.

FEMA, 2011. Coastal Construction Manual. Fourth Edition. FEMA P-259. Available at: www.fema.gov/library/viewRecord.do?id=1671.

FEMA, 2012. Engineering Principles and Practices of Retrofitting Flood-Prone Residential Structures. Third edition. FEMA P-259. Available at: https://www.fema.gov/sites/default/files/2020-08/fema259_complete_rev.pdf.

FEMA, 2013. Floodproofing Non-Residential Buildings. FEMA P-936. Available at: https://www.fema.gov/sites/default/files/2020-07/fema_p-936_floodproofing_non-residential_buiildings_110618pdf.pdf.

Ford JD, Bell T, Couture NJ, 2016. Perspectives on Canada's North Coast region; in Canada's Marine Coasts in a Changing Climate, (ed.) Lemmen DS, Warren FJ, James TS, Mercer CSL. Government of Canada, Ottawa, ON, pp 153-206.

Global News, 2017. Exclusive: Building Codes Across Canada to be updated to Reflect Climate Change. News article by Monique Scotti. Available at: https://globalnews.ca/news/3276145/building-codes-changes-climate-change/.

Goda Y, 2010. Random Seas and Design of Maritime Structures. World Scientific.

Hatch, 2020. Derivation of Flood Water Levels from Floodplain Mapping Studies in Manitoba and Saskatchewan. Summary Report. Hatch, Winnipeg, MB.

Infrastructure Canada, 2016. 2016–17 Departmental Results Report. Available at: http://www.infrastructure.gc.ca/pub/drr-rrm/2017/2017-03-eng.html.

IPCC, 2007. Climate Change 2007: The Physical Science Basis. Contribution of Working Group I to the Fourth Assessment Report of the Intergovernmental Panel on Climate Change DOI: 10.1038/446727a.

IPCC, 2013. Climate Change 2013. The Physical Science Basis. Contribution of Working Group I to the Fifth Assessment Report of the Intergovernmental Panel on Climate Change [Stocker TF, Qin D, Plattner G-K, Tignor M, Allen SK, Boschung J, Nauels A, Xia Y, Bex V, and Midgley PM (eds)]. Cambridge University Press, Cambridge, UK and New York, NY, USA.

IWD, 1976. Hydrologic and Hydraulic Procedures for Flood Plain Delineation. Inland Waters Directorate, Environment Canada, Ottawa, ON.

James TS, Henton JA, Leonard LJ, Darlington A, Forbes DL, Craymer M, 2014. Relative Sea Level Projections in Canada and the Adjacent Mainland United States. Geological Survey of Canada, Open File 7737, pp 72, doi:10.4095/295574.

JFSA, 2015. Etudes Hydrologique et Hydraulique du Ruisseau Clair (No. ref. 1182).

Khaliq MN, Attar A, 2017. Assessment of Canadian Floodplain Mapping and Supporting Datasets for Codes and Standards. NRC Report No. OCRE-TR-2017-026. National Research Council Canada, Ottawa, ON.

Khaliq MN, Attar A, Murphy E, Vouk I, Piche S, 2018. Assessment of Canadian floodplain mapping and supporting datasets for buildings and infrastructure design codes and standards. Canadian Society for Civil Engineering Conference, Fredericton, NB, June 13–16.

Khaliq MN, 2019. An Inventory of Methods for Estimating Climate Change-Informed Design Water Levels for Floodplain Mapping. NRC Report No. NRC-OCRE-2019-TR-011. National Research Council Canada, Ottawa, ON.

Kushner PJ, Mudryk LW, Merryfield W, Ambadan JT, Berg A, Bichet A, Brown R, Derksen C, Déry SJ, Dirkson A, Flato G, Fletcher CG, Fyfe JC, Gillett N, Haas C, Howell S, Laliberté F, McCusker K, Sigmond M, Sospedra-Alfonso R, Tandon NF, Thackeray C, Tremblay B, Zwiers FW, 2018. Canadian snow and sea ice: assessment of snow, sea ice, and related climate processes in Canada's Earth system model and climate-prediction system. The Cryosphere 12, 1137–1156.

LaSalle | NHC, 2018. Ruisseau Clair - Mont Tremblant Analyses Hydrologique et Hydraulique (Ref. No. 08003489).

LaSalle | NHC, 2019. Étude Hydraulique Conception de Deux Passerelles Parc Rivière Beauport (Ref. No. 8004891).

LaSalle | NHC, 2021. Generating Flood Data from Floodplain Mapping Studies for Deriving Flood Loads to Support Building Design for Canadian Codes and Standards: Riverine Case Studies 1 and 2: Beauport River and Clair Creek. Final Report.

McDermid JL, Dickin SK, Winsborough CL, Switzman H, Barr S, Gleeson JA, Krantzberg G, Gray PA, 2015. State of Climate Change Science in the Great Lakes Basin: A Focus on Climatological, Hydrological and Ecological Effects. Prepared jointly by the Ontario Climate Consortium and Ontario Ministry of Natural Resources and Forestry to advise Annex 9 – Climate Change Impacts under the Great Lakes Water Quality Agreement, October 2015.

Ministry of Natural Resources, 1982. HYDSTAT Computer Program for Univariate and Multi-variate Statistical Applications. Conservation Authorities and Water Management Branch.

Ministry of Natural Resources, 1989. Great Lakes System Flood Levels and Water Related Hazards.

Ministry of Natural Resources, 2001. Great Lakes – St. Lawrence River System and Large Inland Lakes. Technical Guides for flooding, erosion and dynamic beaches in support of natural hazards policies 3.1 of the Provincial Policy Statement (1997) of the Planning Act.

NHC, 2012. Serpentine & Nicomekl Rivers, Climate Change Floodplain Review – Phase 1 Final Report. Report prepared for City of Surrey.

NHC, 2015. Serpentine & Nicomekl Rivers, Climate Change Floodplain Review – Phase 2 Final Report. Report prepared for City of Surrey.

NHC, 2017. Peace River Hazard Study. Report for Alberta Environment and Parks.

NHC, 2020. North Saskatchewan River Hazard Study. Report for Alberta Environment and Parks.

NHC, 2021a. Generating Flood Data from Floodplain Mapping Studies for Deriving Flood Loads to Support Building Design for Canadian Codes and Standards. Riverine Case Study 1 – North Saskatchewan River at Edmonton. Final Report.

NHC, 2021b. Generating Flood Data from Floodplain Mapping Studies for Deriving Flood Loads to Support Building Design for Canadian Codes and Standards. Riverine Case Study 2 – Peace River at Peace River. Final Report.

NHC, 2021c. Generating Flood Data from Floodplain Mapping Studies for Deriving Flood Loads to Support Building Design for Canadian Codes and Standards: Coastal Case Study 1 – City of Vancouver. Final Report.

NHC, 2021d. Generating Flood Data from Floodplain Mapping Studies for Deriving Flood Loads to Support Building Design for Canadian Codes and Standards Coastal: Case Study 2 – City of Surrey. Final Report.

Roelvink D, Dastgheib A, Spencer T, Möller I, Christie E, Berenguer M, Sempere-Torres D, 2015. Resilience-increasing Strategies for Coasts – Toolkit. Improvement of Physical Processes. XBeach Improvement & Validation; Wave Dissipation over Vegetated Marshes and Flash Flood Module. Report D.3.2, http://www.risckit.eu/np4/file/23/RISCKIT_D.3.2_Improvement_of_Physical_Pr1.pdf.

Small D, Insurance K, Atallah EH, Gyakum J, 2011. Wind regimes along the Beaufort Sea Coast favorable for strong wind events at Tuktoyaktuk. Journal of Applied Meteorology and Climatology 50(6), DOI: 10.1175/2010JAMC2606.1.

Smit P, Stelling G, Roelvink J, Van Thiel de Vries J, McCall R, Van Dongeren A, Zwinkels C, Jacobs R, 2010. XBeach: Non-hydrostatic Model: Validation, Verification and Model Description. Technical Report, Delft University of Technology.

Swail VR, Cardone VJ, Ferguson M, Gummer DJ, Harris EL, Orelup EA, Cox AT, 2006. The MSC50 wind and wave reanalysis. In Proceedings of the 9th International Workshop on Wave Hindcasting and Forecasting, Vol 25, Victoria, BC, Canada.

Swail VR, Cardone VJ, Callahan B, Ferguson M, Gummer DJ, Cox AT, 2007. The MSC Beaufort wind and wave reanalysis. Proceedings of the 10th International Workshop on Wave Hindcasting and Forecasting and Coastal Hazard Symposium, North Shore, Oahu, Hawaii, WMO/IOC Joint Technical Commission for Oceanography and Marine Meteorology. Available online at http://www.waveworkshop.org/10thWaves/Papers/The%20MSC%20Beaufort%20Wind%20and%20Wave%20Reanalysis.pdf.

Wang XL, Feng Y, Swail VR, Cox A, 2015. Historical changes in the Beaufort–Chukchi–Bering seas surface winds and waves, 1971–2013. Journal of Climate 28 (19), 7457–7469.